

**Understanding and Improving Efficiency  
in Ruthenium Olefin Metathesis**

Thesis by  
Kevin Michael Kuhn

*In Partial Fulfillment of the Requirements  
for the Degree of  
Doctor of Philosophy*

California Institute of Technology  
Pasadena, California  
2010  
(Defended July 13, 2009)



*For My Wife*

## Acknowledgements

I am generally not very good at thanking the people who have helped me along the winding path that is my life. I tend to sputter and ramble, knowing that my words will never be able to match the support that I have been given. Sadly, this case will be no different. Still, before I try my best to acknowledge the many people who deserve to be acknowledged and who have won my infinite respect, I would like to make an attempt at short and sweet. Thank you!

I want to begin by acknowledging my advisor, Professor Robert H. Grubbs. In March 2004, I walked into Bob's office and stated that I wanted to work for him and would be happy to show up in the summer to get started before classes began. It dawned on me later that he was well within his rights to laugh me out of his office, but he did not. Instead, we talked a little about my interest in chemistry and a great deal about California hiking. I joined the Grubbs' group that August and have never looked back.

In lab, Bob has provided me with a great deal of freedom to try my own ideas, make my own mistakes, and learn how to independently approach scientific problems. At the same time, he has always guided me in the right direction, pushed me when I needed a push, and been willing to listen when I needed to vent. Outside of lab, he has taught me how to climb and how to pick a lock. We have shared countless hiking stories and more than one bottle of scotch while camping. It has been refreshing to see that it is possible to be the best in your field and still have a life, family, and hobbies.

My thesis committee — John Bercaw, Brian Stoltz, and Mark Davis — has been excellent. I thank them for their time and effort as I have worked my way through graduate school. Furthermore, they have been willing to take some time and talk about chemistry, politics, and my career path whenever the need arose. I am deeply indebted

for the support they have given me, as well as the numerous recommendation letters they have written, as I have directed my future away from the laboratory and into broader scientific endeavors.

I appreciate the numerous people at Caltech that have provided me with their kind support. I especially thank Linda Syme who keeps the lab running, money flowing, and makes sure Bob is on schedule (a nearly impossible feat). Dian Buchness, Laura Howe, Agnes Tong, Steve Gould, Joe Drew, and Anne Penny have also been incredibly helpful during my time as a graduate student. I also thank Larry Henling and Dr. Mike Day for X-ray crystallography, Dr. Mona Shahgholi for mass spectroscopy, Rick Gerhardt for fixing and building glassware, and Dr. Scott Ross and Dr. David VanderVelde for their help in the NMR facility. Finally, I have to note that if Tom Dunn did not work at Caltech the place would have fallen apart long ago.

While at Caltech, I have had the privilege to work with some amazing collaborators. Dr. Cheol Chung and Dr. J. B. Bourg were instrumental in the synthesis of the complexes described in chapter two. The whole Materia team, especially Dr. Tim Champagne, have been great to work with on screening projects (chapter three), catalyst design, and implementation of the new NHC synthesis (chapter four). Dr. Ian Stewart, Dr. Vincent Lavallo, Keith Keitz, and Jean Li have also spent time working on projects with me and have been excellent teammates. Finally, I have to thank Dr. Scott Virgil who has been essential to a majority of my work. Scott is an amazing chemist, a great sounding board for ideas, and is one of the most diligent people I have ever met. Caltech's 3CS wouldn't be the same without him.

Before highlighting specific individuals, I want to acknowledge all those with whom I have overlapped in the Grubbs' group. First, the graduate students: Isaac Rutenberg (for one day), Dan Sanders, Christie Morrill, Drew Waltman, Diego Benitez, Jacob Berlin, Tim Funk, Andy Hejl, Jason Jordan, Erin Guidry, Irina Gorodestskaya,

Donde Anderson, Soon Hong, Ron Walker, Michelle Robbins, Matt Whited, John Matson, Paul Clark, Yan Xia, Angela Blum, Leslie O'Leary, Jean Li, Chris Daeffler, Keith Keitz, Matt Van Wingerden, and newcomer Renee Thomas. A great many outstanding postdocs have also passed through the labs: Brian Connell, Anatoly Chlenov, Daryl Allen, Anna Wenzel, Tor Kit Goh, Katie Campbell, Greg Beutner, Cheol Chung, Paula Diaconescu, Chris Douglas, Connie Hou, Takashi Koike, Al Nelson, Mike Page, Tobias Ritter, Patricio Romero, Joseph Samec, Ian Stewart, Georgios Vougioukalakis, Masao Yanagawa, A. J. Boydston, J. B. Bourg, Rosemary Conrad, Vince Lavallo, Vlad Iluc, Koji Endo, Peili Teo, Jasim Uddin, Bahar Bingöl, Matteo De Pali, and Jeremiah Johnson.

I want to thank my baymates through the years: Jason Jordan, Katie Campbell, and Matteo. Jason and I became great friends despite having completely different worldviews. I never understood what makes him tick, but it was always fun trying to figure it out. Katie Campbell is an amazing person who I feel privileged to have met. She made my failure-ridden time after candidacy bearable, taught me a lot about Canada, and made me even more liberal. Although I only overlapped with Matteo briefly, he has been a great guy despite my grumbling at thesis time.

I need to thank the other members of the 5th Year Brain Trust: John Matson and Matt Whited. We each think about chemistry a little differently, and I believe our time together has made us all better chemists. Furthermore, they are always available to go drinking at the Ath. I am also indebted to the other Ath-goers in the group: Ian, Rose, Paul, and Keith. Thanks for the beer. Pato and Ian both became really great friends to me, and it is important to acknowledge how important it is to have people you can vent to in the worst of times. Thanks for listening.

Outside of the group, I want to thank John Enquist, Nat Sherden, and Kevin Allan for being great friends. We met the first week at Caltech and have had dinner about once a week for the last five years. On that note, I will miss your indecisiveness. Even

2500 miles away, Michael Morrison has been my best friend. We have backpacked over 300 miles in California over the last couple of years, arguing relentlessly about politics, books, religion, and life along the way.

My family has always been supportive of my decision to become a perpetual student and go on my California Adventure. I will always be grateful that they have been there when I need them, even when I think I know all the answers. Finally, I will always believe that I am just one phone call home away from turning them all into bleeding-heart liberals. Maybe in 2012.

And finally I get to the most important person in my life. My wife Melissa is an amazing, eternally optimistic, beautiful, and intelligent woman. I cannot imagine a day without her. She is the only person that knows what makes me tick, what motivates me, and never laughs when I talk about changing the world. Thank you and I love you.

## Abstract

Olefin metathesis has become an increasingly important and powerful reaction. The development of the well-defined ruthenium alkylidene complexes, in particular, has broadened the scope and utility of the olefin metathesis reaction in both organic synthesis and polymer science. Despite these advances, complete control of the parameters (activity, stability, and selectivity) that affect efficiency in olefin metathesis remains a major challenge, and the development of more efficient catalysts for a variety of applications remains a very important goal. With that in mind, this thesis primarily focuses on understanding the requirements for and improving the efficiency of ruthenium-based olefin metathesis.

In chapter two, a series of ruthenium olefin metathesis catalysts bearing *N*-heterocyclic carbene (NHC) ligands with varying degrees of backbone and *N*-aryl substitution were prepared. These complexes show greater resistance to decomposition through C-H activation of the *N*-aryl group, resulting in increased catalyst lifetimes. This work utilized robotic technology to examine the activity and stability of each catalyst in metathesis, providing insights into the relationship between ligand architecture and catalyst efficiency.

In chapter three, the high-throughput assay developed in the previous chapter was utilized to screen a series of ruthenium catalysts for the ring-closing metathesis (RCM) of acyclic carbamates to form the corresponding di-, tri-, and tetrasubstituted five-, six-, and seven-membered cyclic carbamates. While disubstituted cyclic olefins were easily formed by a variety of catalysts, NHC-bearing catalysts were required to produce trisubstituted cyclic olefin products at low catalyst loadings. Furthermore, only catalysts bearing small *N*-aryl bulk on the NHC ligands were found to effectively

accomplish the RCM reaction for sterically challenging substrates, providing a reminder that more-efficient catalysts still need to be developed.

A process for the preparation of symmetric and unsymmetric imidazolium chlorides that involves reaction of a formamidine with dichloroethane and a base is described in chapter four. This method makes it possible to obtain numerous imidazolium chlorides under solvent-free reaction conditions and in excellent yields with purification by simple filtration.

In chapter five, both chiral triazolylidenes and cyclic alkyl amino carbenes (CAACs) were chosen as ligands for the preparation of chiral ruthenium olefin metathesis catalysts. These  $C_1$  symmetric ligands were chosen to create non-conformationally flexible environments in proximity to the ruthenium center, potentially bringing chirality extremely close to the site of catalysis. These new motifs for ligand architecture show great promise. The moderate enantioselectivities obtained for AROCM and ARCM indicate potential utility toward both synthetic methodology and mechanistic insight.

Finally, appendix A describes the preparation of a series of ruthenium olefin metathesis catalysts bearing acenaphthylene-annulated NHC ligands with varying degrees of *N*-aryl substitution. Initial evaluation of their performance in olefin metathesis demonstrated that these complexes show greater resistance to decomposition, resulting in increased catalyst lifetimes. While this work has significant potential, the results are preliminary.

## Table of Contents

<b>Acknowledgements</b> .....	<b>iv</b>
<b>Abstract</b> .....	<b>viii</b>
<b>Table of Contents</b> .....	<b>x</b>
<b>List of Figures</b> .....	<b>xii</b>
<b>List of Tables</b> .....	<b>xv</b>
<b>List of Schemes</b> .....	<b>xvii</b>
<b>Chapter 1. General Introduction to Olefin Metathesis</b> .....	<b>1</b>
<i>Olefin Metathesis</i> .....	2
Ruthenium-Based Catalysts.....	4
<i>Thesis Research</i> .....	6
<i>References and Notes</i> .....	8
<b>Chapter 2. The Effects of NHC-Backbone Substitution on Efficiency in Olefin Metathesis</b> .....	<b>12</b>
<i>Abstract</i> .....	13
<i>Introduction</i> .....	13
<i>Results and Discussion</i> .....	16
Catalyst Syntheses .....	16
Structural Analyses .....	18
Ring-Closing Metathesis (RCM) Activity.....	20
Development of a ppm Level Assay .....	22
<i>Conclusions</i> .....	30
<i>Experimental</i> .....	31
<i>References and Notes</i> .....	45
<b>Chapter 3. Cyclic Carbamates via Ring-Closing Metathesis with Low Loadings of Ruthenium Catalysts</b> .....	<b>49</b>
<i>Abstract</i> .....	50
<i>Introduction</i> .....	50
<i>Research and Discussion</i> .....	53
<i>Conclusions</i> .....	58
<i>Experimental</i> .....	59
<i>References and Notes</i> .....	69
<b>Chapter 4. A Facile Preparation of Imidazolinium Chlorides</b> .....	<b>71</b>
<i>Abstract</i> .....	72
<i>Introduction</i> .....	72

<i>Results and Discussion</i> .....	74
<i>Conclusions</i> .....	77
<i>Experimental</i> .....	77
<i>References and Notes</i> .....	85
<b>Chapter 5. Chiral Triazolylidenes and CAACs as Ligands for Use in Enantioselective Olefin Metathesis Catalysts</b> .....	<b>88</b>
<i>Abstract</i> .....	89
<i>Enantioselective Olefin Metathesis</i> .....	89
Asymmetric Molybdenum Catalysts .....	90
Asymmetric Ruthenium Catalysts .....	91
<i>Results and Discussion</i> .....	93
Chiral Triazolylidenes.....	93
Complex 5.13.....	93
Activity in Olefin Metathesis .....	95
Complex 5.34.....	98
Chiral CAACs .....	100
Complex 5.39.....	101
Structural Analysis .....	101
Activity in Olefin Metathesis .....	103
Complex 5.49 — Preliminary Work .....	105
Structural Analysis .....	106
Activity in Olefin Metathesis .....	107
<i>Conclusions</i> .....	107
<i>Experimental</i> .....	107
<i>References and Notes</i> .....	115
<b>Appendix A. Ruthenium Olefin Metathesis Catalysts Bearing Acenaphylene-Annulated N-Heterocyclic Carbene Ligands</b> .....	<b>118</b>
<i>Abstract</i> .....	119
<i>Introduction</i> .....	119
<i>Results</i> .....	120
Catalyst Syntheses .....	120
Structural Analyses.....	121
Activity in Olefin Metathesis .....	122
<i>Future Directions</i> .....	125
<i>Experimental</i> .....	125
<i>References and Notes</i> .....	130
<b>Appendix B. Additional Results: Cyclic Carbamates via RCM</b> .....	<b>131</b>
<i>Abstract</i> .....	132
<i>Results</i> .....	132

## List of Figures

### Chapter 1.

Figure 1.1. Types of olefin metathesis reactions commonly employed.....	3
Figure 1.2. Well-defined transition-metal olefin metathesis catalysts .....	3
Figure 1.3. Ruthenium-based olefin metathesis catalysts. ....	5
Figure 1.4. Parameters influencing efficiency in catalysis.. ....	6

### Chapter 2.

Figure 2.1. Representative NHC-bearing olefin metathesis catalysts.....	14
Figure 2.2. N-phenyl substituted complexes. ....	15
Figure 2.3. Imidazolium salts. ....	16
Figure 2.4. Synthesis of ruthenium complexes <b>2.15–2.20</b> .....	18
Figure 2.5. X-ray crystal structures of complexes <b>2.17</b> and <b>2.20</b> .....	19
Figure 2.6. IR carbonyl stretching frequencies of <i>cis</i> -[RhCl(CO) <sub>2</sub> (NHC)] complexes <b>2.21–2.23</b> . ....	20
Figure 2.7. RCM of diene <b>2.24</b> using catalysts <b>2.2</b> and <b>2.15–2.17</b> . ....	21
Figure 2.8. RCM of diene <b>2.26</b> using catalysts <b>2.2</b> and <b>2.15–2.17</b> . ....	21
Figure 2.9. RCM of diene <b>2.28</b> to tetrasubstituted cycloalkene <b>2.29</b> using catalysts <b>2.2</b> and <b>2.15–2.17</b> . ....	22
Figure 2.10. RCM of diene <b>2.24</b> to disubstituted cycloalkene <b>2.25</b> , using catalyst <b>2.2</b> in a variety of solvents.....	24
Figure 2.11. RCM of diene <b>2.24</b> to disubstituted cycloalkene <b>2.25</b> , using catalyst <b>2.2</b> ...25	25
Figure 2.12. Plot of the RCM of diene <b>2.24</b> to disubstituted cycloalkene <b>2.25</b> , with conversion monitored over 24 h using catalysts <b>2.2</b> and <b>2.15–2.17</b> .. ....	26
Figure 2.13. Plot of the RCM of diene <b>2.24</b> to disubstituted cycloalkene <b>2.25</b> , with conversion monitored over 24 h using catalysts <b>2.3</b> and <b>2.20</b> . ....	27
Figure 2.14. RCM of diene <b>2.26</b> to disubstituted cycloalkene <b>2.27</b> , using catalyst <b>2.2</b> ...28	28
Figure 2.15. RCM of diene <b>2.26</b> to trisubstituted cycloalkene <b>2.27</b> , using catalysts <b>2.2</b> , <b>2.3</b> , <b>2.5</b> , <b>2.17</b> , and <b>2.20</b> .....	29
Figure 2.16. RCM of diene <b>2.28</b> to tetrasubstituted cycloalkene <b>2.29</b> , using catalysts <b>2.2</b> , <b>2.3</b> , <b>2.17</b> , and <b>2.20</b> .....	29
Figure 2.17. RCM of diene <b>2.28</b> to tetrasubstituted cycloalkene <b>2.29</b> , using catalysts <b>2.3</b> , <b>2.5</b> , and <b>2.20</b> . ....	30

**Chapter 3.**

Figure 3.1. Ruthenium olefin metathesis catalysts.....	52
Figure 3.2. RCM of <b>3.11</b> utilizing complexes <b>3.1–3.10</b> .....	55
Figure 3.3. RCM of <b>3.13</b> and <b>3.19</b> utilizing complexes <b>3.2–3.5</b> .....	55
Figure 3.4. RCM of <b>3.17</b> , <b>3.19</b> and <b>3.21</b> utilizing complexes <b>3.1–3.8</b> .....	56
Figure 3.5. RCM of <b>3.23</b> utilizing complexes <b>3.7–3.10</b> .....	57
Figure 3.6. RCM of <b>3.25</b> and <b>3.27</b> utilizing complexes <b>3.8–3.10</b> .....	58

**Chapter 5.**

Figure 5.1. Examples of asymmetric olefin metathesis.....	90
Figure 5.2. Representative asymmetric molybdenum catalysts.....	91
Figure 5.3. Examples of ruthenium-based asymmetric olefin metathesis catalysts.....	92
Figure 5.4. C <sub>1</sub> -symmetric monodentate ligands chosen for study.....	93
Figure 5.5. Isomerization of <b>5.16</b> by complex <b>5.13</b> .....	96
Figure 5.6. E/Z ratio of cross-metathesis products.....	97
Figure 5.7. Examples of CAAC-based olefin metathesis catalysts.....	100
Figure 5.8. X-ray crystal structure of complex <b>5.39</b> .....	102
Figure 5.9. Screening of complex <b>5.39</b> in RCM.....	103
Figure 5.10. Screening of complex <b>5.39</b> in ARCM.....	105
Figure 5.11. X-ray crystal structure of complex <b>5.49</b> .....	106

**Appendix A.**

Figure A.1. Acenaphthol-imidazolium chlorides.....	120
Figure A.2. X-ray crystal structure of complex <b>A.3</b> , including side view.....	121
Figure A.3. X-ray crystal structure of complex <b>A.4</b> , including top view.....	122
Figure A.4. RCM of diene <b>A.6</b> to disubstituted cycloalkene <b>A.7</b> .....	123
Figure A.5. RCM of diene <b>A.8</b> to trisubstituted cycloalkene <b>A.9</b> .....	123
Figure A.6. RCM of diene <b>A.10</b> to tetrasubstituted cycloalkene <b>A.11</b> .....	124
Figure A.7. Low ppm assay for RCM of <b>A.6</b> utilizing complexes <b>A.4</b> and <b>A.5</b> .....	125

**Appendix B.**

Figure B.1. Ruthenium-based olefin metathesis catalysts utilized in this study.....	132
Figure B.2. RCM of <b>3.11</b> utilizing complexes <b>3.1–3.10</b> at 50 °C.....	133
Figure B.3. RCM of <b>3.11</b> utilizing complexes <b>3.1–3.10</b> at 30 °C.....	134
Figure B.4. RCM of <b>3.13</b> utilizing complexes <b>3.1–3.10</b> at 50 °C.....	135
Figure B.5. RCM of <b>3.13</b> utilizing complexes <b>3.1–3.10</b> at 30 °C.....	136
Figure B.6. RCM of <b>3.15</b> utilizing complexes <b>3.1–3.10</b> at 50 °C.....	137

<i>Figure B.7. RCM of 3.15 utilizing complexes 3.1–3.10 at 30 °C.</i>	138
<i>Figure B.8. RCM of 3.17 utilizing complexes 3.1–3.10 at 50 °C.</i>	139
<i>Figure B.9. RCM of 3.17 utilizing complexes 3.1–3.10 at 30 °C.</i>	140
<i>Figure B.10. RCM of 3.19 utilizing complexes 3.2–3.5 and 3.7–3.10 at 50 °C.</i>	141
<i>Figure B.11. RCM of 3.21 utilizing complexes 3.2–3.4 and 3.6–3.10 at 50 °C.</i>	142
<i>Figure B.12. RCM of 3.23 utilizing complexes 3.4 and 3.7–3.10 at 50 °C.</i>	143
<i>Figure B.13. RCM of 3.25 utilizing complexes 3.8–3.10 at 50 °C.</i>	144
<i>Figure B.14. RCM of 3.27 utilizing complexes 3.7–3.10 at 50 °C.</i>	145

## List of Tables

### **Chapter 1.**

*Table 1.1. Comparison of activity and functional group tolerance for several metals utilized in olefin metathesis.....4*

### **Chapter 2.**

*Table 2.1. Selected X-ray data for 2.2, 2.17, 2.3, and 2.20..... 19*

### **Chapter 3.**

*Table 3.1. Effects of concentration on the formation of disubstituted five-, six-, and seven-membered cyclic carbamates by complex 3.4.....54*

### **Chapter 4.**

*Table 4.1. Preparation of 1,3-diarylimidazolium chlorides from formamidines. ....75*

*Table 4.2. Preparation of 1,3 diarylimidizolinium chlorides from anilines in one-step. ....76*

### **Chapter 5.**

*Table 5.1. Selected X-ray data for 5.35, 5.39, and 5.40. .... 102*

*Table 5.2. AROCM with complex 5.39. .... 104*

## List of Schemes

<b>Chapter 1.</b>	
Scheme 1.1. <i>General mechanism for olefin metathesis.</i> .....	2
<b>Chapter 2.</b>	
Scheme 2.1. <i>Synthesis of imidazolium chloride 2.8.</i> .....	17
<b>Chapter 3.</b>	
Scheme 3.1. <i>RCM of acyclic carbamates to form the corresponding di-, tri-, and tetrasubstituted five-, six-, and seven-membered cyclic carbamates.</i> .....	53
<b>Chapter 4.</b>	
Scheme 4.1. <i>Deprotonation of imidazol(in)ium salts.</i> .....	72
Scheme 4.2. <i>Common syntheses of imidazolium salts.</i> .....	73
Scheme 4.3. <i>Reaction of 1,3,2-dioxathiolane-2,2-dioxide with lithium-N,N'-bis(2,4,6-trimethylphenyl)formamidine.</i> .....	73
Scheme 4.4. <i>Preparation of 1,3-dimesitylimidazolium chloride.</i> .....	74
<b>Chapter 5.</b>	
Scheme 5.1. <i>Synthesis of aminoindanol-derived triazolium salt 5.12.</i> .....	94
Scheme 5.2. <i>Synthesis of chiral triazolylidene complex 5.13.</i> .....	94
Scheme 5.3. <i>Screening of complex 5.13 in RCM.</i> .....	95
Scheme 5.4. <i>Screening diastereoselectivity of complex 5.13.</i> .....	95
Scheme 5.5. <i>ARCM of 5.24 with complex 5.13.</i> .....	97
Scheme 5.6. <i>AROCM with complex 5.13.</i> .....	98
Scheme 5.7. <i>Synthesis of (S)-2-amino-3-phenyl-1-propanol-derived triazolium salt</i> .....	98
Scheme 5.8. <i>Synthesis of chiral triazolylidene complex 5.34.</i> .....	99
Scheme 5.9. <i>Synthesis of chiral CAAC complex 5.39.</i> .....	101
Scheme 5.10. <i>Synthesis of chiral CAAC complex 5.49.</i> .....	106
<b>Appendix A.</b>	
Scheme A.1. <i>Synthesis of ruthenium complexes A.3 and A.4.</i> .....	121

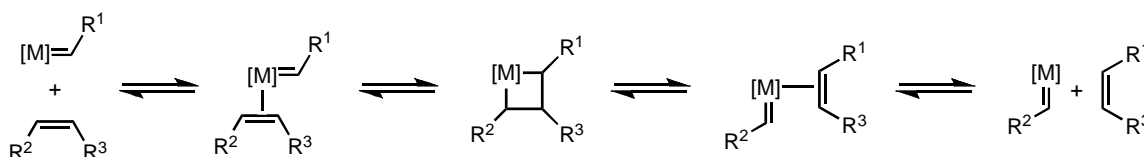
## **Chapter 1**

### **General Introduction to Olefin Metathesis**

## Olefin Metathesis

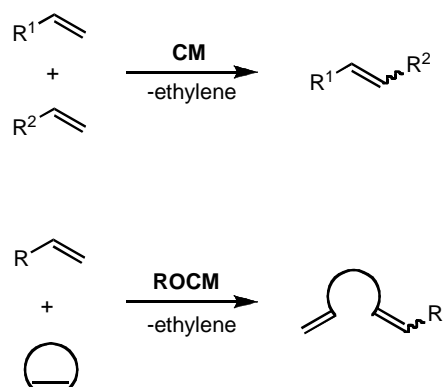
The olefin metathesis reaction is a transition metal-mediated transformation that rearranges the carbon atoms of carbon-carbon double bonds.<sup>1</sup> As illustrated in scheme 1.1, the generally accepted mechanism, originally proposed by Chauvin<sup>2</sup> in 1971 and supported by Grubbs<sup>3</sup> in 1975, involves olefin coordination to a transition metal-alkylidene complex, followed by a [2+2]-cycloaddition reaction that generates a new carbon-carbon bond and affords a metallacyclobutane intermediate, and finally a [2+2]-cycloreversion reaction, which regenerates a metal-alkylidene and a coordinated olefin product.

**Scheme 1.1.** General mechanism for olefin metathesis.



The individual steps in the catalytic cycle of the olefin metathesis reaction are reversible and the substrate-product equilibrium is governed by thermodynamic control. Therefore, most protocols rely on a driving force, such as the formation of ethylene or the release of ring strain, to favor the formation of a single product.<sup>4</sup> The classifications of olefin metathesis reactions are summarized in figure 1.1, including cross metathesis (CM), ring-opening cross metathesis (ROCM), ring-closing metathesis (RCM), ring-opening metathesis polymerization (ROMP), and acyclic diene metathesis polymerization (ADMET). Through the application of these methodologies and others, olefin metathesis has become an increasingly important and powerful reaction that is widely used in both organic synthesis and polymer science.<sup>1,5</sup>

### Intermolecular Metathesis Reactions



### Diene Metathesis Reactions

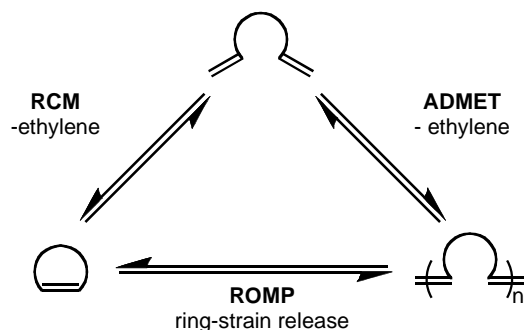


**Figure 1.1.** Types of olefin metathesis reactions commonly employed.

Olefin metathesis was originally observed in the mid-1950s.<sup>6</sup> The earliest metathesis reactions were catalyzed by ill-defined, multi-component systems comprised of transition-metal halides and main-group co-catalysts, such as  $WCl_6/EtAlCl_2$ ,  $WCl_6/BuSn_4$ , or metals on solid supports, such as  $MoO_3/SiO_2$ .<sup>1a,1b,7</sup> The isolation of the first well-defined metal carbene complexes in the 1970s spurred great advances in catalyst design, leading to titanium,<sup>8</sup> tungsten,<sup>9</sup> molybdenum<sup>10</sup> and ruthenium<sup>11</sup> complexes that are active in olefin metathesis reactions (Figure 1.2). The different metals impart different reactivities to the alkylidenes, and, as will be discussed in detail for ruthenium, small adjustments in the ligand environment can cause large changes in catalyst behavior.

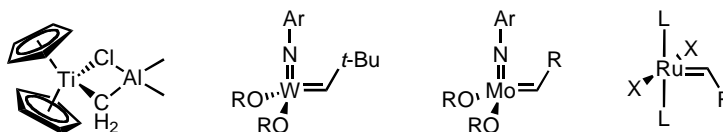


**Figure 1.2.** Well-defined transition-metal olefin metathesis catalysts.

## Ruthenium-Based Catalysts

The development of the well-defined ruthenium alkylidene complexes, in particular, has allowed for olefin metathesis' wide use in both organic synthesis and polymer science.<sup>1,5</sup> Unlike their early transition-metal counterparts, these ruthenium complexes are tolerant to moisture and oxygen, allowing them to be easily handled on the benchtop.<sup>12</sup> Furthermore, the high affinity of ruthenium for olefins over other functional groups makes these complexes generally more useful for synthetic applications (Table 1.1). Despite these comparative advantages, ruthenium systems cannot yet match the overall activity observed with the early metal complexes in many cases.<sup>12</sup>

**Table 1.1.** Comparison of activity and functional group tolerance for several metals utilized in olefin metathesis; adapted from reference 12a.

	Titanium	Tungsten	Molybdenum	Ruthenium
Acids	Acids	Acids	Acids	<b>Olefins</b>
Alcohols, Water	Alcohols, Water	Alcohols, Water	Alcohols, Water	Acids
Aldehydes	Aldehydes	Aldehydes	Aldehydes	Alcohols, Water
Ketones	Ketones	Ketones	<b>Olefins</b>	Aldehydes
Esters, Amides	Esters, Amides	<b>Olefins</b>	Ketones	Ketones
<b>Olefins</b>	<b>Olefins</b>	Esters, Amides	Esters, Amides	Esters, Amides

The ruthenium-based catalysts are based on a  $X_2L_2Ru=CHR$  platform comprised of a ruthenium alkylidene, two anionic, and two neutral ligands (Figure 1.3). Nguyen and co-workers reported the first well-defined ruthenium-alkylidene complex (**1.1**) in 1992.<sup>11b,11c</sup> In 1995, Schwab and co-workers replaced the triphenylphosphine ligands with the more sigma-donating tricyclohexylphosphine ligand and replaced the vinyl carbene with a benzylidene, generating complex **1.2**.<sup>11d,11e</sup> This complex demonstrated

good activity and improved functional group tolerance over **1.1**, greatly expanding the substrate scope. With Scholl and co-workers' development of complex **1.3** ( $(H_2IMes)(PCy_3)Cl_2Ru=CHPh$  ( $H_2IMes = 1,3$ -dimesitylimidazolidine-2-ylidene) in 1999, the activity of the ruthenium catalyst was further increased while retaining the desirable functional group tolerance and stability.<sup>11f,11g</sup> In fact, the activity of **1.3** rivals that of the highly active molybdenum systems.<sup>13</sup> Finally, Hoveyda's exchange of the final phosphine ligand with a chelating ether moiety has provided **1.4**, which shows increased stability relative to previous catalysts.<sup>11h, 11i</sup>

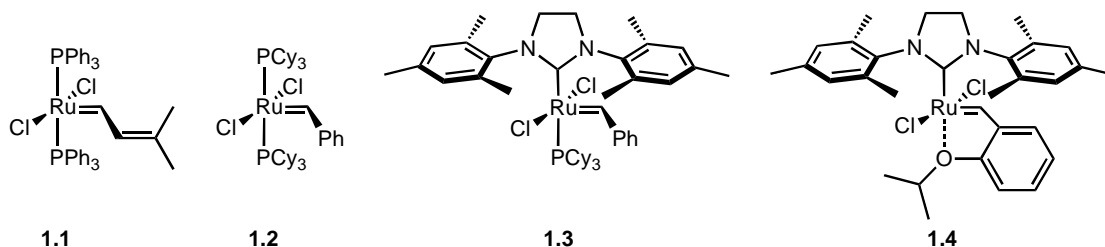


**Figure 1.3.** Ruthenium-based olefin metathesis catalysts.

Despite the aforementioned advances, completely controlling the parameters that affect efficiency in olefin metathesis remains a major challenge. These parameters, best described by Ritter et al., broadly include activity, stability and selectivity (Figure 1.4).<sup>14</sup> Activity encompasses the initiation and propagation rates of given catalyst in olefin metathesis. As such, it is reaction dependent and can be quantified through kinetic experiments.<sup>15</sup> Stability is directly related to activity and refers to the lifetime of a catalyst and its ability to perform productive metathesis events over extended periods of time. Stability can be qualitatively measured by monitoring loss in catalyst activity throughout the course of a reaction. Finally, selectivity describes the ability of a catalyst to react with a certain type of substrate (chemoselectivity) or to provide control over product formation (enantioselectivity and diastereoselectivity).

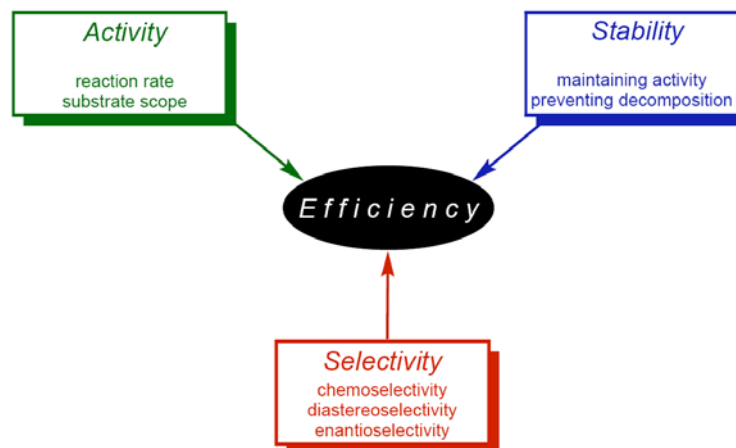


**Figure 1.4.** Parameters influencing efficiency in catalysis; adapted from reference 14.

With that in mind, the development of more efficient catalysts for a variety of applications remains a very important goal and has been actively pursued. In addition to  $\text{H}_2\text{IMes}$ , a variety of other *N*-heterocyclic carbene (NHC) ligands have been examined. These studies have led to, among others, the design and development of ruthenium catalysts utilized in enantioselective olefin metathesis,<sup>16</sup> applications in aqueous or protic solvents,<sup>17</sup> and the metathesis of highly hindered substrates.<sup>18</sup> Other areas of significant interest include the development of catalysts that are both highly stable and highly active or exhibit kinetic selectivity, as in ethenolysis and E/Z-diastereoselective olefin metathesis reactions.<sup>19</sup>

### ***Thesis Research***

This thesis primarily focuses on understanding and improving efficiency in ruthenium-based olefin metathesis. Chapter two describes the effects of NHC-backbone substitution on the activity and stability of ruthenium catalysts and the development of a highly sensitive assay to measure minor modifications in catalyst architecture. The use of this assay to describe trends in catalyst efficiency for the formation of cyclic carbamates is the focus of chapter three, with additional results outlined in appendix B. Chapter four describes a novel, efficient, and environmentally friendly method for the

production of imidazolinium salts, precursors in the synthesis of NHC-based catalysts. The research presented in chapter five describes ongoing efforts to utilize chiral non-racemic  $C_1$ -symmetric ligands, both triazolylidenes and cyclic alkyl amino carbenes, to create rigid chiral space in proximity to the ruthenium center, potentially affording highly efficient and enantioselective olefin metathesis catalysts. Finally, appendix A outlines preliminary results from research utilizing a series of ruthenium olefin metathesis catalysts bearing acenaphthylene-annulated (NHC) ligands.

## References and Notes

---

- (1) (a) Grubbs, R. H. *Handbook of Metathesis*; Wiley-VCH:Weinheim, Germany, 2003 and references cited therein. (b) Ivin, K. J.; Mol, J. C. *Olefin Metathesis and Metathesis Polymerization*; Academic Press: San Diego, CA, 1997 and references cited therein. (c) Noels, A. F.; Demonceau, A. *J. Phys. Org. Chem.* **1998**, *11*, 602–609. (d) Grubbs, R. H. *Tetrahedron*, **2004**, *60*, 7117–7140. (e) Grubbs, R. H. *Angew. Chem. Int. Ed.* **2006**, *45*, 3760–3765. (f) Schrock, R. *Angew. Chem. Int. Ed.* **2006**, *45*, 3748–3759.
- (2) Herrison, J.-L.; Chauvin, Y. *Makromol. Chem.* **1971**, *141*, 161–167.
- (3) (a) Grubbs, R. H.; Burk, P. L.; Carr, D. D. *J. Am. Chem. Soc.* **1975**, *97*, 3265–3267. (b) Grubbs, R. H.; Carr, D. D.; Hoppin, C.; Burk, P. L. *J. Am. Chem. Soc.* **1976**, *98*, 3478–3483.
- (4) Wiberg, K. B. *Angew. Chem., Int. Ed. Engl.* **1986**, *25*, 312–322.
- (5) (a) Hoveyda, A. H.; Zhugralin, A. R. *Nature* **2007**, *450*, 243–251. (b) Schrodi, Y.; Pederson, R. L. *Aldrichimica Acta* **2007**, *40*, 45–52. (c) Nicolaou, K. C.; Bulger, P. G.; Sarlah, D. *Angew. Chem., Int. Ed.* **2005**, *44*, 4490–4527. (d) Furstner, A. *Angew. Chem., Int. Ed.* **2000**, *39*, 3013–3043.
- (6) (a) Banks, R. L. *Chemtech*, **1986**, *16*, 112–117. (b) Eleuterio, H. *Chemtech*, **1986**, *21*, 92–95. (c) Spessard, G. O.; Miessler, G. L. *Organometallic Chemistry*; Prentice-Hall: Upper Saddle River, New Jersey, 1997.
- (7) (a) Calderon, N.; Chem, H. Y.; Scott, K. W. *Tetrahedron Lett.* **1967**, *34*, 3327–3329. (b) Calderon, N. *Acc. Chem. Res.* **1972**, *5*, 127–132.
- (8) (a) Tebbe, F. N.; Parshall, G. W.; Reddy, G. S. *J. Am. Chem. Soc.* **1978**, *100*, 3611–3613. (b) Tebbe, F. N.; Parshall, G. W.; Ovenall, D. W. *J. Am. Chem. Soc.*

- 
- 1979**, *101*, 5074–5075.
- (9) (a) Quignard, F.; Leconte, M.; Basset, J. M. *J. Mol. Catal.* **1986**, *36*, 13–29.  
(b) Wengrovius, J. H.; Schrock, R. R.; Churchill, M. R.; Missert, J. R.; Youngs, W. *J. Am. Chem. Soc.* **1980**, *102*, 4515–4516. (c) Kress, J. R. M.; Russell, M. J. M.; Wesolek, M. G.; Osborn, B. P. *J. Chem. Soc., Chem. Commun.* **1980**, 431–432. (d) Schrock, R. R.; DePue, R. T.; Feldman, J.; Schaverien, C. J.; Dewan, J. C.; Liu, A. H. *J. Am. Chem. Soc.* **1988**, *110*, 1423–1435. (e) Couturier, J.-L.; Paillet, C.; Leconte, M.; Basset, J.-M.; Weiss, K. *Angew. Chem., Int. Ed. Engl.* **1992**, *31*, 628–631.
- (10) (a) Schrock, R. R.; Murdzek, J. S.; Bazan, G. C.; Robbins, J.; DiMare, M.; O'Regan, M. *J. Am. Chem. Soc.* **1990**, *112*, 3875–3886. (b) Bazan, G. C.; Oskam, J. H.; Cho, N.-H.; Park, L. Y.; Schrock, R. R. *J. Am. Chem. Soc.* **1991**, *113*, 6899–6907. (c) Schrock, R. R.; Hoveyda, A. H. *Angew. Chem. Int. Ed. Engl.* **2003**, *42*, 4592–4633.
- (11) (a) Novak, B. M.; Grubbs, R. H. *J. Am. Chem. Soc.* **1988**, *110*, 960–961.  
(b) Nguyen, S. T.; Grubbs, R. H.; Ziller, J. W. *J. Am. Chem. Soc.* **1993**, *115*, 9858–9859. (c) Nguyen, S. T.; Johnson, L. K.; Grubbs, R. H.; Ziller, J. W. *J. Am. Chem. Soc.* **1992**, *114*, 3974–3975. (d) Schwab, P.; France, M. B.; Ziller, J. W.; Grubbs, R. H. *Angew. Chem., Int. Ed.* **1995**, *34*, 2039–2041. (e) Schwab, P.; Grubbs, R. H.; Ziller, J. W. *J. Am. Chem. Soc.* **1996**, *118*, 100–110. (f) Scholl, M.; Ding, S.; Lee, C. W.; Grubbs, R. H. *Org. Lett.* **1999**, *1*, 953–956. (g) Sanford, M. S.; Love, J. A.; Grubbs, R. H. *J. Am. Chem. Soc.* **2001**, *123*, 6543–6554. (h) Kingsbury, J. S.; Harrity, J. P. A.; Bonitatebus, P. J., Jr.; Hoveyda, A. H. *J. Am. Chem. Soc.* **1999**, *121*, 791–799. (i) Garber, S. B.; Kingsbury, J. S.; Gray,

- 
- B. L.; Hoveyda, A. H. *J. Am. Chem. Soc.* **2000**, *122*, 8168–8179.
- (12) (a) Grubbs, R. H. *J. Macromol. Sci. — Pure Applied Chem.* **1994**, *A31*, 1829–1833. (b) Trnka, T. M.; Grubbs, R. H. *Acc. Chem. Res.* **2001**, *34*, 18–29. (c) Novak, B. Ph.D. Thesis, California Institute of Technology, 1989.
- (13) Bielawski, C. W.; Grubbs, R. H. *Angew. Chem. Int. Ed.* **2000**, *39*, 2903–2906.
- (14) Ritter, T.; Hejl, A.; Wenzel, A. G.; Funk, T. W.; Grubbs, R. H. *Organometallics* **2006**, *25*, 5740–5745.
- (15) Sanford, M. S.; Love, J. A.; Grubbs, R. H. *J. Am. Chem. Soc.* **2001**, *123*, 6543–6554.
- (16) (a) Seiders, T. J.; Ward, D. W.; Grubbs, R. H. *Org. Lett.* **2001**, *3*, 3225–3228. (b) Funk, T. W.; Berlin, J. M.; Grubbs, R. H. *J. Am. Chem. Soc.* **2006**, *128*, 1840–1846. (c) Berlin, J. M.; Goldberg, S. D.; Grubbs, R. H. *Angew. Chem. Int. Ed.* **2006**, *45*, 7591–7595. (d) Van Veldhuizen, J. J.; Gillingham, D. G.; Garber, S. B.; Kataoka, O.; Hoveyda, A. H. *J. Am. Chem. Soc.* **2003**, *125*, 12502–12508. (e) Gillingham, D. G.; Kataoka, O.; Garber, S. B.; Hoveyda, A. H. *J. Am. Chem. Soc.* **2004**, *126*, 12288–12290. (f) Van Veldhuizen, J. J.; Campbell, J. E.; Giudici, R. E.; Hoveyda, A. H. *J. Am. Chem. Soc.* **2005**, *127*, 6877–6882.
- (17) (a) Lynn, D. M.; Grubbs, R. H. *J. Am. Chem. Soc.* **2001**, *123*, 3187–3193. (b) Rölle, T.; Grubbs, R. H. *Chem. Commun.* **2002**, 1070–1071. (c) Gallivan, J. P.; Jordan, J. P.; Grubbs, R. H. *Tetrahedron Lett.* **2005**, *46*, 2577–2580. (d) Hong, S. H.; Grubbs, R. H. *J. Am. Chem. Soc.* **2006**, *128*, 3508–3509. (e) Mwangi, M. T.; Runge, M. B.; Bowden, N. B. *J. Am. Chem. Soc.* **2006**, *128*, 14434–14435. (f) Binder, J. B.; Guzei, I. A.; Raines, R. T. *Adv. Synth. Catal.* **2007**, *349*, 395–404. (g) Jordan, J. P.; Grubbs, R. H. *Angew. Chem. Int. Ed.*

---

**2007**, 46, 5152-5155.

- (18) (a) Berlin, J. M.; Campbell, K.; Ritter, T.; Funk, T. W.; Chlenov, A.; Grubbs, R. H. *Org. Lett.* **2007**, 9, 1339–1342. (b) Stewart, I. C.; Ung, T.; Pletnev, A. A.; Berlin, J. M.; Grubbs, R. H.; Schrodi, Y. *Org. Lett.* **2007**, 9, 1589–1592. (c) Chung, C. K. Grubbs, R. H. *Org. Lett.* **2008**, 10, 2693–2696.
- (19) Deshmukh, P. H.; Blechert, S. *Dalton Trans.* **2007**, 24, 2479–2491.

## Chapter 2

### The Effects of NHC-Backbone Substitution on Efficiency in Olefin Metathesis

*The text in this chapter is reproduced in part with permission from:*

Kuhn, K. M.; Bourg, J. B.; Chung, C. K.; Virgil, S. C.; Grubbs, R. H.

*J. Am. Chem. Soc.* **2009**, *131*, 5313-5320.

## **Abstract**

A series of ruthenium olefin metathesis catalysts bearing N-heterocyclic carbene (NHC) ligands with varying degrees of backbone and *N*-aryl substitution have been prepared. These complexes show greater resistance to decomposition through C-H activation of the *N*-aryl group, resulting in increased catalyst lifetimes. This work has utilized robotic technology to examine the activity and stability of each catalyst in metathesis, providing insights into the relationship between ligand architecture and enhanced efficiency. The development of this robotic methodology has also shown that, under optimized conditions, catalyst loadings as low as 25 ppm can lead to 100% conversion in the ring-closing metathesis of diethyl diallylmalonate.

## **Introduction**

Olefin metathesis has emerged as a valuable tool in both organic and polymer chemistry.<sup>1</sup> Ruthenium-based catalysts, in particular, have received considerable attention because of their tolerance to moisture, oxygen, and a large number of organic functional groups.<sup>2</sup> Following the report of the increased activity of complex **2.1** (H<sub>2</sub>IMes)(PCy<sub>3</sub>)Cl<sub>2</sub>Ru=CHPh (H<sub>2</sub>IMes = 1,3-dimesitylimidazolidine-2-ylidene),<sup>3</sup> and Hoveyda's subsequent exchange of the phosphine ligand with a chelating ether moiety (**2.2**),<sup>4</sup> many researchers have focused on increasing catalytic activity, selectivity and stability through modification of the N-heterocyclic carbene (NHC) ligand.<sup>5</sup>

As ligand modification has led to improved catalyst activity, a variety of applications have become possible, including ring-closing metathesis (RCM), cross metathesis (CM), ring-opening cross metathesis (ROCM), acyclic diene metathesis polymerization (ADMET), and ring-opening metathesis polymerization (ROMP). Among those metathesis reactions, ring-closing metathesis has become the most commonly employed metathesis reaction in organic synthesis.<sup>6</sup> For this transformation, NHC

catalysts, such as **2.1**, **2.2**, and more recently **2.3**, have allowed both high activity and increased catalyst lifetime to be realized (Figure 2.1).<sup>3,4,5c</sup>

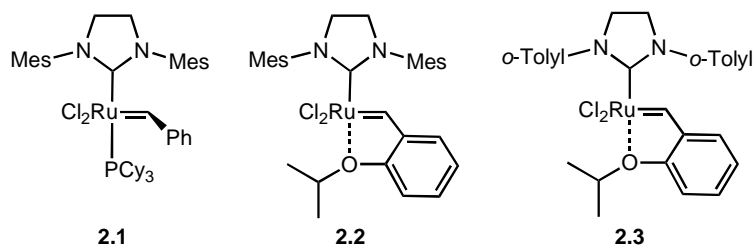


**Figure 2.1.** Representative NHC-bearing olefin metathesis catalysts.

Despite these advances, still more efficient catalysts are sought to increase the applicability of RCM in industry. In many cases, olefin metathesis is still plagued by catalyst deactivation and the requirement of high catalyst loadings.<sup>6</sup> Furthermore, decomposition products of olefin metathesis catalysts have been shown to be responsible for unwanted side reactions such as olefin isomerization.<sup>7</sup> Increased catalyst loading could also potentially increase the level of residual ruthenium impurities in the final products, which becomes especially troublesome where reaction products are intended for pharmaceutical use.<sup>8</sup> Collectively, these issues have a direct influence on the operational cost of metathesis transformations. With these factors in mind, the next challenge in RCM is to substantially decrease the catalyst loading, thereby reducing both reaction cost and the challenges in product purification. To this effect, our goal has been to increase catalyst efficiency by developing even more stable and robust catalysts that still retain a high catalytic activity.

Recently, studies by our group and others have unveiled the decomposition pathways at play during metathesis reactions.<sup>9</sup> Among other degradation products, complexes derived from C-H activation of *N*-aryl substituents were reported. Since the NHC ring and the aryl substituent must approach co-planarity for C-H activation, it was anticipated that decomposition via C-H activation processes might be slowed by



catalysts, they are not sensitive to small variations in the efficiency profile accompanying subtle modification in catalyst architecture.

In order to examine these small changes, we have developed a highly sensitive parts-per-million (ppm) level assay utilizing the precision and consistency of Symyx robotic technology. We utilized these techniques to examine the activity and stability of these catalysts in RCM at low catalyst loadings, providing increased insight into the relationship between ligand architecture and catalyst efficiency. The development of this methodology has also shown that, under optimized conditions, complete conversion in the RCM of diethyl diallylmalonate is observed with catalyst loadings as low as 25 ppm (0.0025 mol%).

## Results and Discussion

### Catalyst Syntheses

The preparation of the 1,1'-dimethyl- and 1,2-dimethyl-substituted imidazolium chlorides **2.6** and **2.7** (Figure 2.3) have been previously reported by Bertrand and Çetinkaya, respectively.<sup>13</sup> Under analogous experimental conditions, imidazolium chlorides **2.9** and **2.10**, featuring 2-methylphenyl (*o*-tolyl) groups were obtained in good yields. Unfortunately, separation of the *syn*- and *anti*- isomers of **2.10** proved to be extremely difficult, requiring the mixture to be carried forward.

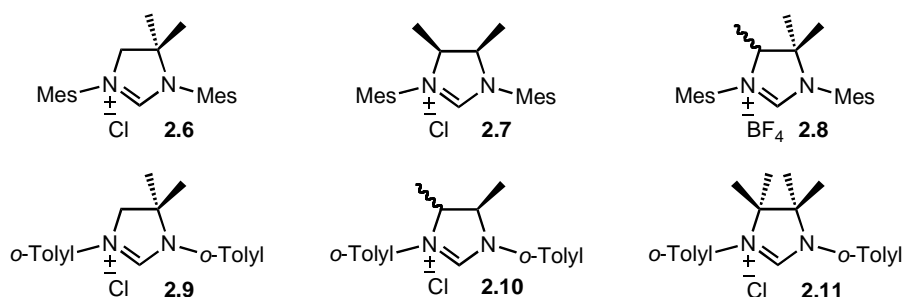
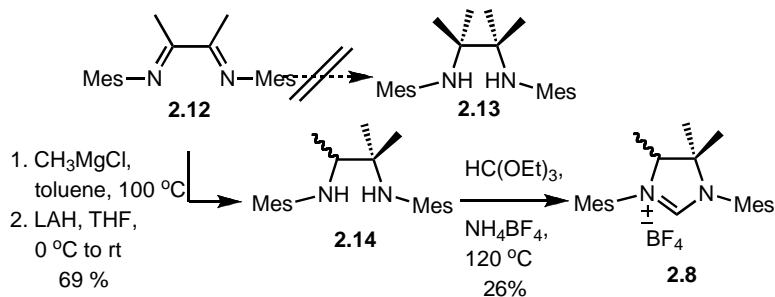


**Figure 2.3.** Imidazolium salts.

Following the procedures previously reported by our group to access the NHC of complex **2.5**, we then attempted the preparation of the highly substituted imidazolium salts bearing four methyl substituents.<sup>5a</sup> While imidazolium chloride **2.11** was prepared without incident, we were unable to synthesize the intermediate tetramethylated diamine **2.13** of the corresponding *N*-mesityl analogue under various conditions (Scheme 2.1). Considering the trimethylated NHC to be sufficiently encumbered to prevent *N*-aryl rotation, we prepared **2.8** instead by Grignard addition followed by reduction and imidazolium salt formation.

**Scheme 2.1.** Synthesis of imidazolium chloride **2.8**.



With precursors **2.6–2.11** in hand, the corresponding free carbenes were generated by treatment of the imidazolium salts with potassium hexamethyldisilazide (KHMDs) at room temperature (Figure 2.4). These carbenes (prepared in situ) were reacted with commercially available  $(\text{PCy}_3)_2\text{RuCl}_2=\text{CH}(\text{o-}i\text{PrC}_6\text{H}_4)$  at  $70\text{ }^\circ\text{C}$ , affording the phosphine-free chelating ether complexes **2.15–2.20**. These complexes were isolated as crystalline green solids after flash column chromatography, and as solids are both air and moisture stable under standard conditions.

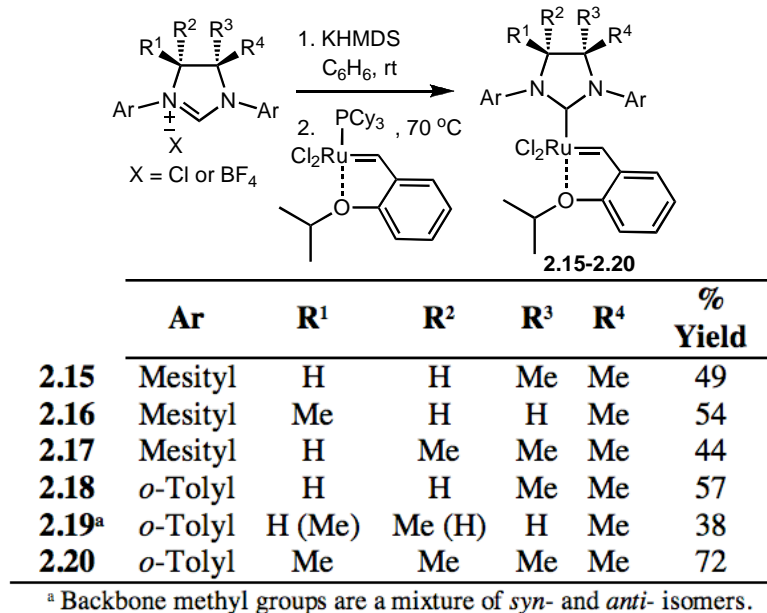


**Figure 2.4.** Synthesis of ruthenium complexes **2.15–2.20**.

### Structural Analyses

To probe the electronic and steric effects of backbone substitution, crystals of **2.17** and **2.20** were grown and their molecular structures were confirmed by single-crystal X-ray crystallographic analysis (Figure 2.5). The complexes exhibit a distorted square pyramidal geometry with the benzylidene moiety occupying the apical position. When compared with its unsubstituted analogue **2.2**, the backbone substitution of **2.17** results in significant differences in three key structural parameters summarized in table 2.1: (1) Ru-C(1) bond length, (2) C(1)-Ru-C(25) bond angle, and (3) the C(3)-N2-C(16) bond angle. Surprisingly, there are no major differences between the solid-state structures of complexes **2.3** and **2.20**.

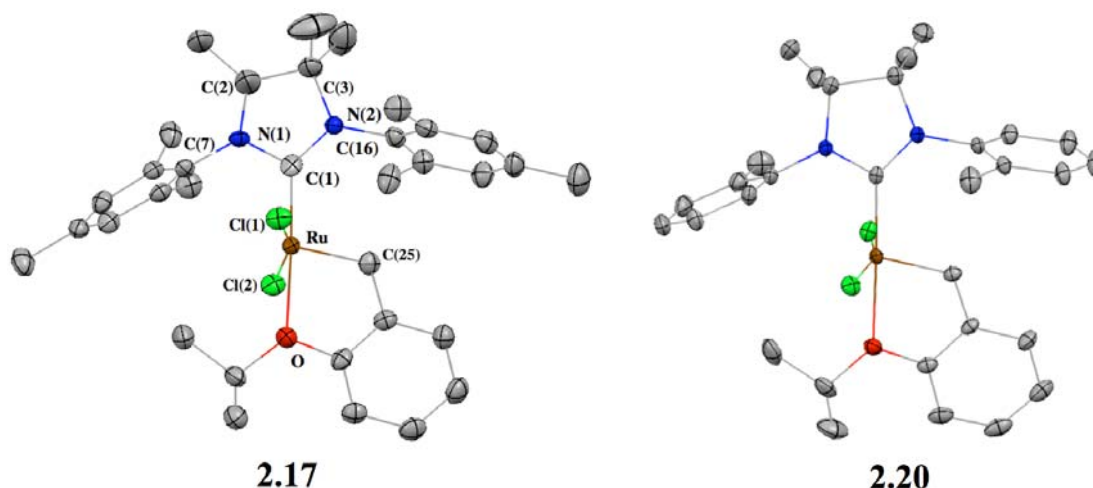


**Figure 2.5.** X-ray crystal structures of complexes **2.17** and **2.20** are shown. Displacement ellipsoids are drawn at 50% probability. For clarity, hydrogen atoms have been omitted.

**Table 2.1.** Selected X-ray data for **2.2**, **2.17**, **2.3**, and **2.20**.

	<b>2.2<sup>b</sup></b>	<b>2.17</b>	<b>2.3<sup>c</sup></b>	<b>2.20</b>
<b>Bond Lengths (Å)</b>				
Ru-C(1)	1.980	1.968	1.962	1.964
Ru-C(25)	1.824	1.840	1.823	1.835
Ru-O	2.262	2.255	2.244	2.261
<b>Bond Angles (deg)</b>				
C(3)-N(2)-C(16)	118.22	122.60	119.91	119.82
C(2)-N(1)-C(7)	118.32	123.82	120.69	120.26
C(1)-Ru-C(25)	101.60	103.08	102.48	103.14
Cl(1)-Ru-Cl(2)	156.42	161.26	159.49	160.80

<sup>a</sup> For a complete list of bond lengths and angles for **2.17** and **2.20**, refer to the SI. <sup>b</sup> See ref 4. <sup>c</sup> See ref. 5c.

The crystal structure of complex **2.17** suggests that the backbone methyl substituents push the *N*-mesityl groups toward the ruthenium center and as a result the NHC-Ru-benzylidene bond angle is also increased. However, the bond distance between the NHC carbene carbon and the Ru center is shorter in **2.17** (1.968 Å) than in **2.2** (1.980 Å). This effect can be explained by noting that the backbone methyl substituents increase the electron-donating ability of the NHC ligand. This effect is also

seen in the IR carbonyl stretching frequencies of the *cis*-[RhCl(CO)<sub>2</sub>(NHC)] complexes **2.21–2.23** (Figure 2.6), where increased substitution resulted in lower frequencies.<sup>14</sup> These structural differences should have a significant impact on the efficiency of the different catalysts.

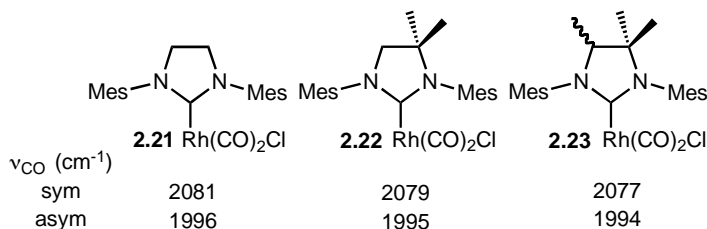


**Figure 2.6.** IR carbonyl stretching frequencies of *cis*-[RhCl(CO)<sub>2</sub>(NHC)] complexes **2.21–2.23**.

### Ring-Closing Metathesis (RCM) Activity

RCM is widely used in organic synthesis and serves as a standard assay to evaluate the relative efficiency of most ruthenium-based catalysts.<sup>6,12</sup> With this in mind, we began our metathesis activity studies by focusing on the catalytic activity of the *N*-mesityl series (**2.2**, **2.15–2.17**) in the RCM of diethyl diallylmalonate **2.24** to cycloalkene **2.25**. The reactions, utilizing 1 mol% catalyst in CD<sub>2</sub>Cl<sub>2</sub> at 30 °C, were monitored by <sup>1</sup>H NMR spectroscopy. Interestingly, the plots of cycloalkene **2.25** concentration versus time (Figure 2.7) revealed that the complexes affect the cyclization of **2.24**, but with slower reaction rates as backbone substitution is increased.

The same trend was observed for the cyclization of diethyl allylmethylmalonate **2.26** to form trisubstituted cyclic olefin **2.27** (Figure 2.8). However, in the very challenging RCM of diethyl dimethylmalonate **2.28**, using 5 mol% catalyst in C<sub>6</sub>D<sub>6</sub> at 60 °C, increased substitution resulted in increased catalyst lifetimes and higher conversions to tetrasubstituted cyclic olefin **2.29** (Figure 2.9).

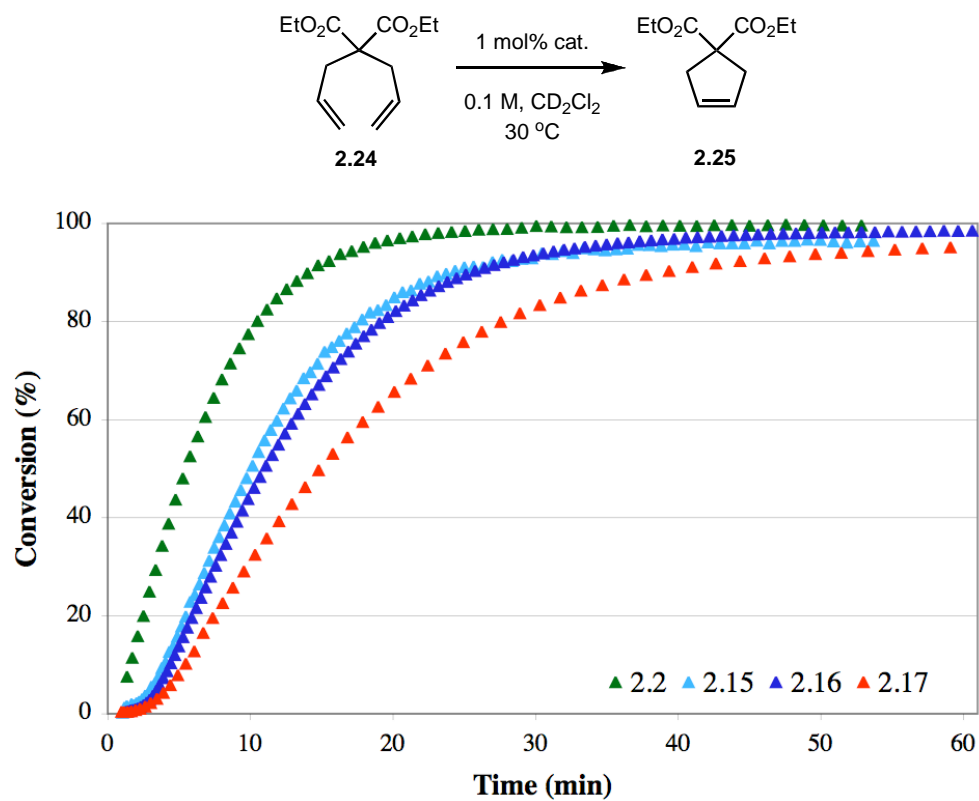


**Figure 2.7.** RCM of diene **2.24** using catalysts **2.2** and **2.15–2.17**.

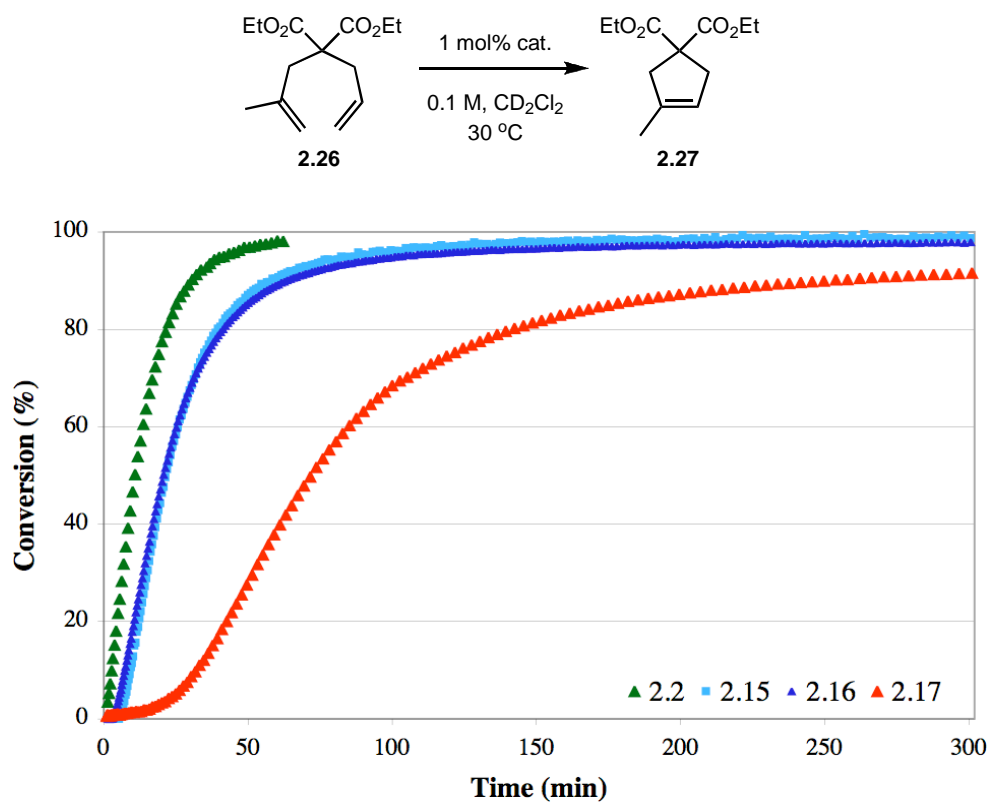


**Figure 2.8.** RCM of diene **2.26** using catalysts **2.2** and **2.15–2.17**.

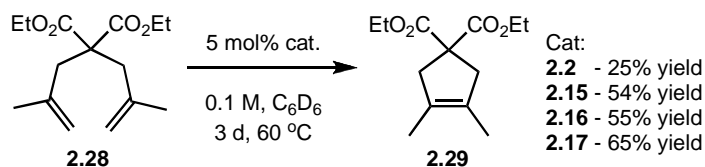


**Figure 2.9.** RCM of diene **2.28** to tetrasubstituted cycloalkene **2.29** using catalysts **2.2** and **2.15–2.17**.

Several explanations could exist to explain these contradictory results. Along with decreased initiation rate, increased backbone substitution could also alter propagation rate, stability, or a combination of both. In any case, the results indicate that the assays reported by Ritter and co-workers, while useful for evaluating the activity of new catalysts,<sup>12</sup> do not distinguish between catalysts that are both highly active<sup>15</sup> and stable.<sup>16</sup> Future improvements in, and understanding of, olefin metathesis catalysts will require a more sensitive assay to evaluate small variations in the efficiency profile accompanying subtle modification in catalyst architecture.

### Development of a ppm Level Assay

In order to study subtle differences in activity and stability, the standard RCM reactions should be observed at the lower limit of productive catalyst loading and under optimized conditions. With this in mind, new techniques were developed using a Symyx robotic system to maintain a high degree of precision and consistency when working with ultra-low catalyst loadings. Our group has recently used these robotic systems to optimize reaction conditions and investigate new applications in olefin metathesis.<sup>17</sup> Similarly, utilizing an automated Vantage system, Grela and co-workers recently reported the successful RCM of **2.24** at just 0.02 mol% **2.2**.<sup>18</sup>

A robotic assay was developed utilizing the RCM of diene **2.24** by complex **2.2**. Stock solutions of catalyst and substrate were prepared in a nitrogen-filled glovebox. While substrate stock solutions could be stored in septum-topped vials, catalyst

solutions were prepared immediately prior to use. The Symyx core module was utilized to add all solutions to reaction vessels as well as to sample the reaction mixtures at programmed time intervals. Aliquots were added into ethyl vinyl ether solution at  $-20\text{ }^{\circ}\text{C}$ ,<sup>19</sup> and then analyzed by gas chromatography with dodecane as an internal standard, measuring the change in the amounts of substrate and product with time. With minimal deviation in reaction results, 1 M (1 mL vials) and 0.1 M (20 mL vials) concentrations were employed depending on reaction scale and glassware to minimize substrate usage. The large vials were used in experiments where aliquots were withdrawn over the course of the reaction.

For practical reasons, most standard metathesis assays are performed in a closed system under inert atmosphere.<sup>12,18</sup> However, we have observed variations in reaction rate and total conversion depending on the headspace of the reaction vessel. To circumvent this problem, reactions were carried out in open vials. Additionally, in order to minimize the potential for decomposition pathways related to oxygen, all reactions were conducted in a nitrogen-filled glovebox. While ruthenium-based catalysts are relatively stable under ambient conditions, at low catalyst loadings oxygen-related decomposition becomes relevant. Control reactions were completed on a Symyx core module open to atmosphere, confirming the importance for oxygen-free reaction conditions. Other reaction considerations, including temperature and solvent, were optimized based on our recent complementary studies on the RCM of diallylamines with low catalyst loadings (chapter 3).<sup>17a</sup> A solvent screen identified toluene as the optimal solvent for RCM of these diallyl substrates (Figure 2.10).

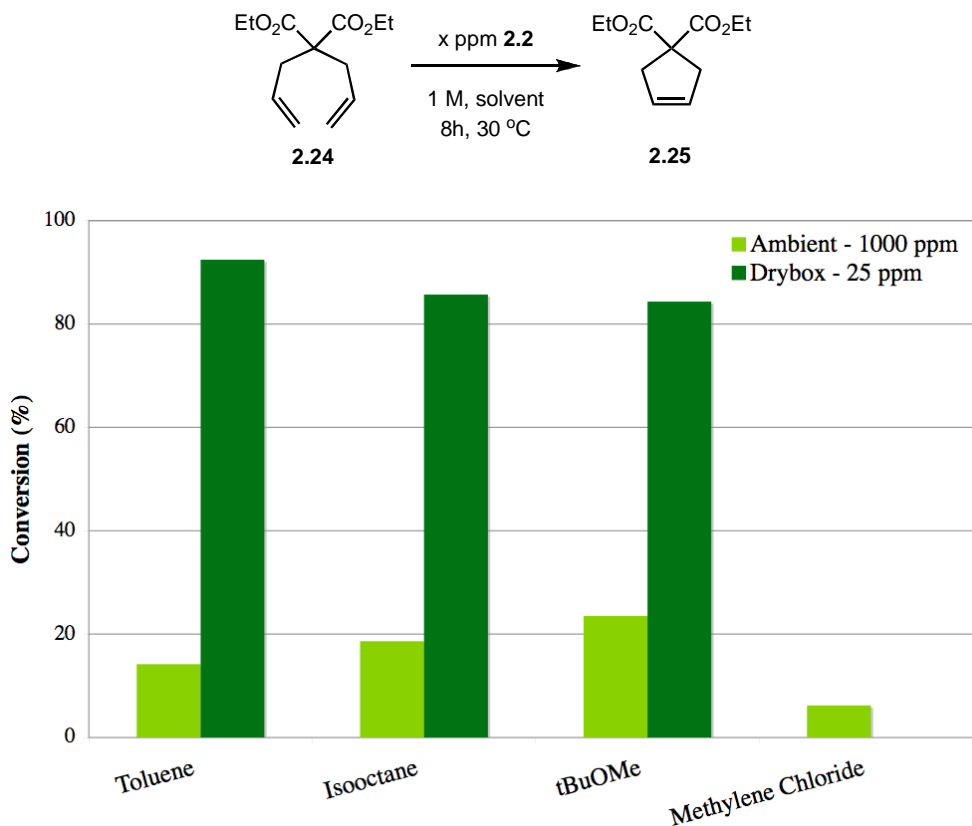


**Figure 2.10.** RCM of diene **2.24** to disubstituted cycloalkene **2.25**, using catalyst **2.2** in a variety of solvents.

Toluene as solvent also allowed for an increased temperature of 50 °C. While increased temperatures have previously been shown to increase metathesis reaction rates,<sup>18,20</sup> temperatures above 50 °C decreased assay consistency and resulted in significant solvent losses throughout the course of the reaction. The use of methylene chloride, the solvent most commonly used for RCM, resulted in considerable solvent loss even at 30 °C. Furthermore, its use resulted in decreased conversions, relative to other solvents. The RCM of **2.24** was then monitored over a variety of catalyst loadings to calibrate the new assay (Figure 2.11). Under optimized conditions (0.1 M, toluene, 50 °C), complex **2.2** afforded almost quantitative yields of **2.25** after 1 hour at just 50 ppm.

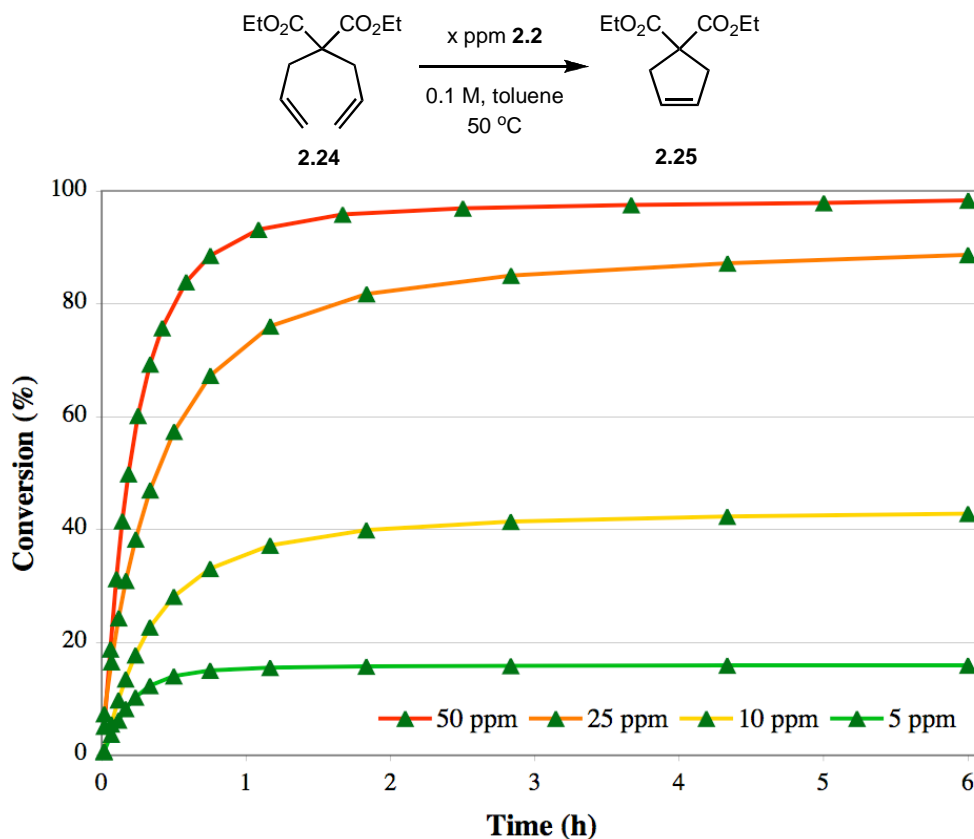


**Figure 2.11.** RCM of diene **2.24** to disubstituted cycloalkene **2.25**, using catalyst **2.2**.

Under the optimized conditions, trimethylated complex **2.17** required only 25 ppm to reach full conversion to disubstituted cycloalkene **2.25**; a catalyst loading near pharmaceutical impurity limits.<sup>8</sup> In order to directly compare the *N*-mesityl series (**2.2** and **2.15–2.17**), catalyst loadings were further decreased to 15 ppm to ensure that no reactions would reach completion before the catalyst had completely decomposed. Again, at very low catalyst loadings, increased backbone substitution resulted in higher conversions to cyclic olefin **2.25**. When conversions were monitored over the course of the reaction, the effects of backbone substitution became evident (Figure 2.12). The data suggest that the higher conversions are a direct result of longer catalyst lifetimes. However, as observed during the NMR studies, increased backbone substitution decreases catalyst reaction rate. These results were supported through observation of

the same trends when complexes **2.3** and **2.20** were studied using the same assay (Figure 2.13).<sup>21</sup>

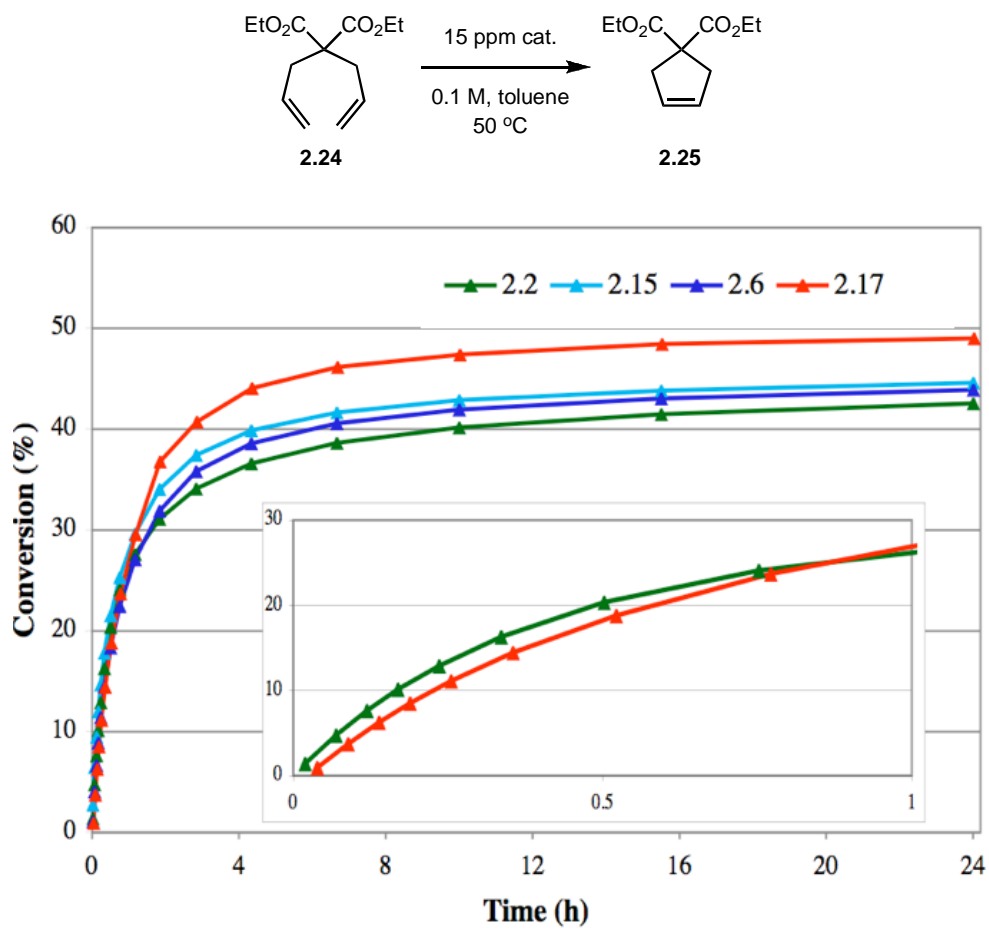


**Figure 2.12.** Plot of the RCM of diene **2.24** to disubstituted cycloalkene **2.25**, with conversion monitored over 24 h using catalysts **2.2** and **2.15–2.17**. The inset depicts a plot expansion over 1 h of the reaction.

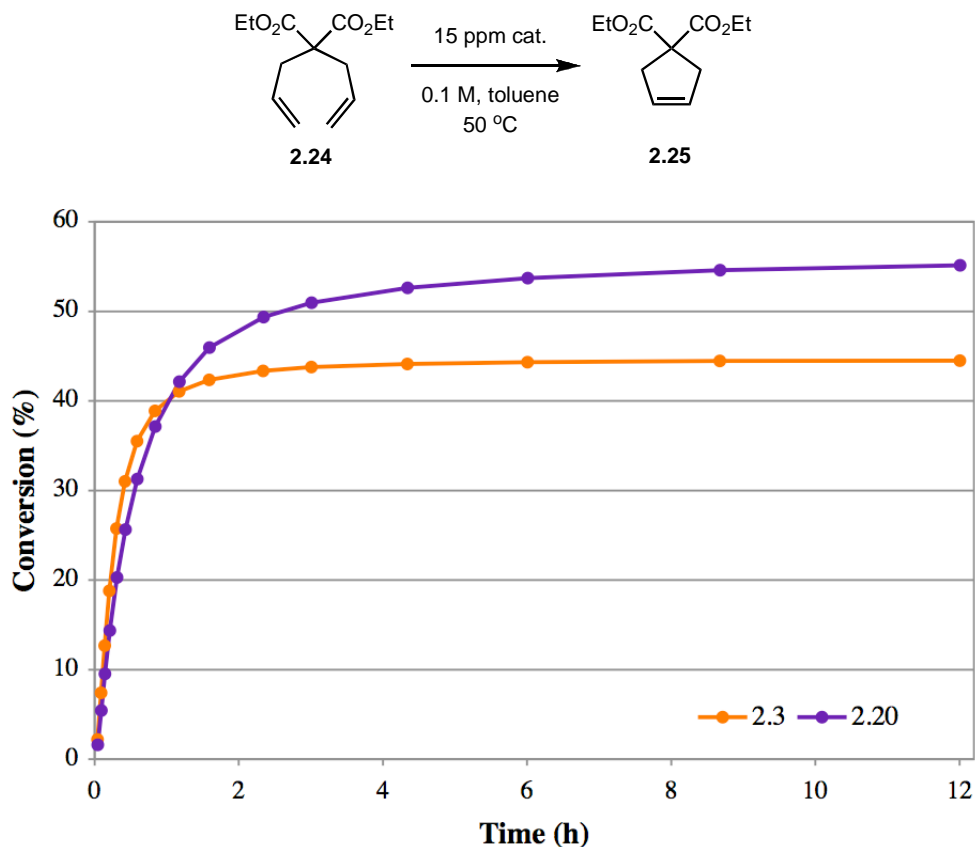


**Figure 2.13.** Plot of the RCM of diene **2.24** to disubstituted cycloalkene **2.25**, with conversion monitored over 24 h using catalysts **2.3** and **2.20**.

The catalyst efficiency assay was then expanded to study the RCM of **2.26** to give trisubstituted cycloalkene **2.27**. Calibration using the more sterically challenging substrate revealed that significantly more catalyst is necessary to effect full conversion to **2.27**, with complex **2.2** affording yields over 90% at 400 ppm catalyst loadings (Figure 2.14). The increase in required catalyst loading due to the addition of a single methyl group demonstrates the importance and effect of the olefin substrates steric environment.

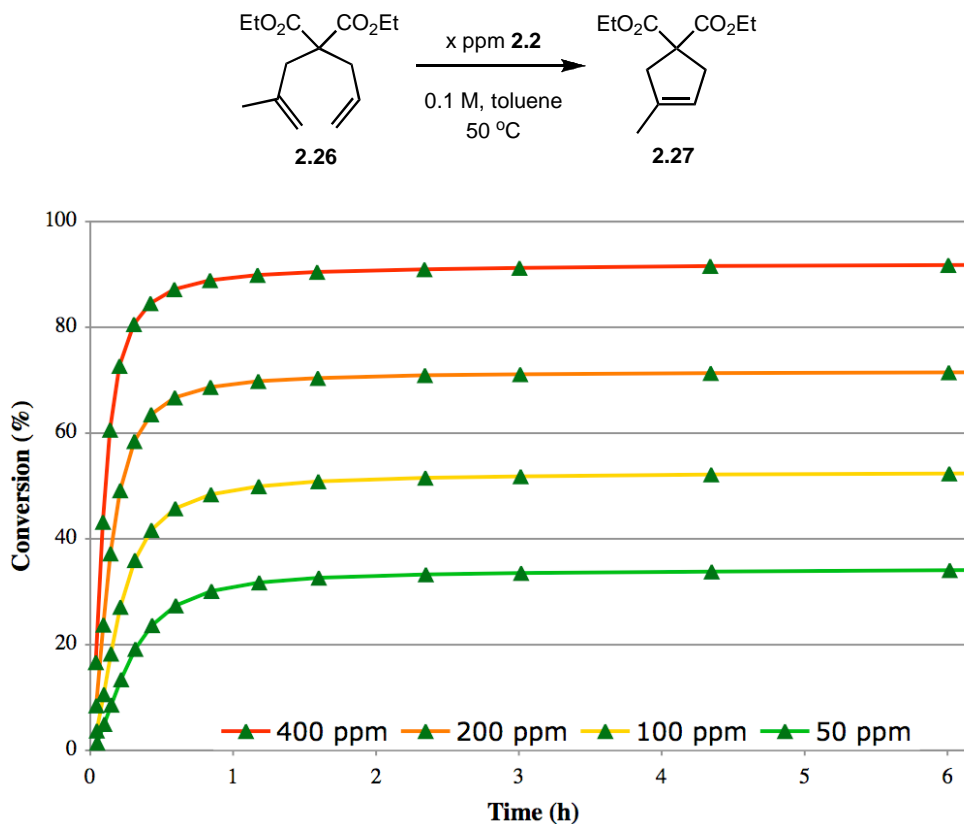


**Figure 2.14.** RCM of diene **2.26** to disubstituted cycloalkene **2.27**, using catalyst **2.2**.

Catalyst comparison reactions, performed at 200 ppm, reveal that the addition of substituents to the NHC ligands has greater impact on the efficiency of the metathesis catalysts than with the previous substrate, with **2.17** and **2.20** both outperforming their unsubstituted analogues (Figure 2.15). Notably, the RCM of **2.26** also clearly highlights the difference in stability between the *N*-mesityl (**2.2** and **2.17**) and the *N*-*o*-tolyl catalysts (**2.3** and **2.20**). For this trisubstituted olefin substrate, catalyst stability is more significant than activity for success in RCM. Complex **2.5** is the most active ruthenium-based catalyst to date, but is not particularly stable under prolonged reaction conditions. As expected, while **2.5** performs exceptionally well at standard loadings (1 mol%), it falters at low catalyst loadings.

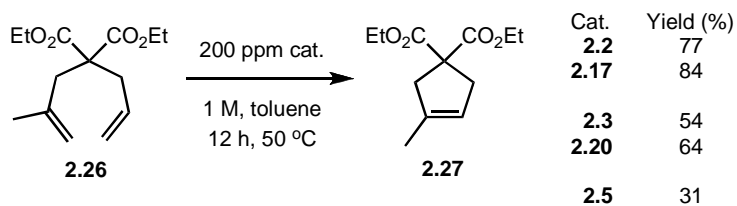


**Figure 2.15.** RCM of diene **2.26** to trisubstituted cycloalkene **2.27**, using catalysts **2.2**, **2.3**, **2.5**, **2.17**, and **2.20**.

Finally, the ring-closing metathesis of **2.28** to tetrasubstituted cycloalkene **2.29** was examined using the same catalyst assay. Continuing the trend, at 0.2 mol% loading, complex **2.17** outperforms **2.2**, yielding just 15% and 7% of the tetrasubstituted cycloalkene respectively (Figure 2.16). Despite the expected low yields, the result reaffirmed the conclusion that backbone substitution increases the stability of the resulting complex. In the case of the *N*-mesityl series, this increase in stability has not resulted in a detrimental decrease in activity.

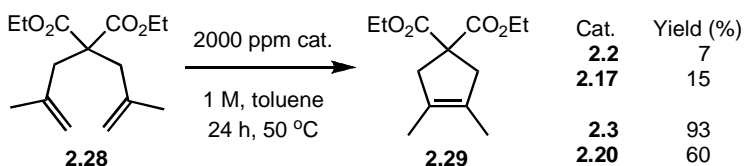


**Figure 2.16.** RCM of diene **2.28** to tetrasubstituted cycloalkene **2.29**, using catalysts **2.2**, **2.3**, **2.17**, and **2.20**.

Surprisingly, the *N*-*o*-tolyl series does not continue in the expected trend. Complexes **2.3**, and **2.20** were compared at 0.2 mol% catalyst loading (Figure 2.16), revealing complex **2.3** to be the most efficient catalyst for this tetrasubstituted olefin. To confirm this result, complexes **2.3**, **2.5**, and **2.20** were tested at a lower loading of 0.1 mol% and the reactions were monitored over time (Figure 2.17). At this loading, the effectiveness of the catalysts to complete the RCM dropped significantly, providing a reminder that more efficient catalysts still need to be developed.

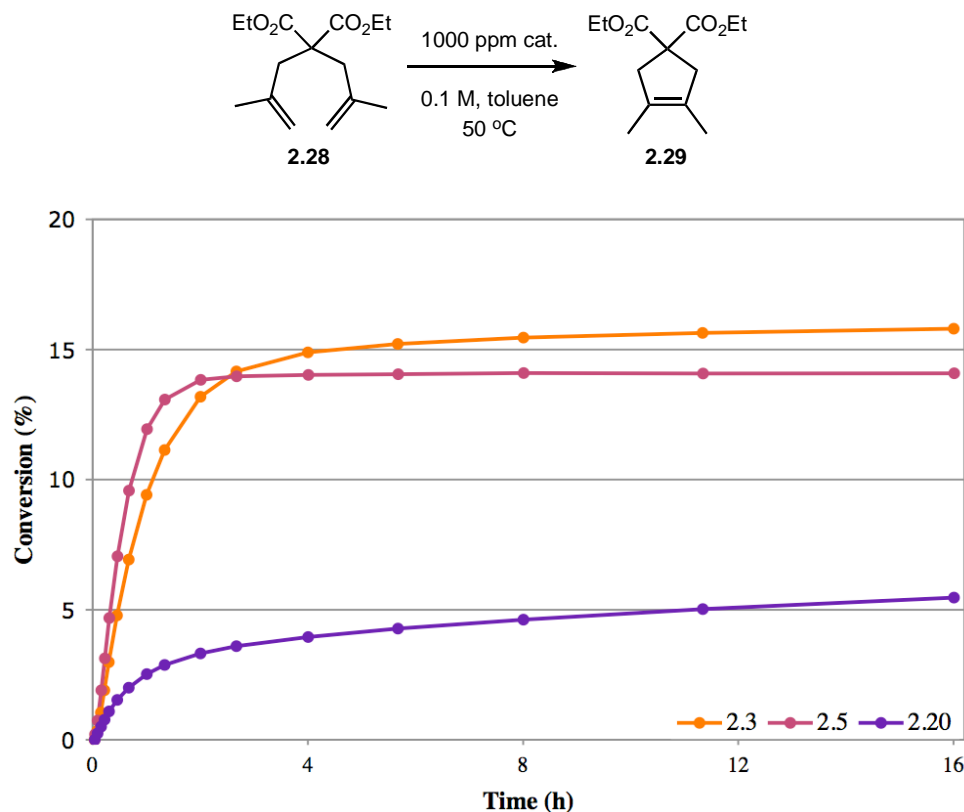


**Figure 2.17.** RCM of diene **2.28** to tetrasubstituted cycloalkene **2.29**, using catalysts **2.3**, **2.5**, and **2.20**.

Complex **2.3** outperformed both the more stable **2.20** and the more active **2.5**. At low catalyst loadings, the decreased stability of **2.5** becomes a larger factor than its increased activity. Complex **2.20** faces the opposite challenge of substantially decreased activity. The differences between **2.3**, **2.5**, and **2.20** suggest that increased activity becomes more important than, but does not negate, increased stability for the RCM of very challenging substrates. While conversions were low, the experiment gives a clear result and is a reminder that the key to catalyst efficiency is the ratio of the rate of productive olefin metathesis relative to the rate of catalyst decomposition.

### Conclusions

In summary, we describe the synthesis and characterization of a series of ruthenium-based olefin metathesis catalysts bearing NHCs with varying degrees of

backbone and aryl substitution. In order to study their subtle differences in activity and stability, a highly sensitive assay was developed to operate at the lower limit of productive catalyst loading. These techniques were developed using a Symyx robotic system to maintain a high degree of precision and consistency when working with ultra-low catalyst loadings.

The development of this highly sensitive assay has provided increased insight into the relationship between ligand architecture and efficiency. In this study, both backbone and aryl substitution were found to significantly impact catalyst stability and activity. Whereas low *N*-aryl bulk on the NHC ligands led to increased activity, it also decreased stability. Increased backbone substitution, however, led to increased catalyst lifetimes and decreased reaction rates. Furthermore, it was found that the relative importance of stability and activity on efficiency is dependent on the steric encumbrance of the RCM reaction. For substrates with low steric demands, catalyst stability is quite important for success at low catalyst loadings. For sterically encumbered substrates, catalyst activity becomes much more important than increased stability. The ability to study the relationship between small changes in ligand architecture and efficiency will allow us to better explore new opportunities in catalyst design.

## ***Experimental***

### ***General Information***

NMR spectra were recorded using a Varian Mercury 300 or Varian Inova 500 MHz spectrometer. NMR chemical shifts are reported in parts per million (ppm) downfield from tetramethylsilane (TMS) with reference to internal solvent for  $^1\text{H}$  and  $^{13}\text{C}$ . Spectra are reported as follows: chemical shift ( $\delta$  ppm), multiplicity, coupling constant (Hz), and integration. IR spectra were recorded on a Perkin-Elmer Paragon 1000

Spectrophotometer. Gas chromatography data was obtained using an Agilent 6850 FID gas chromatograph equipped with a DB-Wax Polyethylene Glycol capillary column (J&W Scientific). High-resolution mass spectroscopy (FAB) was completed at the California Institute of Technology Mass Spectrometry Facility. X-ray crystallographic structures were obtained by the Beckman Institute X-ray Crystallography Laboratory of the California Institute of Technology. Crystallographic data have been deposited at the CCDC, 12 Union Road, Cambridge CB2 1EZ, U.K., and copies can be obtained on request, free of charge, by quoting the publication citation and the deposition numbers 670930 (**2.17**) and 651007 (**2.20**).

All reactions involving metal complexes were conducted in oven-dried glassware under a nitrogen atmosphere with anhydrous and degassed solvents, using standard Schlenk and glovebox techniques. Anhydrous solvents were obtained via elution through a solvent column drying system.<sup>22</sup> Silica gel used for the purification of organometallic complexes was obtained from TSI Scientific, Cambridge, MA (60 Å, pH 6.5–7.0).  $\text{RuCl}_2(\text{PCy}_3)(=\text{CH}-o\text{-O}i\text{PrC}_6\text{H}_4)$ , **2.2**, and **2.3** were obtained from Materia, Inc. Unless otherwise indicated, all compounds were purchased from Aldrich or Fisher and used as obtained. The compounds **2.6**,<sup>13a</sup> **2.7**,<sup>13b</sup> **2.12**,<sup>13b</sup> **2.21**,<sup>14</sup> **2.24-2.29**,<sup>12</sup> have been described previously and were prepared according to literature procedures or identified by comparison of their spectroscopic data. The initial screening of the catalysts, in RCM via  $^1\text{H}$  NMR spectroscopy was conducted according to literature procedures.<sup>12</sup>

### ***Low ppm Level Assays***

Experiments on the RCM of **2.24**, **2.26**, and **2.28** using the catalysts described were conducted using a Symyx Technologies Core Module (Santa Clara, CA) housed in a Braun nitrogen-filled glovebox and equipped with Julabo LH45 and LH85 temperature-control units for separate positions of the robot tabletop.

For experiments where aliquots were not taken during the course of the reaction, up to 576 reactions (6×96 well plates) could be performed simultaneously in 1 mL vials by an Epoch software-based protocol as follows. To prepare catalyst stock solutions (0.25 mM), 20 mL glass scintillation vials were charged with catalyst (5  $\mu$ mole) and diluted to 20.0 mL total volume in THF. Catalyst solutions, 6 to 800  $\mu$ L depending on desired final catalyst loading, were transferred to reaction vials and solvent was removed via centrifugal evaporation. The catalysts were preheated to the desired temperature using the LH45 unit, and stirring was started. Substrates (0.1 mmol), containing dodecane (0.025 mmol) as an internal standard, were dispensed simultaneously to 4 reactions at a time using one arm of the robot equipped with a 4-needle assembly. Immediately following substrate addition, solvent was added to reach the desired reaction molarity, generally 1 M. All reactions were quenched by injection of 0.1 mL 5% v/v ethyl vinyl ether in toluene at a preprogrammed time. Samples were then analyzed by gas chromatography

Alternatively, where aliquots were taken during the course of the reaction, the entire operation was performed on 12 reactions simultaneously (4 catalyst loadings in triplicate or 2 catalysts at 3 catalyst loadings in duplicate) by an Epoch software-based protocol as follows. To prepare catalyst stock solutions (1.0 mM), 20 mL glass scintillation vials were charged with catalyst (5  $\mu$ mole) and diluted to 5.0 mL total volume in toluene. Catalyst solutions, 10 to 400  $\mu$ L depending on desired final catalyst loading, were transferred to glass 20 mL scintillation vials each capped with a septum having a 3 mm hole for the purpose of needle access, and were diluted to 10 mL total volume in toluene. The catalysts were preheated to 50.0  $^{\circ}$ C using the LH45 unit and stirred. Substrates (1 mmol), containing dodecane (0.25 mmol) as an internal standard, were dispensed simultaneously to 4 reactions at a time using one arm of the robot equipped with a 4-needle assembly. After the 2 minutes required for completion of the transfer, 50

$\mu\text{L}$  aliquots of each reaction were withdrawn using the other robot arm and dispensed to 1.2 mL septa-covered vials containing 5% v/v ethyl vinyl ether in toluene cooled to  $-20\text{ }^{\circ}\text{C}$  in two 96-well plates. The needle was flushed and washed between dispenses to prevent transfer of the quenching solution into the reaction vials. 16 time points were sampled at preprogrammed intervals and the exact times were recorded by the Epoch protocol. Samples were then analyzed by gas chromatography.

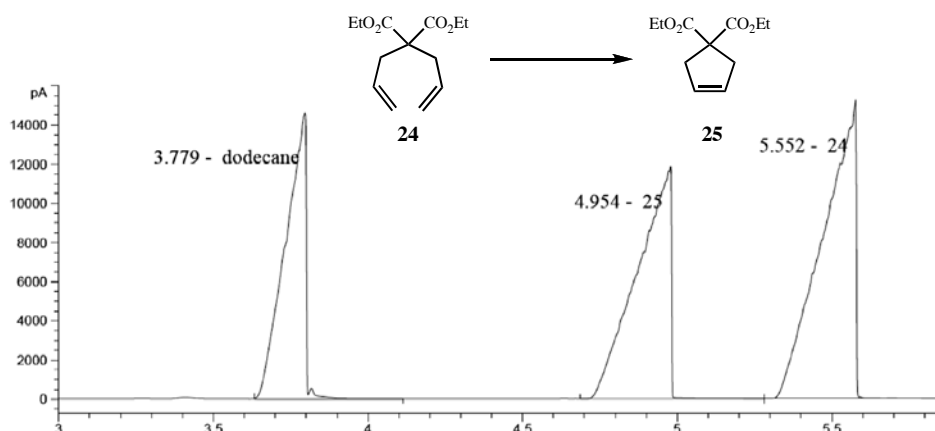
### GC Data Analysis

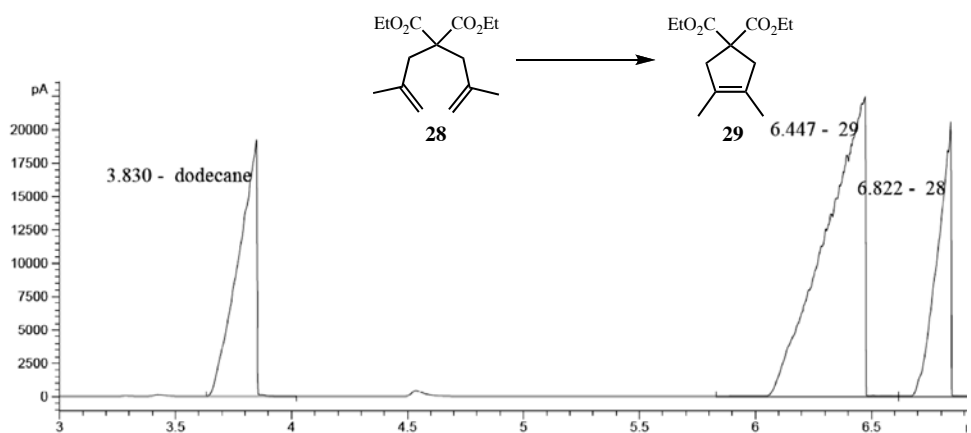
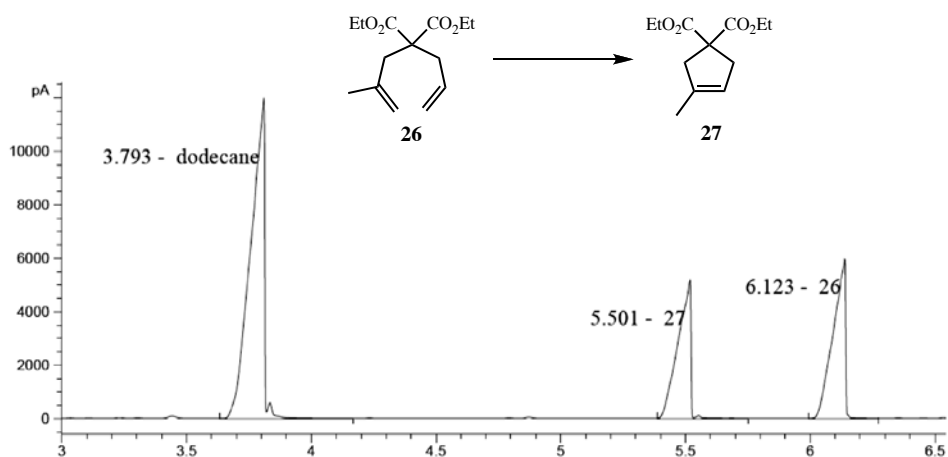
Samples were analyzed by gas chromatography with dodecane as an internal standard, measuring the change in the amounts of substrate and product with time. To obtain accurate conversion data, GC response factors were obtained for all starting materials and products.<sup>12</sup>

Relevant instrument conditions: Inlet temperature =  $250\text{ }^{\circ}\text{C}$ ; detector temperature =  $250\text{ }^{\circ}\text{C}$ ; hydrogen flow =  $32\text{ mL/min}$ ; air flow =  $400\text{ mL/min}$ ; constant col + makeup flow =  $30\text{ mL/min}$ .

GC Method:  $85\text{ }^{\circ}\text{C}$  for 1.5 minutes, followed by a temperature increase of  $15\text{ }^{\circ}\text{C/min}$  to  $160\text{ }^{\circ}\text{C}$ , followed by a temperature increase of  $80\text{ }^{\circ}\text{C/min}$  to  $200\text{ }^{\circ}\text{C}$  and a subsequent isothermal period at  $210\text{ }^{\circ}\text{C}$  for one minute (total run time = 8 minutes).

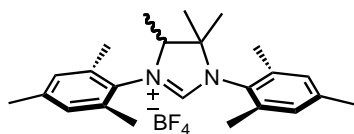
### Representative GC Traces





## Syntheses

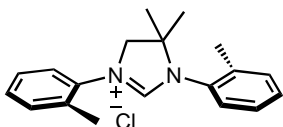
### 1,3-dimesityl-4,4,5-trimethyl-imidazolium tetrafluoroborate (**2.8**)



A solution of the diimine **2.12** (2.00 g, 6.24 mmol) in dry benzene was placed in a flask equipped with a reflux condenser, to it was added a solution of methylmagnesium chloride in tetrahydrofuran (3.0 M, 8.3 ml, 24.96 mmol). The resulting solution was stirred at refluxing temperature for one day. The solvents were removed under vacuum, the residue was dissolved in diethyl ether and treated lithium aluminium hydride (120 mg, 3.1 mmol). After workup and purification by flash column chromatography, the diamine was obtained as a white solid in 69% yield. A mixture of diamine (1.62 g, 4.78

mmol), ammonium tetrafluoroborate (0.75 g, 7.17 mmol), and triethyl orthoformate (12 ml) was stirred at 120 °C for 10 min and cooled to room temperature. The precipitation was collected by filtration, and the solid was redissolved in CH<sub>2</sub>Cl<sub>2</sub>. After the insoluble material was filtered off, the filtrate was evaporated under vacuum, and the residue was recrystallized in ethyl acetate to give **2.8** as a white solid (543 mg, 1.24 mmol, Y = 26%).  
<sup>1</sup>H NMR (300 MHz, DMSO-*d*<sub>6</sub>): δ 9.00 (s, 1H), 7.13 (s, 2H), 7.11 (s, 2H), 4.71 (q, J = 6.9 Hz, 1H), 2.34-2.29 (m, 18H), 1.52 (s, 3H), 1.36 (s, 3H), 1.19 (d, J = 6.9 Hz, 3H). <sup>13</sup>C NMR (75 MHz, DMSO-*d*<sub>6</sub>): δ 159.0, 139.7, 137.5, 136.9, 136.0, 135.8, 130.2, 130.1, 129.8, 129.2, 128.3, 73.5, 67.7, 26.3, 20.5, 20.5, 19.3, 19.1, 18.2, 17.9, 11.9. <sup>19</sup>F NMR (282 MHz, DMSO-*d*<sub>6</sub>): δ -148.7. HRMS calculated for C<sub>24</sub>H<sub>33</sub>N<sub>2</sub>: 349.2644. Found: 349.2648.

### 1,3-Ditolyl-4,4-Dimethyl-imidazolinium chloride (**2.9**)

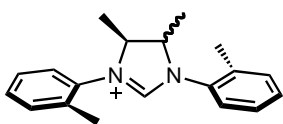


To a THF solution (40 mL) of the formamidine (1 equiv) at -78 °C was added a solution of *n*-BuLi in hexanes (1 equiv). The mixture was stirred for 30 minutes, then was allowed to warm to room temperature and stirred for a further 12 hours. The mixture was again cooled to -78 °C, and 3-bromopropene (1 equiv) or 3-bromo-2-methylpropene (1 equiv) was slowly added. The mixture was stirred for 30 minutes at -78 °C then heated at 50 °C for 12 hours. Removal of the volatiles under vacuum and extraction with hexanes afforded the corresponding alkylated derivative.

An oven-dried, argon-flushed, sealable Schlenk tube with a Teflon stopcock was loaded with the alkylated derivative (1 equiv), toluene and was cooled to 0 °C, at which point was added a solution of HCl in Et<sub>2</sub>O (2.0 M, 1 equiv). Precipitation of a white powder was immediately observed. After 15 minutes at 0 °C the mixture was left to warm to r.t.

and stirred for an additional 15 minutes. The mixture was heated at 110 °C for 24 hours, after which time the volatiles were removed under vacuum and the resulting salt washed with toluene and ether to afford salt **2.9** (overall yield = 77%). <sup>1</sup>H NMR (300 MHz, CDCl<sub>3</sub>): δ 9.00 (s, 1H), 7.86 (d, J = 7.2 Hz, 1H), 7.60 (d, J = 7.8 Hz, 1H), 7.37-7.15 (m, 6H), 4.32 (s, 2H), 2.42 (s, 3H), 2.40 (s, 3H), 1.62 (s, 6H). <sup>13</sup>C NMR (75 MHz, CDCl<sub>3</sub>): 157.8, 136.2, 134.6, 133.6, 131.9, 131.7, 131.1, 130.6, 130.1, 130.0, 128.0, 127.3.0, 127.1, 69.8, 64.6, 26.4, 18.8, 18.3.

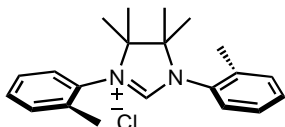
### 1,3-Ditolyl-4,5-Dimethyl-imidazolinium chloride (**2.10**)



A mixture of 2,3-butanedione (2.00 g, 23.23 mmol), *o*-toluidine (5.00 g, 46.66 mmol), and ethanol (ca. 2 ml) was stirred at room temperature for 1 day. The yellow crystalline solid was collected by filtration and rinsed with a small amount of ethanol to yield 3.42 g (12.97 mmol, Y = 56%) of the desired diimine. After reduction, the diamine was obtained as a mixture of isomers. A diethyl ether solution of the diamine was treated with a solution of hydrogen chloride (2 equiv) to precipitate the diamine hydrochloride salt. The white solid was collected by filtration and washed with copious amount of diethyl ether. The solid was placed in a flask and triethyl orthoformate (large excess) was added. The resulting mixture was stirred at 130 °C for 5 to 10 min then cooled. After cooling to room temperature, the white solid was collected by filtration washing with large amount of diethyl ether and then with acetone to give the desired imidazolidinium chloride salt **2.10**. <sup>1</sup>H NMR (300 MHz, CDCl<sub>3</sub>): δ 9.04 (s, 0.3H, *trans*), 8.45 (s, 0.7H, *cis*), 8.00-7.93 (m, 2H), 7.39-7.25 (m, 6H), 5.54 (m, 1.4H, *cis*), 4.64 (m, 0.6H, *trans*), 2.47 (s, 4.2H, *cis*), 2.45 (s, 1.8H, *trans*), 1.53 (d, J = 6.0 Hz, 1.8H, *trans*), 1.32 (d, J = 5.7 Hz, 4.2H, *cis*). <sup>13</sup>C NMR (75 MHz, CDCl<sub>3</sub>): δ 157.2 (*trans*), 156.2 (*cis*), 134.4 (*cis*), 134.3 (*trans*), 132.8 (*cis*),

132.6 (*trans*), 131.7 (*trans*), 131.6 (*cis*), 130.0 (*trans*), 129.8 (*cis*), 127.9 (*trans*), 127.6 (*cis*), 127.55 (*trans*), 127.5 (*cis*), 66.9 (*trans*), 62.8 (*cis*), 18.3 (*cis*), 18.2 (*trans*), 17.6 (*trans*), 12.5 (*cis*). HRMS Calculated for  $C_{19}H_{23}N_2$ : 279.1861. Found: 279.1853.

### 1,3-Ditolyl-4,4,5,5-Tetramethyl-imidazolinium chloride (2.11)



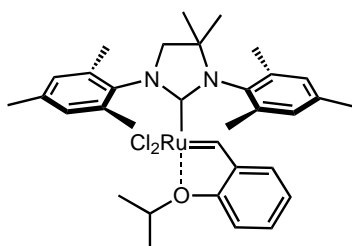
A solution of the diimine (3.00 g, 11.35 mmol) in dry benzene was placed in a flask equipped with a reflux condenser, and to it was added a solution of methylmagnesium chloride in tetrahydrofuran (3.0 M, 11.3 ml, 45.4 mmol). The resulting solution was stirred at refluxing temperature overnight. After being cooled to room temperature, a saturated aqueous solution of ammonium chloride was slowly added to the reaction mixture. The organic layer was separated and the aqueous layer was extracted with ethyl acetate three times. The combined organic layer was washed with brine, dried over magnesium sulfate, and purified by flash chromatography on silica (eluent: hexanes/ethyl acetate = 30/1) to yield the desired diamine as a yellow oil (2.25 g, 7.60 mmol, Y = 67%). The diamine was dissolved in diethyl ether (10 ml) and treated with a solution of hydrogen chloride (4 M in dioxane) to precipitate the diamine hydrochloride salt. The solid was collected by filtration and rinsed with an ample amount of diethyl ether then with acetone to give the desired amine salt as a white powder (2.19 g, 5.93 mmol, Y = 78%). A mixture of the diamine salt (330 mg, 0.89 mmol) and triethyl orthoformate (1.5 ml) was placed in a vial and stirred at 120 °C for 18 hours. After being cooled to room temperature, the tan colored solid was collected by filtration and washed with diethyl ether. (11, 64 mg, 0.187 mmol, Y = 21%).  $^1H$  NMR (300 MHz,  $CDCl_3$ ):  $\delta$  9.38 (br s, 1H), 7.58 (deformed d, 2H), 7.40-7.30 (m, 6H), 2.47 (s, 6H), 1.50 (s, 12H).  $^{13}C$  NMR (75 MHz,  $CDCl_3$ ):  $\delta$  157.9, 136.3, 131.8, 131.3, 130.4, 130.4, 127.2, 74.0, 21.6, 18.8. HRMS Calculated for  $C_{21}H_{27}N_2$ : 307.2174. Found: 307.2162.

### General procedure for the preparation of catalysts 2.15-2.20:

To a solution of imidazolium salt in toluene (or benzene) was added KHMDS, and the resulting solution was stirred at room temperature for a few minutes.  $\text{RuCl}_2(\text{PCy}_3)(=\text{CH}-o\text{-O}i\text{PrC}_6\text{H}_4)$  was then added, and the mixture was stirred for the designated time and temperature (*vide infra*). After cooling to room temperature, the mixture was purified by column chromatography on TSI silica (eluent: hexane/ether = 2/1  $\rightarrow$  1/1) to give the compounds as green solids.

### $\text{RuCl}_2(4,4\text{-dimethyl-1,3-dimesitylimidazolin-2-ylidene})(=\text{CH}-o\text{-O}i\text{PrC}_6\text{H}_4)$ (2.15).

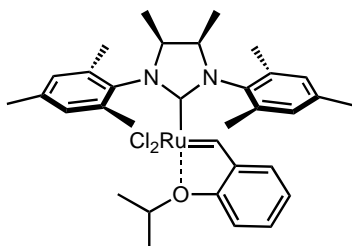
**2.6** (200 mg, 0.54 mmol), potassium hexamethyldisilazide (140 mg, 0.70 mmol), and



$\text{RuCl}_2(\text{PCy}_3)(=\text{CH}-o\text{-O}i\text{PrC}_6\text{H}_4)$  (250 mg, 0.42 mmol) were reacted according to the general procedure (stirred for 2 hours at 70 °C) to give the desired ruthenium complex **2.15** as a green powder (135 mg, 0.21 mmol, 49%).

$^1\text{H}$  NMR (500 MHz,  $\text{CD}_2\text{Cl}_2$ , 25 °C):  $\delta$  16.46 (br s, 1H), 7.55 (ddd,  $J = 8.3$  Hz,  $J = 2.0$  Hz, 1H), 7.10 (br s, 2H), 7.05 (br s, 2H), 6.95 (dd,  $J = 7.5$  Hz,  $J = 2.0$  Hz, 1H), 6.91 (t,  $J = 7.5$  Hz, 1H), 6.82 (d,  $J = 8.0$  Hz, 1H), 4.86 (sept,  $J = 6.1$  Hz, 1H), 3.93 (s, 2H), 2.50-2.25 (m, 18H), 1.47 (s, 6H), 1.21 (d,  $J = 6.1$  Hz, 6H).  $^{13}\text{C}$  NMR (125 MHz,  $\text{C}_6\text{D}_6$ ):  $\delta$  293.3 (m), 213.3, 153.0, 146.4, 141.3, 139.0, 138.6, 130.7, 130.0, 129.3, 122.7, 122.5, 113.6, 75.4, 68.2 (br), 65.6 (br), 28.1, 21.8, 21.5, 21.4. HRMS Calculated for  $\text{C}_{33}\text{H}_{42}\text{Cl}_2\text{N}_2\text{ORu}$ : 654.1718. Found: 654.1725.

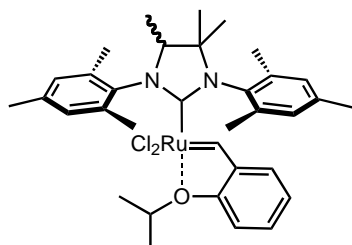
**RuCl<sub>2</sub>(1,3-dimesityl-4,5-dimethyl-imidazolin-2-ylidene)(=CH-*o*-O*Pr*C<sub>6</sub>H<sub>4</sub>) (2.16).**



**2.7** (100 mg, 0.27 mmol), KHMDS (70 mg, 0.35 mmol), and RuCl<sub>2</sub>(PCy<sub>3</sub>)(=CH-*o*-O*Pr*C<sub>6</sub>H<sub>4</sub>) (100 mg, 0.17 mmol) were reacted according to the general procedure (stirred for 2 hours at 70 °C) to give the desired ruthenium complex **2.16**

as a green powder (60 mg, 0.092 mmol, 54%). <sup>1</sup>H NMR (500 MHz, C<sub>6</sub>D<sub>6</sub>, 25 °C): δ 16.74 (s, 1H), 7.14 (dd, J = 7.5 Hz, J = 1.5 Hz, 1H), 7.11 (ddd, J = 7.5 Hz, J = 1.5 Hz, 1H), 7.00 (br s, 4H), 6.65 (dt, J = 7.5 Hz, J = 1.0 Hz, 1H), 6.32 (d, J = 8.0 Hz, 1H), 4.49 (sept, J = 6.1 Hz, 1H), 4.12 (s, 2H), 3.00-2.30 (br s, 12H), 2.25 (s, 6H), 1.31 (br s, 6H), 0.81 (d, J = 6.5 Hz, 6H). <sup>13</sup>C NMR (125 MHz, C<sub>6</sub>D<sub>6</sub>): δ 293.8, 213.4, 153.0, 146.4, 140.7, 138.7, 130.2, 129.9, 128.8, 122.8, 122.5, 113.6, 75.3, 62.4 (br), 21.8, 21.4, 13.9 (br). HRMS Calculated for C<sub>33</sub>H<sub>42</sub>Cl<sub>2</sub>N<sub>2</sub>ORu: 654.1718. Found: 654.1738.

**RuCl<sub>2</sub>(1,3-dimesityl-4,4,5-trimethyl-imidazolin-2-ylidene)(=CH-*o*-O*Pr*C<sub>6</sub>H<sub>4</sub>) (2.17).**

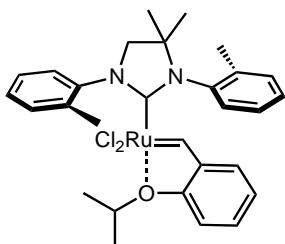


**2.8** (200 mg, 0.46 mmol), KHMDS (120 mg, 0.60 mmol), and RuCl<sub>2</sub>(PCy<sub>3</sub>)(=CH-*o*-O*Pr*C<sub>6</sub>H<sub>4</sub>) (200 mg, 0.33 mmol) were reacted according to the general procedure (stirred for 2.5 hrs at room temperature and 4 hrs at 60 °C) to give the

desired ruthenium complex **2.17** as a green powder (97 mg, 0.15 mmol, 44%). Crystals suitable for X-ray crystallography were grown at room temperature by slow diffusion of pentane into a solution of **2.17** in benzene. <sup>1</sup>H NMR (500 MHz, C<sub>6</sub>D<sub>6</sub>, 25 °C): δ 16.65 (br s, 1H), 7.13-7.07 (m, 3H), 6.94 (br m, 3H), 6.63 (td, J = 7.6, 0.8 Hz, 1H), 6.31 (d, J = 8.0 Hz, 1H), 4.46 (sept, J = 6.1 Hz, 1H), 4.20 (br s, 1H), 2.85-2.47 (m, 12H), 2.24 (s, 3H), 2.21 (s, 3H), 1.28 (d, J = 6.1 Hz, 6H), 1.15 (br s, 3H), 0.88 (br s, 3H), 0.69 (br d, J = 6.9 Hz, 3H). <sup>13</sup>C NMR (125 MHz, C<sub>6</sub>D<sub>6</sub>): δ 293.8 (m), 213.4 (br), 152.9, 146.5, 140.7, 138.7,

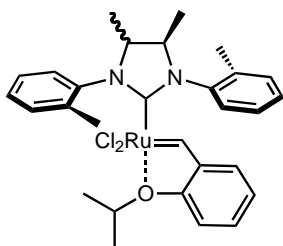
138.6, 130.9, 130.6, 130.3, 129.4, 122.7, 122.4, 113.6, 75.3, 71.0 (br), 68.4 (br), 25.1, 23.1 (br), 21.8, 21.5, 21.4, 12.1. HRMS Calculated for  $C_{34}H_{44}Cl_2N_2ORu$ : 668.1875. Found: 668.1898.

**$RuCl_2(1,3\text{-ditolyl-4,4-dimethyl-imidazolin-2-ylidene})(=CH\text{-}o\text{-}O\text{-}iPrC_6H_4)$  (**2.18**).**



**2.9** (190 mg, 0.60 mmol), KHMDS (157 mg, 0.78 mmol), and  $RuCl_2(PCy_3)(=CH\text{-}o\text{-}O\text{-}iPrC_6H_4)$  (200 mg, 0.33 mmol) were reacted according to the general procedure (stirred for 2 hours at 70 °C) to give the desired ruthenium complex **2.18** as a green powder (112 mg, 0.19 mmol, 57%).  $^1H$  NMR (500 MHz,  $CD_2Cl_2$ , 25 °C):  $\delta$  16.41 (br s, 0.40H), 16.24 (br s, 0.60H), 8.59 (br s, 1.20H), 8.59 (br s, 0.80H), 7.60-7.20 (m, 7H), 6.88-6.81 (m, 3H), 4.91 (m, 1H), 4.40-3.60 (m, 2H), 2.62-2.40 (m, 6H), 1.64-1.07 (m, 12H).  $^{13}C$  NMR (125 MHz,  $CD_2Cl_2$ ):  $\delta$  232.5, 152.2, 144.3, 141.9, 138.6, 134.3, 132.5, 131.4, 129.9, 129.5, 129.2, 128.9, 128.8, 127.6, 126.9, 122.3, 122.0, 121.8, 112.9, 74.8, 68.1, 66.6, 29.7, 27.3, 27.0, 26.9, 26.3, 24.6, 23.9, 21.5, 19.5. HRMS Calculated for  $C_{29}H_{34}Cl_2N_2ORu$ : 598.1092. Found: 598.1064.

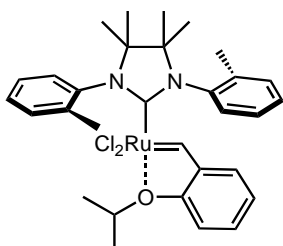
**$RuCl_2(1,3\text{-ditolyl-4,5-dimethyl-imidazolin-2-ylidene})(=CH\text{-}o\text{-}O\text{-}iPrC_6H_4)$  (**2.19**).**



**2.10** (100 mg, 0.32 mmol), potassium hexamethyldisilazide (70 mg, 0.35 mmol), and  $RuCl_2(PCy_3)(=CH\text{-}o\text{-}O\text{-}iPrC_6H_4)$  (100 mg, 0.17 mmol) were reacted according to the general procedure (stirred for 2 hours at 70 °C) to give the desired ruthenium complex **2.19** as a green powder (39 mg, 0.065 mmol, 38%).  $^1H$  NMR (500 MHz,  $C_6D_6$ , 25 °C):  $\delta$  16.64-16.41 (m, 1H), 9.00 (br s, 2H), 7.11-6.71 (m, 8H), 6.65 (m, 1H), 6.42 (t,  $J$  = 7.8 Hz, 1H), 4.57 (sept,  $J$  = 6.4 Hz, 1H), 4.29-3.55 (m, 2H), 2.65-2.25 (m, 6H), 1.20-

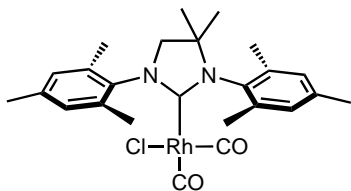
1.60 (m, 6H), 1.05-0.60 (m, 6H).  $^{13}\text{C}$  NMR (125 MHz,  $\text{C}_6\text{D}_6$ ):  $\delta$  291.7, 290.9, 232.5, 210.74, 152.8, 144.2, 140.0, 139.6, 138.6, 137.4, 132.4, 132.2, 131.5, 131.3, 130.6, 130.3, 121.9, 121.8, 113.0, 112.8, 74.4, 61.1, 61.0, 60.4, 21.7, 21.6, 13.2, 12.9. HRMS Calculated for  $\text{C}_{29}\text{H}_{34}\text{Cl}_2\text{N}_2\text{ORu}$ : 598.1092. Found: 598.1097.

**$\text{RuCl}_2(1,3\text{-ditolyl-4,4,5,5\text{-tetramethyl-imidazolin-2-ylidene})(=\text{CH-}o\text{-O/PrC}_6\text{H}_4)$  (**2.20**).**



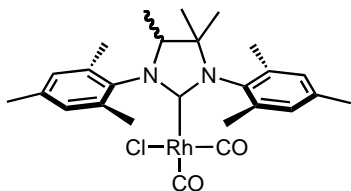
**2.11** (41 mg, 0.12 mmol), potassium hexamethyldisilazide (24 mg, 0.12 mmol), and  $\text{RuCl}_2(\text{PCy}_3)(=\text{CH-}o\text{-O/PrC}_6\text{H}_4)$  (60 mg, 0.1 mmol) were reacted according to the general procedure described above to give the desired ruthenium complex **2.20** as a green powder as a ca. 3:1 mixture of isomers (45 mg, 0.072 mmol, 72%). Crystals suitable for X-ray crystallography were grown at room temperature by slow diffusion of pentane into a solution of **2.20** in benzene.  $^1\text{H}$  NMR (500 MHz,  $\text{C}_6\text{D}_6$ ):  $\delta$  16.64 (s, 0.75H), 16.33 (s, 0.25H), 8.89 (d,  $J = 7.7$  Hz, 0.75H), 8.84 (d,  $J = 7.9$  Hz, 0.25H), 7.43-7.25 (m, 4H), 7.20-7.05 (m, 4H), 6.99-6.94 (m, 1H), 6.70-6.62 (m, 1H), 6.34 (d,  $J = 8.3$  Hz, 1H), 4.45 (sept,  $J = 6.1$  Hz, 1H), 2.74 (s, 0.75H), 2.68 (s, 2.25H), 2.47 (s, 0.75H), 2.44 (s, 2.25H), 1.38-1.20 (m, 10H), 1.04 (s, 2H), 0.76-0.70 (m, 6H).  $^{13}\text{C}$  NMR (125 MHz,  $\text{C}_6\text{D}_6$ ):  $\delta$  214.0, 211.5, 153.1, 153.0, 145.8, 143.3, 143.2, 141.6, 140.8, 140.3, 139.8, 137.3, 136.5, 136.0, 134.7, 134.4, 132.3, 132.2, 131.9, 129.6, 129.5, 129.4, 129.1, 128.9, 127.6, 127.3, 126.9, 126.6, 122.7, 122.6, 122.6, 122.5, 113.5, 75.2, 75.1, 72.3, 71.8, 71.7, 71.4, 24.9, 24.3, 24.1, 23.9, 22.7, 22.5, 22.4, 22.2, 22.1, 22.0, 20.3, 20.1, 19.7, 19.4, 19.3. HRMS Calculated for  $\text{C}_{31}\text{H}_{38}\text{Cl}_2\text{N}_2\text{ORu}$ : 626.1405. Found: 626.1427.

**RhCl(CO)<sub>2</sub>(4,4-dimethyl-1,3-dimesityl-imidazolin-2-ylidene) (2.22)**



The imidazolidinium salt **2.6** (40 mg, 0.10 mmol), KHMDS (22 mg, 0.11 mmol), and toluene (2 mL) was stirred at room temperature under N<sub>2</sub> for 5 min, and added to a suspension of [RhCl(COD)]<sub>2</sub> (25 mg, 0.05 mmol) in toluene (1 mL). The resulting mixture was stirred at room temperature for 1 hour, and then the solvent was removed under vacuum. The residue was purified by column chromatography on TSI silica (eluent: 2% EtOH in CH<sub>2</sub>Cl<sub>2</sub>) to give [(NHC)RhCl(COD)] as a yellow powder. A solution of the prepared complex in CH<sub>2</sub>Cl<sub>2</sub> (3 mL) was bubbled with CO for 1 hour. The mixture was then concentrated under vacuum and the residue was washed with dry hexane (2 mL × 3). The resulting solid was dried under vacuum to give **2.22** (38 mg, 0.071 mmol, Y = 71% two steps). <sup>1</sup>H NMR (300 MHz, CD<sub>2</sub>Cl<sub>2</sub>): δ 7.01 (s, 2H), 6.97 (s, 2H), 3.74 (s, 2H), 2.43 (s, 12H), 2.33 (s, 6H), 1.41 (s, 6H). <sup>13</sup>C NMR (125 MHz, CD<sub>2</sub>Cl<sub>2</sub>): δ 205.6 (*J*<sub>C-Rh</sub> = 41 Hz), 185.7 (*J*<sub>C-Rh</sub> = 53 Hz), 183.4 (*J*<sub>C-Rh</sub> = 75 Hz), 138.6, 138.3, 135.5, 132.8, 130.0, 129.7, 69.7, 69.7, 65.0, 25.0, 21.4, 21.0, 20.9, 18.8. IR (CD<sub>2</sub>Cl<sub>2</sub>): 2079, 1995 cm<sup>-1</sup>. HRMS Calculated for C<sub>25</sub>H<sub>29</sub>ClN<sub>2</sub>O<sub>2</sub>Rh: 527.0973. Found: 527.0960.

**RhCl(CO)<sub>2</sub>(1,3-dimesityl-4,4,5-trimethyl-imidazolin-2-ylidene) (2.23).**



The imidazolidinium **2.8** (46 mg, 0.10 mmol) was treated as described above to give **2.23** (36 mg, 0.066 mmol, Y = 66% two steps). IR (CD<sub>2</sub>Cl<sub>2</sub>): 2078, 1994 cm<sup>-1</sup>. HRMS Calculated for C<sub>26</sub>H<sub>32</sub>ClN<sub>2</sub>O<sub>2</sub>Rh: 542.1207. Found: 542.1228.

<b>Complex</b>	<b>2.17</b>	<b>2.20</b>
<b>CCDC #</b>	670930	651007
<b>Empirical formula</b>	$C_{34}H_{44}N_2OCl_2Ru, \frac{1}{2}(C_5H_{12})$	$C_{31}H_{38}N_2OCl_2Ru$
<b>Formula weight</b>	704.25	626.60
<b>Crystallization solvent</b>	Benzene/pentane	Benzene/pentane
<b>Crystal color</b>	Blue	Dichroic - green/blue
<b>T (K)</b>	100(2)	100(2)
<b><math>\theta</math> range (°)</b>	2.37 to 30.72	2.37 to 41.27
<b>a (Å)</b>	11.5182(8)	9.1757(3)
<b>b (Å)</b>	12.3831(8)	10.6130(4)
<b>c (Å)</b>	12.4144(8)	16.2638(6)
<b><math>\alpha</math> (Å)</b>	99.737(3)	85.3300(10)
<b><math>\beta</math> (Å)</b>	92.627(4)	77.2650(10)
<b><math>\gamma</math> (Å)</b>	92.065(4)	72.2060(10)
<b>V (Å<sup>3</sup>)</b>	1741.6(2)	1470.76(9)
<b>Crystal system</b>	Triclinic	Triclinic
<b>Space group</b>	P-1	P-1
<b><math>d_{calc}</math> (g/cm<sup>3</sup>)</b>	1.343	1.415
<b><math>\mu</math> (mm<sup>-1</sup>)</b>	0.634	0.741
<b>GOF on F<sup>2</sup></b>	2.665	1.187
<b>R<sub>1</sub>, wR<sub>2</sub> [I &gt; 2<math>\sigma</math>(I)]</b>	0.0605, 0.0916	0.0444, 0.0893

## References and Notes

---

- (1) (a) Grubbs, R. H. *Handbook of Metathesis*; Wiley-VCH:Weinheim, Germany, 2003 and references cited therein. (b) Hoveyda, A. H.; Zhugralin, A. R. *Nature* **2007**, *450*, 243–251. (c) Schrodi, Y.; Pederson, R. L. *Aldrichimica Acta* **2007**, *40*, 45–52. (d) Nicolaou, K. C.; Bulger, P. G.; Sarlah, D. *Angew. Chem., Int. Ed.* **2005**, *44*, 4490–4527. (e) Grubbs, R. H. *Tetrahedron* **2004**, *60*, 7117–7140. (f) Fürstner, A. *Angew. Chem., Int. Ed.* **2000**, *39*, 3013–3043.
- (2) (a) Grubbs, R. H. *J. Macromol. Sci. — Pure Applied Chem.* **1994**, *A31*, 1829–1833. (b) Trnka, T. M.; Grubbs, R. H. *Acc. Chem. Res.* **2001**, *34*, 18–29.
- (3) Scholl, M.; Ding, S.; Lee, C. W.; Grubbs, R. H. *Org. Lett.* **1999**, *1*, 953–956.
- (4) Garber, S. B.; Kingsbury, J. S.; Gray, B. L.; Hoveyda, A. H. *J. Am. Chem. Soc.* **2000**, *122*, 8168–8179.
- (5) (a) Chung, C. K. Grubbs, R. H. *Org. Lett.* **2008**, *10*, 2693–2696. (b) Berlin, J. M.; Campbell, K.; Ritter, T.; Funk, T. W.; Chlenov, A.; Grubbs, R. H. *Org. Lett.* **2007**, *9*, 1339–1342. (c) Stewart, I. C.; Ung, T.; Pletnev, A. A.; Berlin, J. M.; Grubbs, R. H.; Schrodi, Y. *Org. Lett.* **2007**, *9*, 1589–1592. (d) Vougioukalakis, G. C.; Grubbs, R. H. *J. Am. Chem. Soc.* **2008**, *130*, 2234–2245. (e) Vehlow, K.; Maechling, S.; Blechert, S. *Organometallics* **2006**, *25*, 25–28. (f) Despagnet-Ayoub, E.; Grubbs, R. H. *Organometallics* **2005**, *24*, 338–340. (g) Van Veldhuizen, J. J.; Garber, S. B.; Kingsbury, J. S.; Hoveyda, A. H. *J. Am. Chem. Soc.* **2002**, *124*, 4954–4955. (h) Funk, T. W.; Berlin, J. M.; Grubbs, R. H. *J. Am. Chem. Soc.* **2006**, *128*, 1840–1846. (i) Anderson, D. R.; Lavallo, V.; O’Leary, D. J.; Bertrand, G.; Grubbs, R. H. *Angew. Chem., Int. Ed.* **2007**, *46*, 7262–7265.

- 
- (j) Kuhn, K. M.; Grubbs, R. H. *Org. Lett.* **2008**, *10*, 2075–2077. (k) Weigl, K.; Köhler, K.; Dechert, S.; Meyer, F. *Organometallics* **2005**, *24*, 4049–4056.
- (6) For recent examples, see: (a) Enquist, J. E.; Stoltz, B. M. *Nature* **2008**, *453*, 1228–1231. (b) White, D. E.; Stewart, I. C.; Grubbs, R. H.; Stoltz, B. M. *J. Am. Chem. Soc.* **2008**, *130*, 810–811. (c) Pfeiffer, M. W. B.; Phillips, A. J. *J. Am. Chem. Soc.* **2005**, *127*, 5334–5335. (d) Humphrey, J. M.; Liao, A.; Rein, T.; Wong, Y.-L.; Chen, H.-J.; Courtney, A. K.; Martin, S. F. *J. Am. Chem. Soc.* **2002**, *124*, 8584–8592. (e) Martin, S. F.; Humphrey, J. M.; Ali, A.; Hillier, M. C. *J. Am. Chem. Soc.* **1999**, *121*, 866–867. (f) Yang, Z.; He, Y.; Vourloumis, D.; Vallberg, H.; Nicolaou, K. C. *Angew. Chem., Int. Ed.* **1997**, *36*, 166–168.
- (7) (a) Maynard, H. D.; Grubbs, R. H. *Tetrahedron Lett.* **1999**, *40*, 4137–4140. (b) Hong, S. H.; Sanders, D. P.; Lee, C. W.; Grubbs, R. H. *J. Am. Chem. Soc.* **2005**, *127*, 17160–17161.
- (8) Governmental recommendations for residual ruthenium are now routinely less than 10 ppm. For recent guidelines, see: (a) Zaidi, K. *Pharmacopeial Forum* **2008**, *34*, 1345–1348. (b) Criteria given in the EMEA Guideline on the Specification Limits for Residues of Metal Catalysts, available at: [www.emea.europa.eu/pdfs/human/swp/444600.pdf](http://www.emea.europa.eu/pdfs/human/swp/444600.pdf)
- (9) (a) Ulman, M.; Grubbs, R. H. *J. Org. Chem.* **1999**, *64*, 7202–7207. (b) Hong, S. H.; Day, M. W.; Grubbs, R. H. *J. Am. Chem. Soc.* **2004**, *126*, 7414–7415. (c) Hong, S. H.; Wenzel, A. G.; Salguero, T. T.; Day, M. W.; Grubbs, R. H. *J. Am. Chem. Soc.* **2007**, *129*, 7961–7968. (d) Hong, S. H.; Chlenov, A.; Day, M. W.; Grubbs, R. H. *Angew. Chem., Int. Ed.* **2007**, *46*, 5148–5151. (e) Vehlow, K.; Gessler, S.; Blechert, S. *Angew. Chem., Int. Ed.* **2007**, *46*, 8082–8085. (f) Leitao,

- 
- E. M.; Dubberley, S. R.; Piers, W. E.; Wu, Q.; McDonald, R. *Chem. Eur. J.* **2008**, *14*, 11565–11572.
- (10) Under inert atmosphere, heating a C<sub>6</sub>D<sub>6</sub> solution of catalyst **5** for 3 days at 70 °C leads to its total decomposition, while catalyst **2** does not readily decompose under those conditions.
- (11) Occhipinti, G.; Bjorsvik, H.-R.; Jensen, V. R. *J. Am. Chem. Soc.* **2006**, *128*, 6952–6964.
- (12) Ritter, T.; Hejl, A.; Wenzel, A. G.; Funk, T. W.; Grubbs, R. H. *Organometallics* **2006**, *25*, 5740–5745 and literature cited therein.
- (13) (a) Jazzar, R.; Bourg, J.-B.; Dewhurst, R. D.; Donnadieu, B.; Bertrand, G. *J. Org. Chem.* **2007**, *72*, 3492–3499. (b) Türkmen, H.; Çetinkaya, B. *J. Organomet. Chem.* **2006**, *691*, 3749–3759.
- (14) Denk, K.; Sirsch, P.; Herrmann, W. A. *J. Organomet. Chem.* **2002**, *649*, 219–224.
- (15) In this paper, catalyst activity encompasses initiation and propagation rates. For more insight into initiation kinetic studies, see Sanford, M. S.; Love, J. A.; Grubbs, R. H. *J. Am. Chem. Soc.* **2001**, *123*, 6543–6554.
- (16) Catalyst stability refers to the ability of a catalyst to do productive metathesis after extended period of time.
- (17) (a) Champagne, T. M.; Hong, S. H.; Lee, C. W.; Ung, T. A.; Stoianova, D. S.; Pederson, R. L.; Kuhn, K. M.; Virgil, S. C.; Grubbs, R. H. *Abstracts of Papers*, 236th ACS National Meeting, Philadelphia, PA; American Chemical Society; Washington, DC, 2008; ORGN-077. (b) Matson, J. M.; Virgil, S. C.; Grubbs, R. H. *J. Am. Chem. Soc.* **2009**, *131*, 3355–3362.
- (18) Bieniek, M.; Michrowska, A.; Usanov, D. L.; Grela, K. *Chem. Eur. J.* **2008**, *14*, 806–818.

- 
- (19) Ethyl vinyl ether functions as an effective catalyst quench, as the corresponding Fischer carbene complex is metathesis inactive. See: Louie, J.; Grubbs, R. H. *Organometallics*, **2002**, *21*, 2153–2164.
- (20) Wang, H.; Goodman, S. N.; Dai, Q.; Stockdale, G. W.; Clark Jr., W. M. *Org. Process Res. Dev.* **2008**, *12*, 226–234.
- (21) Complexes **15**, **16**, **18** and **19** underwent no further testing as experimentation continually demonstrated that complexes bearing disubstituted backbone ligands consistently gave results between the two extremes.
- (22) Pangborn, A. B.; Giardello, M. A.; Grubbs, R. H.; Rosen, R. K.; Timmers, F. J. *Organometallics* **1996**, *15*, 1518–1520.

## Chapter 3

### **Cyclic Carbamates via Ring-Closing Metathesis with Low Loadings of Ruthenium Catalysts**

*The text in this chapter is reproduced in part with permission from:*

Kuhn, K. M.; Champagne, T. M.; Hong, S. H.; Wei, W.-H.; Nickel, A.; Lee, C. W.; Ung, T. A.; Virgil, S. C.; Grubbs, R. H.; Pederson, R. L. *unpublished manuscript.*

## **Abstract**

Utilizing a high throughput and sensitive assay, a series of ruthenium catalysts have been screened for the ring closing metathesis (RCM) of acyclic carbamates to form the corresponding di-, tri-, and tetrasubstituted five-, six-, and seven-membered cyclic carbamates. While disubstituted cyclic olefins were easily formed by a variety of catalysts, NHC-bearing catalysts were required to produce trisubstituted cyclic olefin products at low catalyst loadings. Furthermore, only catalysts bearing small *N*-aryl bulk on the NHC ligands were found to effectively accomplish the RCM reaction for sterically challenging substrates, providing a reminder that more efficient catalysts still need to be developed.

## **Introduction**

Olefin metathesis has become an indispensable tool for the formation of new carbon-carbon bonds; its success in organic synthesis and materials chemistry driven by the development of increasingly efficient catalysts.<sup>1</sup> Ruthenium-based catalysts have received considerable attention because of their tolerance to moisture, oxygen, and a large number of organic functional groups.<sup>2</sup> Ring-closing metathesis (RCM), in particular, has become the most commonly employed metathesis reaction in organic synthesis.<sup>3</sup> RCM has had an especially large impact on the pharmaceutical industry since the reaction allows for an efficient and direct formation of heterocycles from acyclic dienes. Unfortunately, pharmaceutical efforts and applications typically use unnecessarily high catalyst loadings.

With this in mind, an important challenge in RCM is to substantially decrease “standard” catalyst loading, thereby reducing both reaction cost and the challenges in product purification, especially critical where reaction products are intended for pharmaceutical use.<sup>4</sup>

Herein, we report studies to optimize conditions for olefin metathesis and explore the viability of RCM of acyclic carbamates with low catalyst loadings of ruthenium-based catalysts. In order to examine the widest possible variety of catalysts and conditions, we have employed a highly sensitive ppm level assay utilizing the precision and consistency of Symyx robotic technology. Our group and others have recently used robotic systems to study catalyst efficiency, reaction optimization and new applications in olefin metathesis.<sup>5</sup>

The evolution of ruthenium-based catalysts (Figure 3.1) from first generation catalyst **3.1** (PCy<sub>3</sub>)<sub>2</sub>RuCl<sub>2</sub>(=CHPh) to the highly active complex **3.10** bearing a tetramethyl-substituted NHC ligand, has been driven by a continued need for increasingly efficient catalysts. Generally, phosphine-ligated complexes, such as **3.1** and **3.3**, have been suitable for the formation of disubstituted cyclic olefins.<sup>6, 7a</sup> The increased activity of H<sub>2</sub>IMes-ligated complexes (H<sub>2</sub>IMes = 1,3-dimesitylimidazolidine-2-ylidene), such as **3.2**, **3.4**, **3.5** and **3.6**, have allowed for the facile production of trisubstituted olefins.<sup>7b-e</sup> Finally, decreasing N-aryl steric bulk (**3.7** and **3.8**) on the N-heterocyclic carbene (NHC) and adding methyl-groups to the backbone (**3.9** and **3.10**) have greatly increased activity and stability, allowing for efficient synthesis of highly hindered olefin products.<sup>5a, 7f,g</sup>

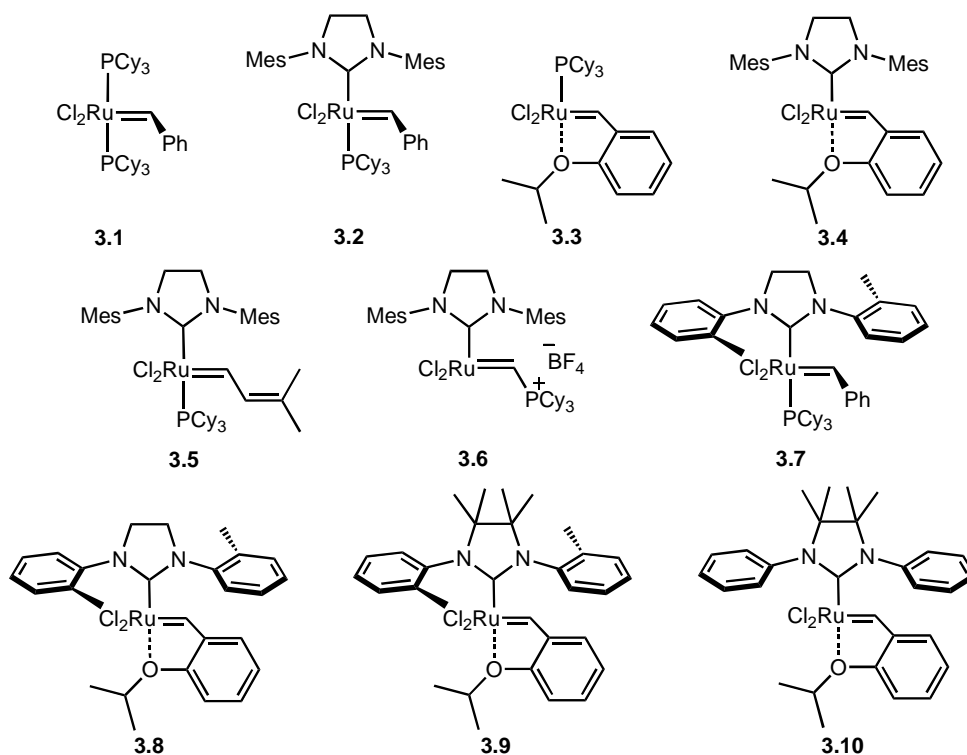


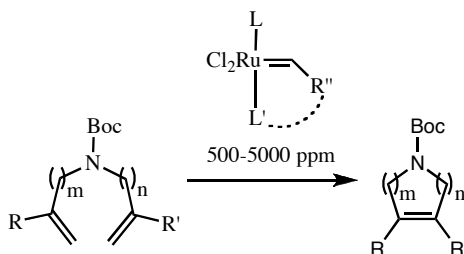
**Figure 3.1.** Ruthenium olefin metathesis catalysts (Mes = 2,4,6-trimethylphenyl).<sup>5a,7</sup>

Due to the wide variety of catalysts now available, the judicious choice of one catalyst for any particular application can be a daunting challenge. There are many substrate-dependent variables as well as catalyst stability, activity, and initiation rate considerations that determine catalyst efficiency for a given reaction. Therefore, it is important to examine and understand trends in relative catalyst efficiencies based on both reaction conditions and substrate design. With this in mind, the performance of several commercially available catalysts along with recently reported variants were utilized in this study (Figure 3.1), reaffirming the notion that no single catalyst is best for all olefin metathesis applications.<sup>1f, 5c, 5d</sup>

## Research and Discussion

Research focused on the RCM of acyclic carbamates to form the corresponding di-, tri-, and tetrasubstituted five-, six-, and seven-membered cyclic carbamates: valuable intermediates in organic synthesis (Scheme 3.1).

**Scheme 3.1.** RCM of acyclic carbamates to form the corresponding di-, tri-, and tetrasubstituted five-, six-, and seven-membered cyclic carbamates.



Reaction conditions including solvent, concentration, and temperature, were chosen based on recent complementary studies on catalyst efficiency.<sup>5a</sup> Methylene chloride, a solvent often used in olefin metathesis reactions, was shown to greatly decrease catalyst efficiency and was not utilized in our experiments.<sup>5a</sup> Instead, methyl *tert*-butyl ether (MTBE) and toluene were utilized and consistently provided excellent conversions throughout our studies. MTBE, in particular, is an exciting alternative to chlorinated solvents and other peroxide forming ethers.

While increased temperatures have previously shown to improve metathesis efficiency,<sup>5c,8</sup> temperatures above 50 °C decreased assay consistency and resulted in significant solvent losses throughout the course of the reaction. With this in mind, assays were generally completed at 50 °C.

There is a clear substrate dependence for optimized concentration. Five- and six-membered rings can be formed in high concentration. Notably, RCM conversions to form five-membered rings are only marginally lower without any solvent. However, as

ring size is increased, there is an evident trend for lower concentrations leading to higher conversions (Table 3.1).

**Table 3.1.** Effects of concentration on the formation of di-substituted five, six, and seven-membered cyclic carbamates by complex **3.4**.

500 ppm **3.4**  
50 °C  
x M, Toluene, 8 h

Substrate	Product	Conc. [M]	Conv. (%)
 <b>3.11</b>	 <b>3.12</b>	neat	87
		1 M	>99
		0.2 M	>99
 <b>3.13</b>	 <b>3.14</b>	1 M	96
		0.2 M	>99
		0.05 M	92
 <b>3.15</b>	 <b>3.16</b>	1 M	46
		0.2 M	82
		0.05 M	90

This is exemplified in the formation of disubstituted five-, six-, and seven-membered cyclic carbamates by complex **3.4**. Under varying concentrations, complex **3.4** afforded excellent yields of **3.12**, **3.14**, and **3.16** at just 500 ppm.

The ring-closing metathesis of **3.11** was then examined utilizing the full battery of catalysts (Figure 3.2). Results indicate that lower conversions were attained with catalysts containing labile phosphine (**3.1**, **3.2**, **3.5**, and **3.7**) than the Hoveyda and Piers type catalysts. The lower conversions with catalysts containing labile phosphine may be a result of competitive phosphine-based decomposition pathways.<sup>9</sup> On average, complexes **3.3** and **3.4** perform this RCM most efficiently.

Any change in substrate, either increased steric hindrance or chain length, resulted in dramatic differences in relative catalyst efficacy. For example, an increase in chain length of one methylene unit from substrate **3.11** to substrate **3.13** results in a

large increase in efficiency for complex **3.5**. Notably, **3.5** is easier to prepare but generally less active than benzylidene analogue **3.2** and less stable than the chelating 2-isopropoxy-benzylidene analogue **3.4**. However, **3.5** matches the performance of both **3.2** and **3.4** in the RCM of **3.13** at just 500 ppm (Figure 3.3). Furthermore, **3.5** continues to perform exceptionally well in the RCM of **3.19**—a substrate designed to study increased steric hindrance.

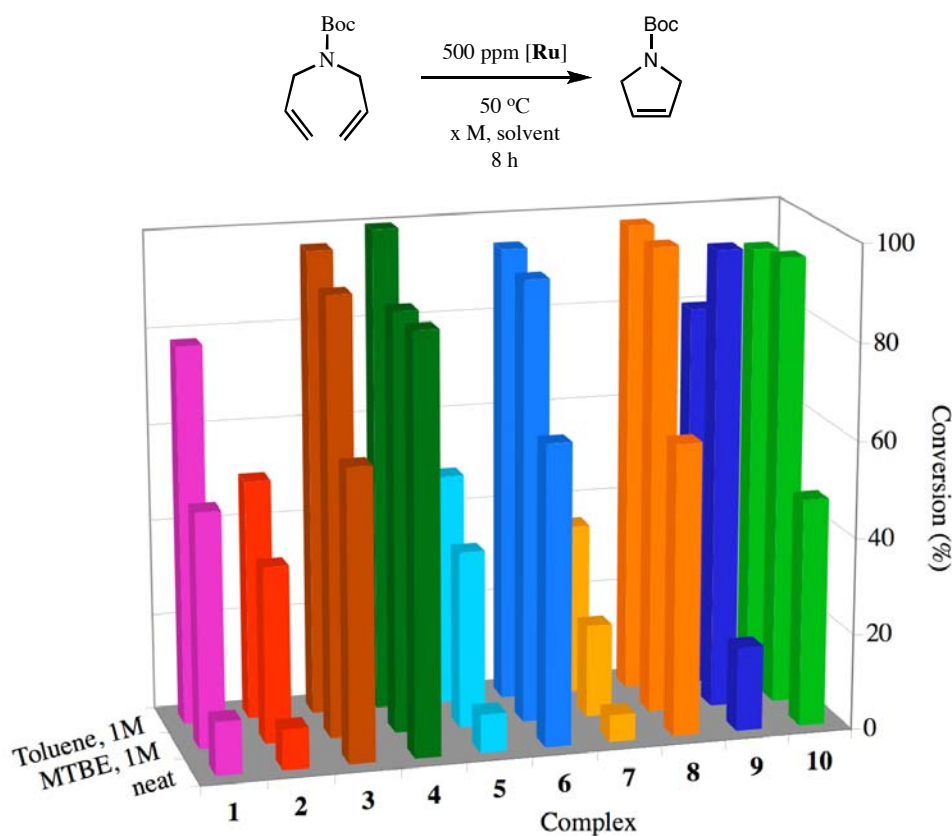


**Figure 3.2.** RCM of **3.11** utilizing complexes **3.1–3.10**.

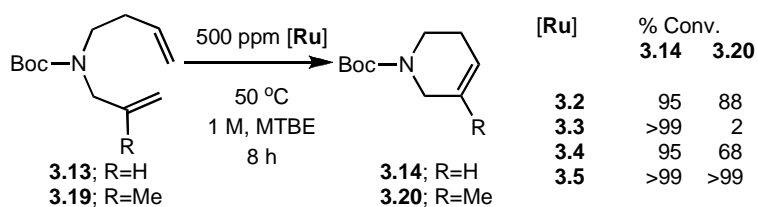


**Figure 3.3.** RCM of **3.13** and **3.19** utilizing complexes **3.2–3.5**.

While disubstituted cyclic olefins are easily formed by a variety of catalysts, NHC-bearing catalysts are required to produce trisubstituted cyclic olefin products at low catalyst loadings, as seen in the failure of **3.3** to perform the ring-closing of substrate **3.19** (Figure 3.3). As a general trend, the increased activity of H<sub>2</sub>I-Mes-ligated catalysts is demonstrated in the RCM of sterically challenging substrates **3.17**, **3.19** and **3.21** (Figure 3.4).

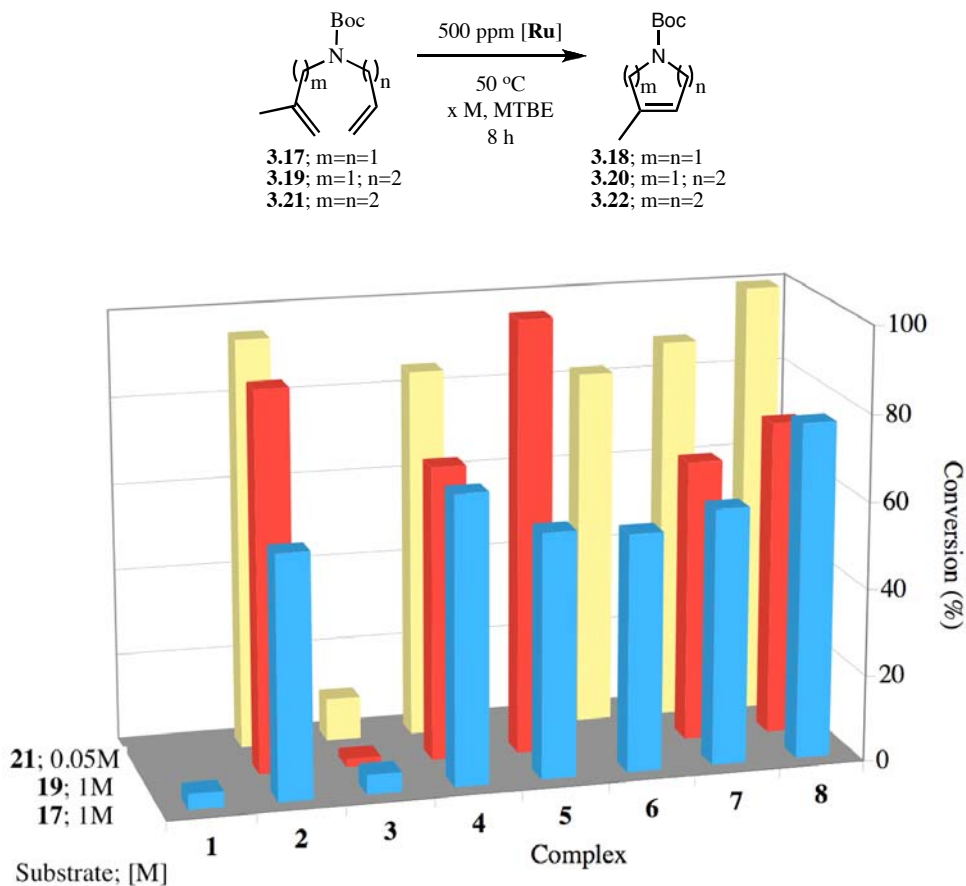


**Figure 3.4.** RCM of **3.17**, **3.19** and **3.21** utilizing complexes **3.1**–**3.8**.

Surprisingly, in the RCM of **3.17** by quickly initiating phosphonium alkylidene **3.6**, conversions increase to >99% at 30 °C from 92% at 50 °C. We hypothesize that decreased reaction temperatures increase conversion to product by decreasing the relative rate of complex decomposition compared to productive metathesis. This could

be quite relevant when utilizing thermally unstable substrates and products in organic synthesis and will be further explored in our laboratories.

Recent catalyst design and synthesis has focused on increasing the utility of olefin metathesis when working with highly hindered substrates.<sup>5a,7f,g</sup> Our comparison of **3.8–3.10** for the RCM of diethyl dimethylallylmalonate prompted further comparison in this study.<sup>5a</sup> We began this study with the RCM of N-Boc-Dimethylallylamine, **3.23**, utilizing 1000 ppm catalyst loadings (Figure 3.5).

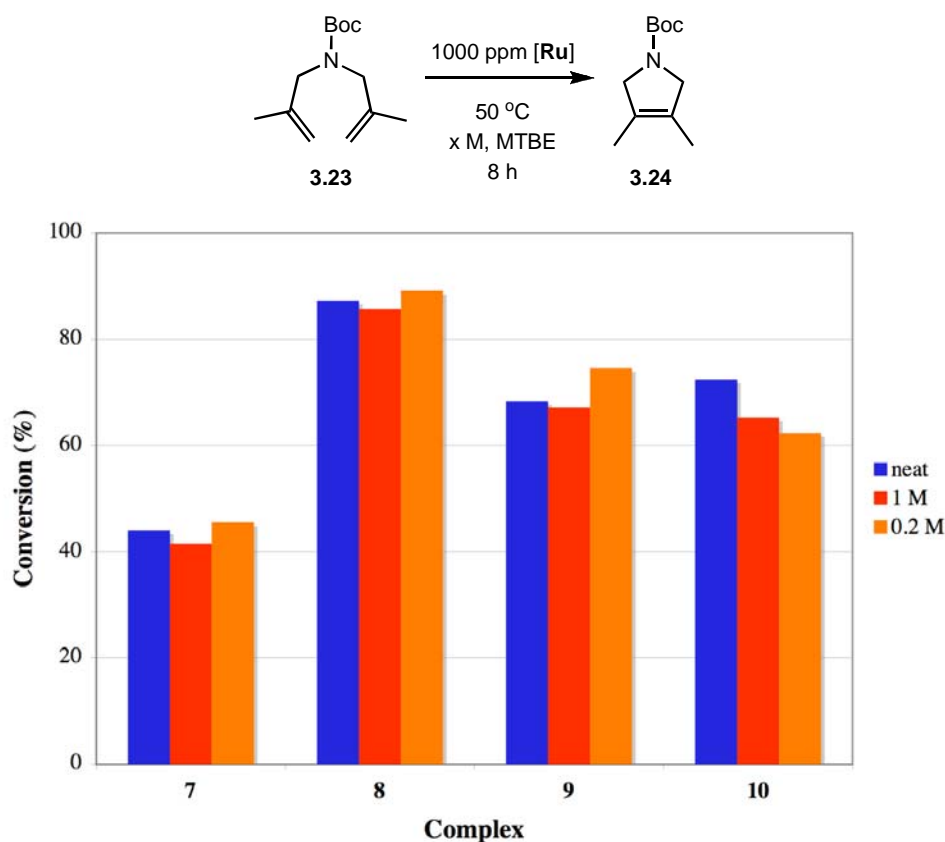


**Figure 3.5.** RCM of **3.23** utilizing complexes **3.7–3.10**.

Changes in concentration had a negligible effect on reaction conversion. As in previous examples, the Grubbs-Hoveyda catalysts outperformed the phosphine variants. The delicate balance between activity and stability is also suggested by this reaction; complex **3.8** is more stable than **3.10** yet more active than **3.9**, and leads to the highest conversions for this reaction.

This balance is altered by the addition of methylene units to the substrate, increasing the significance of catalyst stability. The low catalyst loading of 1000 ppm, which was adequate for **3.23**, was not sufficient for the RCM of **3.25**. Catalysts **3.8** and **3.9** were comparable in activity, however, low conversions resulted: 17%-34%. Thus, the RCM of the more challenging substrates **3.25** and **3.27** required catalysts loadings up to 0.5 mol% (Figure 3.6) to achieve high yields. Furthermore, only catalysts **3.8–3.10** were found to effectively accomplish the RCM reaction for these substrates, providing a reminder that more efficient catalysts still need to be developed.

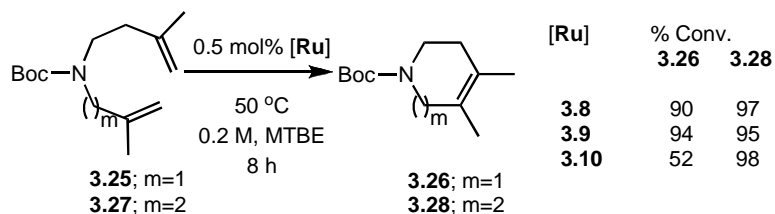


**Figure 3.6.** RCM of **3.25** and **3.27** utilizing complexes **3.8–3.10**.

### Conclusions

We have synthesized di-, tri-, and tetrasubstituted five-, six-, and seven-membered cyclic carbamates via RCM using low loadings of Ru-based catalysts. A high throughput and sensitive assay was developed and implemented using a Symyx robotic technology. This method has provided an overall assessment of catalyst activity with the carbamate substrates. This chapter focuses on just a small portion of the results from this study. Additional results can be found in appendix B.

In general, catalyst loadings as low as 500 ppm gave high yields of the cyclic carbamates. The di, tri, and tetrasubstituted *five*-membered cyclic carbamates were more dependent on catalyst choice and less dependent on concentration. Among the *six*- and *seven*-membered carbamates, lower concentrations gave higher yields. Furthermore, increasing steric bulk in the substrate required less bulky aryl substitution

on NHC-bearing catalysts. The use of MTBE as a substitute for chlorinated solvents provides a useful option for scale optimization.

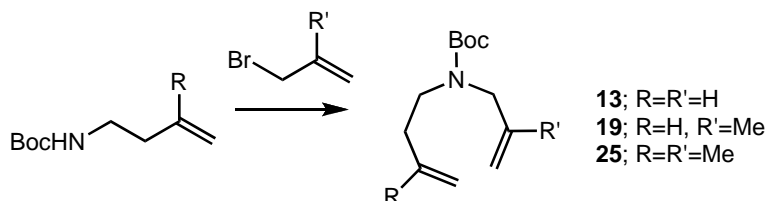
## ***Experimental***

### ***General Information***

NMR spectra were recorded using Varian Mercury 300, Inova 500, and VNMRs 400 MHz NMR spectrometers. NMR chemical shifts are reported in parts per million (ppm) downfield from tetramethylsilane (TMS) with reference to internal solvent for  $^1\text{H}$  and  $^{13}\text{C}$  nuclei. Spectra are reported as follows: chemical shift ( $\delta$  ppm), multiplicity, coupling constant (Hz), and integration. Gas chromatography data was obtained using an Agilent 6850 FID gas chromatograph equipped with a DB-Wax Polyethylene Glycol capillary column (J&W Scientific). High-resolution mass spectroscopy (FAB) was completed at the California Institute of Technology Mass Spectrometry Facility.

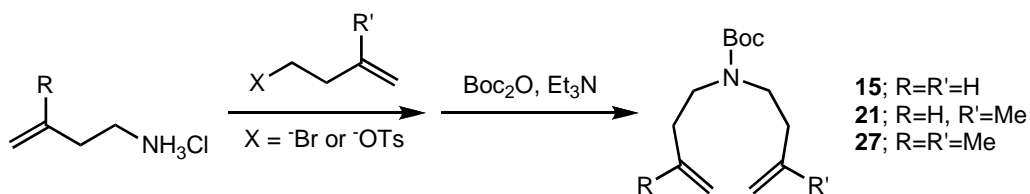
Catalysts **3.1-3.10** were obtained from Materia, Inc. Unless otherwise indicated, all compounds were purchased from Aldrich or Fisher and used as obtained. The compounds **3.11**, **3.12**, **3.14**,<sup>10</sup> **3.16-3.18**,<sup>11</sup> and **3.23-3.24**<sup>12</sup> have been described previously and were prepared according to literature procedures or identified by comparison of their spectroscopic data. The initial screening of the catalysts, in ring-closing metathesis (RCM) via  $^1\text{H}$  NMR was conducted according to literature procedures.<sup>13</sup>

**General procedure for the synthesis of N-Boc-1-(3-butenyl)allylamine (3.13), N-Boc-1-(3-butenyl)methallylamine (3.19), and N-Boc-1-(3-methyl-3-butenyl)methallylamine (3.25) RCM substrates:**



The Boc-protected olefin (1 equiv) was added at room temperature to a suspension of 60% NaH (1.5 equiv) mineral oil dispersion in 150 mL of DMF. The slurry was stirred for 2 h followed by addition of the allylbromide (1.3 equiv) at 0 °C. The reactions were monitored by gas chromatography until all of the Boc-protected olefin was consumed. The reaction was quenched with MeOH and water followed by extraction with hexanes (3 x 60 mL). The organic phases were combined and dried over MgSO<sub>4</sub>; the organic solvent was removed to give light-yellow oil. The crude product was purified by column chromatography on silica and eluted with 0%-4% EtOAc in hexanes. The pure products (97% by GC) were clear colorless oils and 60%-70% yields were obtained.

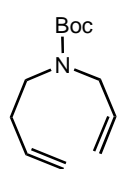
**General procedure for the synthesis of N-Boc-1-(3-dibutenyl)amine (3.15), N-Boc-1-(3-butenyl)-1-(3-methyl-3-butenyl)amine (3.21), N-Boc-1-(3-methyl-3-dibutenyl)amine (3.27) RCM substrates:**



The 4-bromo-1-butene or 4-tosylic-1-butene (1 equiv), butenylamine hydrochloride (1.1 equiv), and NaHCO<sub>3</sub> (1.1 equiv) were suspended in 150 mL of THF and heated to 60°C for 2 days. After cooling to room temperature, triethylamine (2.8

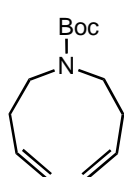
equiv) was added followed by addition of di-*tert*-butyl dicarbonate (1.1 equiv) over 15 minutes maintaining a constant gas evolution. The suspension was stirred for 90 minutes and the solids were removed by filtration. The filtrate was concentrated, re-dissolved in 50 mL of MeOH, and 5 mL of 1M NaOH (aq) was added. This mixture was stirred at room temperature for 16h and formed a cream-colored slurry. The solids were removed by filtration, and the filtrate was concentrated, and the residue partitioned between Et<sub>2</sub>O and saturated NaHCO<sub>3</sub> (aq). The organic phase was washed with water and brine, dried over Na<sub>2</sub>SO<sub>4</sub>, filtered, and concentrated to yield a brown oil. The crude product was purified by column chromatography on silica and eluted with 0%-4% EtOAc in hexanes. The pure products were clear, pale-yellow oils and 40%-50% yields were obtained.

#### N-Boc-1-(3-butenyl)allylamine (3.13)

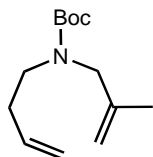


<sup>1</sup>H NMR (400 MHz, CDCl<sub>3</sub>): δ 5.75 (m, 2H), 4.97-5.12 (m, 4H), 3.80 (br, 2H), 3.21 (br, 2H), 2.25 (br, 2H), 1.44 (s, 9H). <sup>13</sup>C NMR (75 MHz, CDCl<sub>3</sub>): δ 155.54 (s), 135.66 (s), 134.47 (s), 116.51 (s), 79.49 (s), 49.96/49.65 (s, rotamers), 46.32 (s), 33.16/32.86 (s, rotamers), 28.51 (s). HRMS Calculated for C<sub>13</sub>H<sub>23</sub>O<sub>2</sub>N: 212.1650. Found: 212.1640.

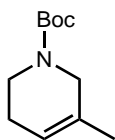
#### N-Boc-1-(3-dibutenyl)amine (3.15)



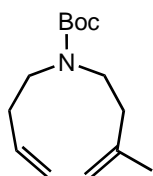
<sup>1</sup>H NMR (400 MHz, CDCl<sub>3</sub>): δ 5.75 (m, 2H), 5.07 (m, 1H), 5.02 (m, 2H), 4.99 (m, 1H), 3.22 (br, 4H), 2.26 (br, 4H), 1.44 (s, 9H). <sup>13</sup>C NMR (75 MHz, CDCl<sub>3</sub>): δ 155.58 (s), 135.69 (s), 116.54 (s), 79.36 (s), 47.09 (s), 33.49/32.94 (s, rotamers), 28.57 (s). HRMS Calculated for C<sub>14</sub>H<sub>25</sub>O<sub>2</sub>N: 226.1807. Found: 226.1797.

**N-Boc-1-(3-butenyl)methylamine (3.19)**

$^1\text{H}$  NMR (400 MHz,  $\text{CDCl}_3$ ):  $\delta$  5.76 (m, 1H), 5.06 (d, 1H,  $J^3 = 32$  Hz), 5.02 (d, 1H,  $J^2 = 4$  Hz), 4.82 (s, 1H), 4.76 (s, 1H), 3.75 (br, 2H), 3.20 (br, 2H), 2.26 (br, 2H), 1.67 (s, 3H), 1.45 (s, 9H).  $^{13}\text{C}$  NMR (75 MHz,  $\text{CDCl}_3$ ):  $\delta$  140.17 (s), 134.25 (s), 115.50 (s), 110.61 (s), 79.43 (s), 53.67/53.11 (s, rotamers), 46.83 (s), 34.16/33.61 (s, rotamers), 29.76 (s), 21.46 (s). HRMS Calculated for  $\text{C}_{13}\text{H}_{23}\text{O}_2\text{N}$ : 226.1807. Found: 226.1807.

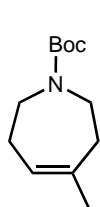
**1-(tert-Butoxycarbonyl)-3-methyl-1,2,5,6-tetrahydropyridine (3.20)**

$^1\text{H}$  NMR (400 MHz,  $\text{CDCl}_3$ ):  $\delta$  5.50 (br, 1H), 3.72 (br, 2H), 3.42 (t, 2H,  $J^3 = 6$  Hz), 2.06 (s, 2H), 1.66 (s, 1H), 1.46 (s, 9H).  $^{13}\text{C}$  NMR (75 MHz,  $\text{CDCl}_3$ ):  $\delta$  155.05 (s), 119.83 (s), 79.51 (s), 47.30 / 46.05 (s, rotamers), 40.86/39.55 (s, rotamers), 28.62 (s), 28.41 (s), 20.60 (s). HRMS Calculated for  $\text{C}_{13}\text{H}_{23}\text{O}_2\text{N}$ : 196.1338. Found: 196.1333.

**N-Boc-1-(3-butenyl)-1-(3-methyl-3-butenyl)amine (3.21)**

$^1\text{H}$  NMR (400 MHz,  $\text{CDCl}_3$ ):  $\delta$  5.76 (m, 1H), 5.07 (d, 1H,  $J^3 = 34$  Hz), 5.02 (d, 1H,  $J^2 = 5$  Hz), 4.74 (s, 1H), 4.68 (s, 1H), 3.23 (br, 4H), 2.18-2.27 (br m, 4H), 1.74 (s, 3H), 1.45 (s, 9H).  $^{13}\text{C}$  NMR (75 MHz,  $\text{CDCl}_3$ ):  $\delta$  153.51 (s), 134.19 (s), 115.51 (s), 111.01 (s), 110.70 (s), 79.28 (s), 46.98/47.23 (s, rotamers), 47.60/47.85 (s, rotamers), 37.44/38.10 (s, rotamers), 34.06/34.59 (s, rotamers), 29.79 (s), 23.99 (s). HRMS Calculated for  $\text{C}_{14}\text{H}_{25}\text{O}_2\text{N}$ : 240.1964. Found: 240.1974.

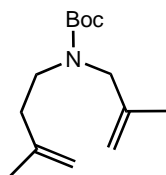
**1-(tert-Butoxycarbonyl)-4-methyl-2,3,6,7-tetrahydroazepine (3.22)**



$^1\text{H}$  NMR (400 MHz,  $\text{CDCl}_3$ ):  $\delta$  5.46 (m, 1H), 3.44 (br, 4H), 2.20 (br, 4H), 1.70 (br, 3H), 1.44 (s, 9H).  $^{13}\text{C}$  NMR (75 MHz,  $\text{CDCl}_3$ ):  $\delta$  155.33 (s), 123.50/123.17 (s, rotamers), 79.22 (s), 47.18/46.44 (s, rotamers), 45.33/44.61 (s, rotamers), 35.32/35.11 (s, rotamers), 28.62 (s), 26.65 (s).

HRMS Calculated for  $\text{C}_{12}\text{H}_{21}\text{O}_2\text{N}$ : 211.1572. Found: 211.1564.

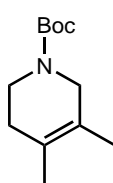
**N-Boc-1-(3-methyl-3-butenyl)methylamine (3.25)**



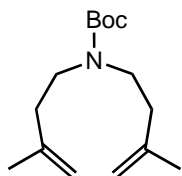
$^1\text{H}$  NMR (400 MHz,  $\text{CDCl}_3$ ):  $\delta$  4.83 (s, 1H), 4.76 (s, 1H), 4.74 (s, 1H), 4.74 (s, 1H), 4.68 (s, 1H), 3.75 (d, 2H, rotamers), 3.24 (d, 2H, rotamers), 2.20 (br, 2H), 1.73 (s, 3H), 1.67 (s, 3H), 1.45 (br s, 9H).  $^{13}\text{C}$  NMR (75 MHz,  $\text{CDCl}_3$ ):  $\delta$  140.22 (s), 111.04 (s), 110.71 (s), 79.41 (s), 53.54/52.93 (s, rotamers), 46.11 (s), 37.67/37.00 (s, rotamers), 29.76 (s), 23.97 (s), 21.44 (s). HRMS

Calculated for  $\text{C}_{14}\text{H}_{25}\text{O}_2\text{N}$ : 240.1964. Found: 240.1963.

**1-(tert-Butoxycarbonyl)-3,4-dimethyl-1,2,5,6-tetrahydropyridine (3.26)**

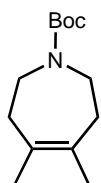


$^1\text{H}$  NMR (400 MHz,  $\text{CDCl}_3$ ):  $\delta$  3.68 (br, 2H), 3.43 (t, 2H,  $J^{\beta} = 5.6$  Hz), 1.99 (s, 2H), 1.63 (s, 3H), 1.59 (s, 3H), 1.45 (s, 9H).  $^{13}\text{C}$  NMR (75 MHz,  $\text{CDCl}_3$ ):  $\delta$  154.95 (s), 79.30 (s), 47.80 (br, rotamers), 41.47/40.16 (s, rotamers), 31.26 (s), 28.60 (s), 18.77 (s), 16.13 (s).

**N-Boc-1-(3-methyl-3-dibutenyl)amine (3.27)**

$^1\text{H}$  NMR (400 MHz,  $\text{CDCl}_3$ ):  $\delta$  4.74 (s, 2H), 4.68 (s, 2H), 3.25 (br, 4H), 2.21 (br, 4H), 1.74 (s, 6H), 1.44 (s, 9H).  $^{13}\text{C}$  NMR (75 MHz,  $\text{CDCl}_3$ ):  $\delta$  153.44 (s), 141.62 (s), 111.02 (s), 110.74 (s), 79.26 (s), 47.08 / 46.77 (s, rotamers), 38.13/37.47 (s, rotamers), 29.81 (s), 24.00 (s). HRMS

Calculated for  $\text{C}_{15}\text{H}_{27}\text{O}_2\text{N}$ : 254.2120. Found: 254.2121.

**1-(tert-Butoxycarbonyl)-4,5-dimethyl-2,3,6,7-tetrahydroazepine (3.28)**

$^1\text{H}$  NMR (400 MHz,  $\text{CDCl}_3$ ):  $\delta$  3.29 (br, 4H), 2.24 (br, 4H), 1.67 (s, 6H), 1.46 (s, 9H).  $^{13}\text{C}$  NMR (75 MHz,  $\text{CDCl}_3$ ):  $\delta$  155.62 (s), 79.35 (s), 45.22/44.41 (s, rotamers), 37.10/36.43 (s, rotamers), .35.32/35.11 (s, rotamers), 28.62 (s), 21.76 (s). HRMS Calculated for  $\text{C}_{13}\text{H}_{24}\text{O}_2\text{N}$ : 226.1807. Found: 226.1812.

**Low Catalyst Loading Assay.**

Experiments on the RCM of **3.11**, **3.13**, **3.15**, **3.17**, **3.19**, **3.21**, **3.23**, **3.25**, and **3.27** using the catalysts described were conducted using a Symyx Technologies Core Module (Santa Clara, CA) housed in a Braun nitrogen-filled glovebox and equipped with Julabo LH45 and LH85 temperature-control units for separate positions of the robot tabletop.

Up to 576 reactions (6x96 well plates) could be performed simultaneously in 1 mL vials by an Epoch software-based protocol as follows. To prepare catalyst stock solutions (0.25 mM), 20 mL glass scintillation vials were charged with catalyst (5  $\mu\text{mole}$ ) and diluted to 20.0 mL total volume in THF. Catalyst solutions, 6 to 800  $\mu\text{L}$  depending on desired final catalyst loading, were transferred to reaction vials and solvent was removed via centrifugal evaporation. The catalysts were preheated to the desired

temperature using the LH45 unit, and stirring was started. Substrates (0.1 mmol), containing dodecane (0.025 mmol) as an internal standard, were dispensed simultaneously to 4 reactions at a time using one arm of the robot equipped with a 4-needle assembly. Immediately following substrate addition, solvent was added to reach the desired reaction molarity. All reactions were quenched by injection of 0.1 mL 5% v/v ethyl vinyl ether in toluene.

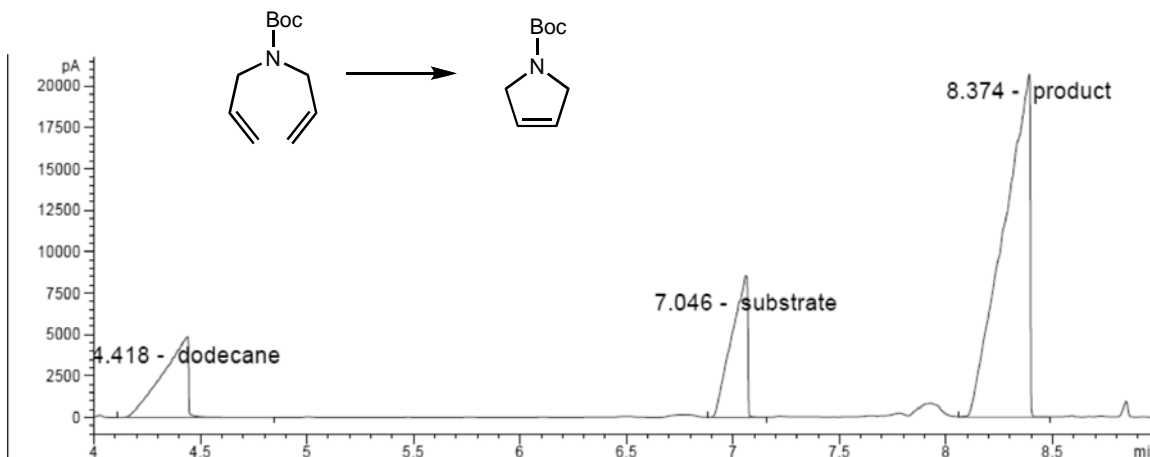
### **GC Data Analysis.**

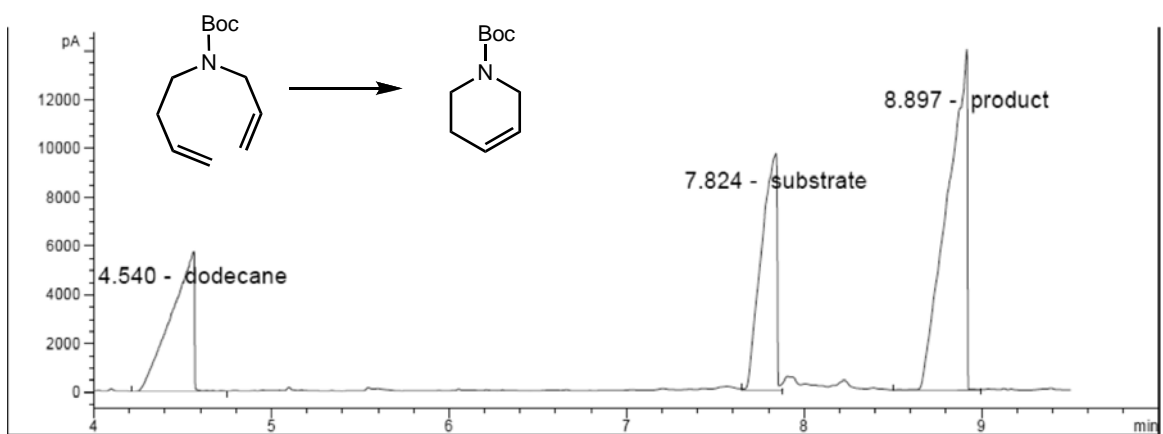
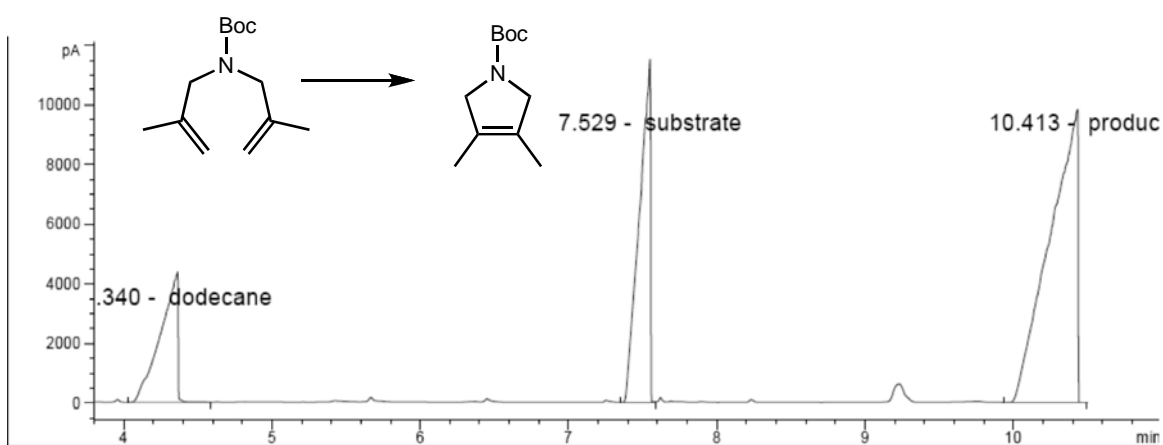
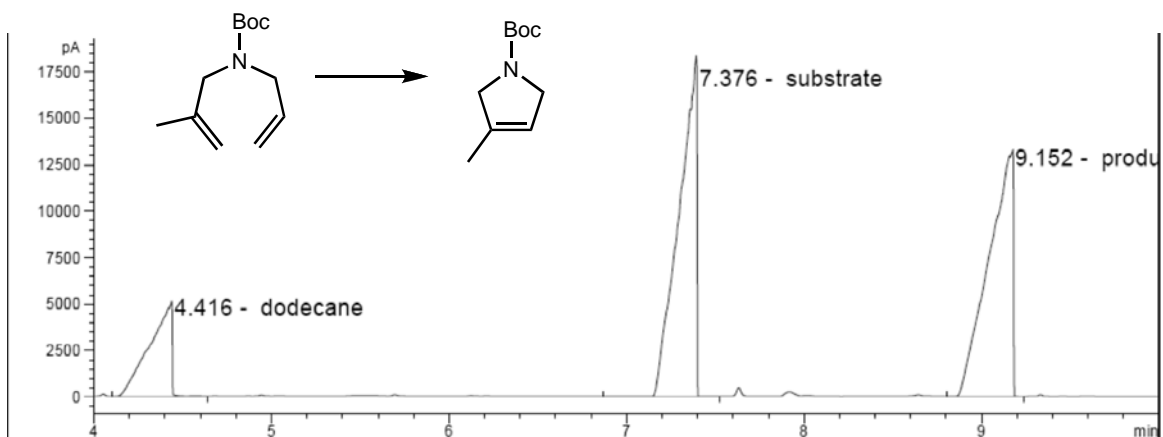
Samples were analyzed by gas chromatography with dodecane as an internal standard, measuring the change in the amounts of substrate and product with time.

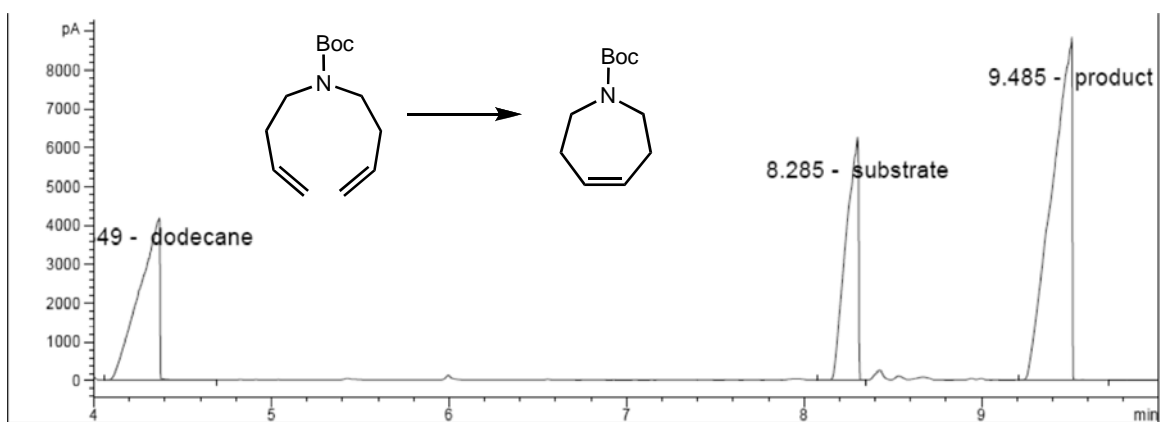
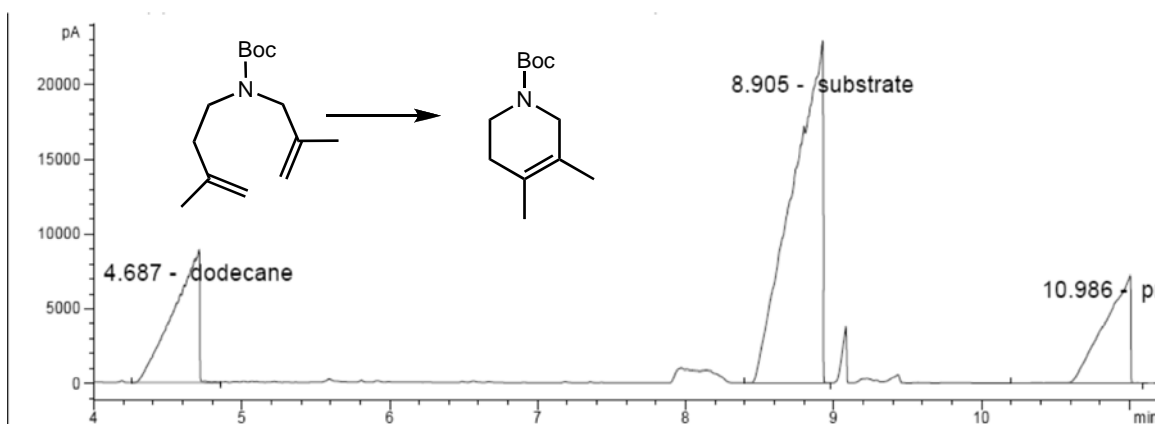
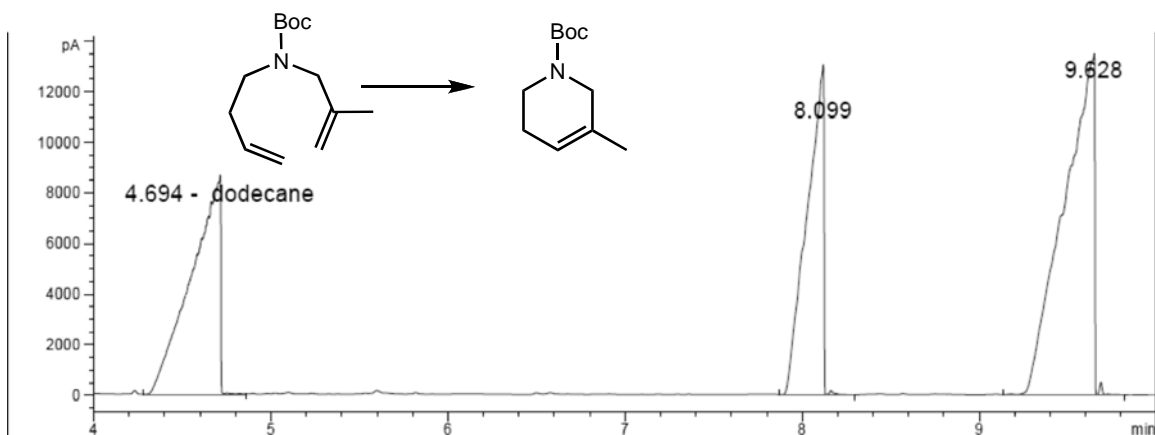
Relevant instrument conditions: Inlet temperature = 150 °C; detector temperature = 250 °C; hydrogen flow = 32mL/min; air flow = 400 mL/min; constant col + makeup flow = 30 mL/min.

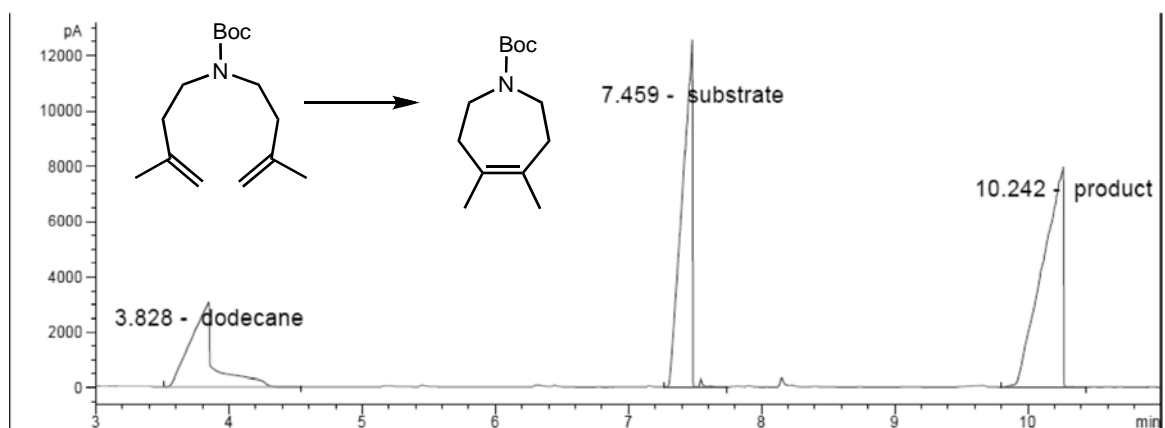
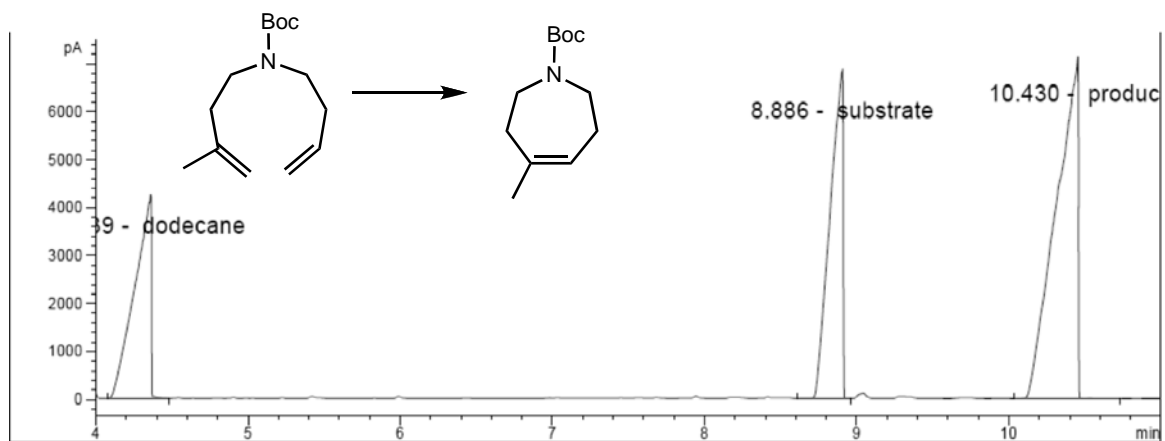
GC Method: 75 °C for 4 minutes, followed by a temperature increase of 25 °C/min to 160 °C, and a subsequent isothermal period at 160 °C for between 2 and 8 minutes, depending on substrate mass. (total run time = 10-16 minutes). Method for **3.27** and **3.28** began at 80 °C.

### **Representative GC traces.**









## References and Notes

---

- (1) (a) Grubbs, R. H. *Handbook of Metathesis*; Wiley-VCH:Weinheim, Germany, 2003 and references cited therein. (b) Hoveyda, A. H.; Zhugralin, A. R. *Nature* **2007**, *450*, 243–251. (c) Schrodi, Y.; Pederson, R. L. *Aldrichimica Acta* **2007**, *40*, 45–52. (d) Nicolaou, K. C.; Bulger, P. G.; Sarlah, D. *Angew. Chem., Int. Ed.* **2005**, *44*, 4490–4527. (e) Grubbs, R. H. *Tetrahedron* **2004**, *60*, 7117–7140. (f) Furstner, A. *Angew. Chem., Int. Ed.* **2000**, *39*, 3013–3043.
- (2) (a) Grubbs, R. H. *J. Macromol. Sci. — Pure Applied Chem.* **1994**, *A31*, 1829–1833. (b) Trnka, T. M.; Grubbs, R. H. *Acc. Chem. Res.* **2001**, *34*, 18–29.
- (3) For recent examples, see: (a) Enquist, J. E.; Stoltz, B. M. *Nature* **2008**, *453*, 1228–1231. (b) White, D. E.; Stewart, I. C.; Grubbs, R. H.; Stoltz, B. M. *J. Am. Chem. Soc.* **2008**, *130*, 810–811. (c) Pfeiffer, M. W. B.; Phillips, A. J. *J. Am. Chem. Soc.* **2005**, *127*, 5334–5335. (d) Humphrey, J. M.; Liao, A.; Rein, T.; Wong, Y.-L.; Chen, H.-J.; Courtney, A. K.; Martin, S. F. *J. Am. Chem. Soc.* **2002**, *124*, 8584–8592. (e) Martin, S. F.; Humphrey, J. M.; Ali, A.; Hillier, M. C. *J. Am. Chem. Soc.* **1999**, *121*, 866–867.
- (4) Governmental recommendations for residual ruthenium are now routinely less than 10 ppm. For recent guidelines, see: (a) Zaidi, K. *Pharmacopeial Forum* **2008**, *34*, 1345–1348. (b) Criteria given in the EMEA Guideline on the Specification Limits for Residues of Metal Catalysts, available at: [www.emea.europa.eu/pdfs/human/swp/444600.pdf](http://www.emea.europa.eu/pdfs/human/swp/444600.pdf)
- (5) (a) Kuhn, K. M.; Bourg, J. B.; Chung, C. K.; Virgil, S. C.; Grubbs, R. H. *J. Am. Chem. Soc.*, **2009**, *131*, 5313–5320. (b) Matson, J. M.; Virgil, S. C.; Grubbs, R. H. *J. Am. Chem. Soc.* **2009**, *131*, 3355–3362. (c) Bieniek, M.; Michrowska, A.;

- 
- Usanov, D. L.; Grela, K. *Chem Eur. J.* **2008**, *14*, 806–818. (d) Blacquiere, J. M.; Jurca, T.; Weiss, J.; Fogg, D. E. *Adv. Synth. Catal.* **2008**, *350*, 2849–2855.
- (6) Fu, G. C.; Nguyen, S.; Grubbs, R. H. *J. Am. Chem. Soc.* **1993**, *115*, 9856–9857.
- (7) (a) Schwab, P.; Grubbs, R. H.; Ziller, J. W. *J. Am. Chem. Soc.* **1996**, *118*, 100–110. (b) Scholl, M.; Ding, S.; Lee, C. W.; Grubbs, R. H. *Org. Lett.* **1999**, *1*, 953–956. (c) Garber, S. B.; Kingsbury, J. S.; Gray, B. L.; Hoveyda, A. H. *J. Am. Chem. Soc.* **2000**, *122*, 8168–8179. (d) Chatterjee, A. K.; Grubbs, R. H. *Org. Lett.* **1999**, *1*, 1751–1753. (e) Romero, P. E.; Piers, W. E.; McDonald, R. *Ang. Chem. Int. Ed.* **2004**, *43*, 6161–6165. (f) Stewart, I. C.; Ung, T.; Pletnev, A. A.; Berlin, J. M.; Grubbs, R. H.; Schrodi, Y. *Org. Lett.* **2007**, *9*, 1589–1592. (g) Chung, C. K. Grubbs, R. H. *Org. Lett.* **2008**, *10*, 2693–2696.
- (8) Wang, H.; Goodman, S. N.; Dai, Q.; Stockdale, G. W.; Clark Jr., W. M. *Org. Process Res. Dev.* **2008**, *12*, 226–234.
- (9) (a) Hong, S. H.; Day, M. W.; Grubbs, R. H. *J. Am. Chem. Soc.* **2004**, *126*, 7414–7415. (b) Hong, S. H.; Wenzel, A. G.; Salguero, T. T.; Day, M. W.; Grubbs, R. H. *J. Am. Chem. Soc.* **2007**, *129*, 7961–7968.
- (10) Nordmann, R.; Graff, P.; Maurer, R.; Gaehwiler, B. H. *J. Med. Chem.* **1985**, *28*, 1109–1111.
- (11) (a) MaGee, D. I.; Beck, E. J. *J. Org. Chem.* **2000**, *65*, 8367–8371. (b) Hodgson, D. M.; Miles, T. J.; Witherington, J. *Tetrahedron*, **2003**, *59*, 9729–9742.
- (12) Del Sol Moreno, G. *et al.* Sanofi Synthelabo. Aminoalkylimidazole derivatives preparation and therapeutic use thereof, WO03011856.
- (13) Ritter, T.; Hejl, A.; Wenzel, A. G.; Funk, T. W.; Grubbs, R. H. *Organometallics* **2006**, *25*, 5740–5745, and literature cited therein.

## Chapter 4

### A Facile Preparation of Imidazolinium Chlorides

*The text in this chapter is reproduced in part with permission from:*

Kuhn, K. M.; Grubbs, R. H. *Org. Lett.* **2008**, *10*, 2075–2077.

## Abstract

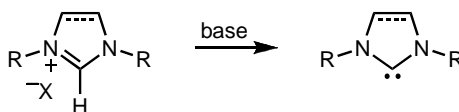
A process for the preparation of symmetric and unsymmetric imidazolium chlorides that involves reaction of a formamidine with dichloroethane and a base is described. This method makes it possible to obtain numerous imidazolium chlorides under solvent-free reaction conditions and in excellent yields with purification by simple filtration. Alternatively, symmetric imidazolium chlorides can be prepared directly in moderate yields from substituted anilines by utilizing half of the formamidine intermediate as sacrificial base.

## Introduction

Since the first isolation of a stable N-heterocyclic carbene (NHC) by Arduengo,<sup>1</sup> their use as ligands in organometallic complexes has become routine. NHCs, as neutral, two-electron donors with little  $\pi$ -accepting character, have replaced phosphines in a variety of applications.<sup>2</sup> Particularly, the use of NHCs as ligands in ruthenium-based olefin metathesis has allowed for great gains in both activity and stability.<sup>3</sup> There is also increasing interest in the use of NHCs as nucleophilic reagents and organocatalysts, with wide application in reactions such as the benzoin condensation, among others.<sup>4</sup>

NHCs are often prepared in situ via the deprotonation of their corresponding imidazol(in)ium salts (Scheme 4.1).<sup>5</sup> Therefore, facile and high-yielding methods for the synthesis of imidazol(in)ium salts are of great interest.

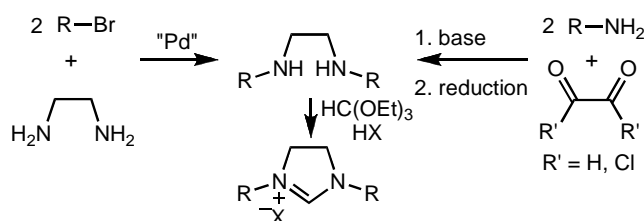
**Scheme 4.1.** Deprotonation of imidazol(in)ium salts.



The synthesis of unsaturated imidazolium salts, previously optimized by Arduengo and co-workers, involves a one-pot procedure from glyoxal, substituted aniline, formaldehyde, and acid starting materials.<sup>6</sup> Saturated imidazolium salts, however, are

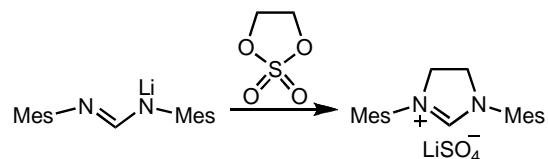
prepared from the reaction of triethylorthoformate with the corresponding diamine.<sup>7</sup> This approach suffers several drawbacks: the preparation of the diamine generally includes either a palladium C-N coupling or a condensation and reduction sequence (Scheme 4.2);<sup>8</sup> moreover, purification of the unstable diamine sometimes requires careful chromatography. Unsymmetric imidazolium salts are especially challenging synthetic targets due to the introduction of the differing substituents.<sup>9</sup>

**Scheme 4.2.** Common syntheses of imidazolium salts.



Recently, Bertrand and co-workers developed an alternative retrosynthetic disconnection and prepared a range of five-, six-, and seven membered imidazolium salts from the addition of “di-electrophiles” to lithiated formamidines.<sup>10</sup> For example, 1,3-dimesitylimidazolium lithium sulfate was prepared in high yield with 1,3,2-dioxathiolane-2,2-dioxide as the dielectrophile (Scheme 4.3).

**Scheme 4.3.** Reaction of 1,3,2-dioxathiolane-2,2-dioxide with lithium-*N,N'*-bis(2,4,6-trimethylphenyl)formamide.



Following Bertrand's report, we reasoned that imidazolium chlorides could be more easily prepared directly from the reaction of formamidines with dichloroethane (DCE) in the presence of a base. Formamidines are ideal precursors for the preparation of imidazolium chlorides because they are generally prepared in a one-step solvent-

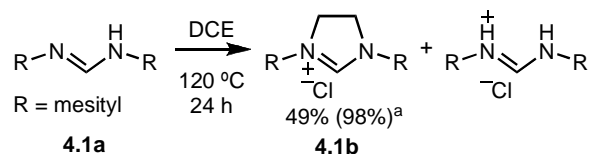
free reaction from materials already utilized in imidazolinium salt synthesis, namely anilines and triethylorthoformate.

Herein, we report this new synthetic strategy for the preparation of imidazolinium chlorides under solvent-free reaction conditions and in excellent yields with purification by simple filtration. This strategy also allows for the preparation of symmetric imidazolinium chlorides in a one-step, three-component procedure directly from substituted anilines.

### Results and Discussion

Our preliminary efforts focused on the preparation of 1,3-dimesitylimidazolinium chloride (**4.1b**) from *N,N'*-bis(mesityl)formamidine (**4.1a**).<sup>11</sup> The formamidine can act as both substrate and sacrificial base in the reaction. After optimization, the reaction led to nearly quantitative, reproducible yields of pure **4.1b** (Scheme 4.4). *N,N'*-bis(mesityl)formamidine hydrochloride could also be isolated and easily reverted to the formamidine for future use by solvation in pyridine and precipitation into water.<sup>12</sup>

**Scheme 4.4.** Preparation of 1,3-dimesitylimidazolinium chloride (**4.1b**).<sup>13</sup>



Numerous bases were screened to find an effective replacement for the sacrificial formamidine. Only diisopropylethylamine (DIPA) was shown to perform well in the reaction. Bases such as pyridine and triethylamine were too nucleophilic and reacted preferentially with dichloroethane. Strong bases such as sodium hydride deprotonated the final product.

The two methods were both successful in preparing a series of other imidazolinium chlorides starting from a variety of anilines (Table 4.1). In all cases,

reactions were completed neat in ten to twenty equivalents of dichloroethane and a slight excess of base. Products were easily purified by removal of excess dichloroethane, trituration in acetone, hot toluene or water, and filtration.

**Table 4.1.** Preparation of 1,3-diarylimidazolium chlorides from formamidines.<sup>14</sup>

Method A

$$\text{R}^1\text{-N}=\text{C}(\text{H})\text{-N-R}^2 \xrightarrow[\text{DIPA, 120 }^\circ\text{C}]{\text{DCE}} \text{R}^1\text{-N}^+\text{C}(\text{H})\text{-N-R}^2 + \text{DIPA-HCl}$$

Method B

$$\text{R}^1\text{-N}=\text{C}(\text{H})\text{-N-R}^2 \xrightarrow[\text{120 }^\circ\text{C}]{\text{DCE}} \text{R}^1\text{-N}^+\text{C}(\text{H})\text{-N-R}^2 + \text{R}^1\text{-N}^+\text{C}(\text{H})\text{-N-R}^2 + \text{R}^1\text{-N}=\text{C}(\text{H})\text{-N-R}^2$$

entry	product	time (h)	A yield (%) <sup>a</sup>	B yield (%) <sup>a,b</sup>
4.1		24	92	49 (98)
4.2		24	43 <sup>c</sup>	48 (96)
4.3		36	91	46 (92)
4.4		168 <sup>d</sup>	42	19 (38)
4.5		36	75	41 (82)
4.6		24	80	43 (86)

Notably, two challenging unsymmetrical imidazolium chlorides were prepared in good yields (entries 4.5 and 4.6). Our synthesis of 1-(2,6-difluorophenyl)-3-(mesityl)imidazolium chloride (**4.5b**), prepared here in two steps and a 65% overall yield, is a marked improvement over its previous four-step synthesis.<sup>9a</sup> This method should allow for the properties and applications of unsymmetrical NHCs to be further explored.

In our ongoing efforts we have found several substrate limitations. As steric bulk at the N-aryl ortho positions is increased, the steric hinderance decreases reaction rate, and longer reaction times are necessary. This is exemplified by the reaction of *N,N'*-bis(2-tertbutylphenyl)formamidinium, which only reached 60% conversion after 7 days (entry 4.4). Highly electron withdrawing N-aryl substituents also hinder the reaction; the reaction of *N,N'*-bis(2,6-trifluoromethylphenyl)formamidinium was unsuccessful. Finally, reaction of a dialkyl formamidinium, *N,N'*-bis(cyclohexyl)formamidinium, gave only poor yields of the desired product, most likely due to the increased basicity of dialkyl formamidines.

Further efforts focused on a one-step, three-component synthesis of commonly utilized symmetric 1,3-diarylimidazolium chlorides from substituted anilines (Table 4.2). The formamidinium, as base and intermediate, is formed in situ and the cyclization then proceeds as normal. Regretably, replacement of the sacrificial formamidinium with diisopropylethylamine hindered the initial reaction and resulted in very limited product formation. While yields are lower than the two-step procedure, reaction optimization and recycling of the formamidinium hydrochloride could be successful on the large scale. In our studies, 1,3-dimesitylimidazolium chloride has been prepared on a 20 gram scale without loss in yield or ease of purification.

**Table 4.2.** Preparation of 1,3 diarylimidazolium chlorides from anilines in one step.<sup>15</sup>

$$2 \text{ R-NH}_2 + 1 \text{ HC(OEt)}_3 \xrightarrow[120^\circ\text{C}]{\text{DCE}} \text{R-N}^+\text{C}(\text{H})\text{N-R} + \text{R-N}^+\text{C}(\text{H})\text{N-R}^- \text{Cl}^-$$

entry	product	time (h)	yield (%) <sup>a,b</sup>
1		24	45 (90)
2		24	26 (52)
3		36	42 (84)

## **Conclusions**

We have devised a new synthetic strategy for the preparation of symmetric and unsymmetric imidazolinium chlorides from formamidines in excellent yields. Because the formamidine precursors and imidazolinium products are both formed in solvent-free conditions and purified by simple trituration and filtration, this approach is more straightforward as well as more atom economical than the previously available methods. We have also demonstrated that symmetric imidazolinium chlorides can be prepared directly in moderate yields from substituted anilines. We believe these experimentally convenient procedures will find wide application as N-heterocyclic carbenes become even more common as ligands and organocatalysts.

## **Experimental**

### **General Information**

NMR spectra were recorded on an Oxford 300 MHz NMR spectrometer running Varian VNMR Software. Chemical shifts are reported in parts per million (ppm) downfield from tetramethylsilane (TMS) with reference to internal solvent for  $^1\text{H}$  NMR and  $^{13}\text{C}$  NMR spectra. Spectra are reported as follows: chemical shift ( $\delta$  ppm), integration, multiplicity, and coupling constant (Hz). (Multiplicities are abbreviated as follows: singlet (s), doublet (d), triplet (t), quartet (q), quintet (quint), septet (sept), multiplet (m), and broad (br). All new compounds were also characterized by high-resolution mass spectrometry (FAB) at the California Institute of Technology Mass Spectrometry Facility. Compounds are numbered according to their entry number in Table 4.1; (a) denotes the formamidine and (b) denotes the imidazolinium chloride. All commercial chemicals were used as obtained.

### A Note on Formamidinium Isomerization and NMR Spectra

Although many diarylformamidines are well known and highly utilized compounds, their NMR spectra are rarely found in the literature. While this is presumed to be a result of their age in the literature, it could also be a result of their surprisingly complex NMR spectra. Formamidines have two rotational isomers that interconvert at rates dependent on both substituents and solvent. This often leads to spectra that are considerably more complex than expected for these small molecules. Because the NMR spectra of a single formamidinium can vary significantly depending on the solvent, we have tried to provide spectral data for the known formamidines in solvents that supply the most information about each compound.

### General Procedure for the Preparation of Symmetric Formamidines

Acetic acid (86  $\mu$ L, 1.5 mmol) was added to a round bottom flask charged with the corresponding aniline (60 mmol, 2 equiv) and triethyl orthoformate (5 mL, 30 mmol, 1 equiv). The flask was fitted with a distillation head and was heated with stirring overnight. Upon cooling to room temperature, the solution solidified. The crude product was triturated with cold hexanes (30 mL), collected by vacuum filtration and dried *in vacuo*, providing pure product as a colorless powder (80%-92%). The following formamidines were prepared by the following procedure:

***N,N'*-Bis(2,4,6-trimethylphenyl)formamidinium (1a).** Prepared according to the above general procedure (140 °C) in 92% yield as a white semi-crystalline solid. In  $C_6D_6$  (25 °C) the formamidinium exists in two isomeric forms in a 1:1 ratio.  $^1H$  NMR chemical shifts for the two isomers will be listed separately. Isomer 1:  $^1H$  NMR ( $C_6D_6$ ):  $\delta$  1.86 [s, 6H], 2.03 [s, 3H], 2.23 [s, 3H], 2.31 [s, 3H], 4.99 [d, 1H,  $J_{HH} = 7.2$  Hz], 6.55 [s, 2H], 6.90 [s, 2H], 6.94 [d, 1H,  $J_{HH} = 7.2$  Hz]. Isomer 2:  $^1H$  NMR ( $C_6D_6$ ):  $\delta$  2.12 [s, 6H], 2.16 [s, 12H], 6.74

[s, 4H], 6.83 [s, 1H].  $^{13}\text{C}\{^1\text{H}\}$  NMR ( $\text{C}_6\text{D}_6$ ):  $\delta$  18.62, 18.86, 19.14, 21.18, 21.27, 21.29, 129.50, 129.74, 129.83, 134.52, 134.93, 135.97, 144.44, 146.77.

***N,N'*-Bis(2-methylphenyl)formamidine (2a)**. Prepared according to the above general procedure (140 °C) in 90% yield as a white semi-crystalline solid.  $^1\text{H}$  NMR ( $\text{C}_6\text{D}_6$ ):  $\delta$  2.03 [s, 6H], 6.87-7.04 [m, 8H], 7.68 [s, 1H].  $^{13}\text{C}\{^1\text{H}\}$  NMR ( $\text{C}_6\text{D}_6$ ):  $\delta$  18.20, 118.50, 123.95, 127.59, 131.24, 147.92.

***N,N'*-Bis(2,6-diisopropylphenyl)formamidine (3a)**. Prepared according to the above general procedure (160 °C) in 85% yield as a white semi-crystalline solid. Major isomer(>95%):  $^1\text{H}$  NMR ( $\text{C}_6\text{D}_6$ ):  $\delta$  1.12 [d, 24H,  $J_{\text{HH}} = 6.7$  Hz], 3.42 [sept, 4H,  $J_{\text{HH}} = 6.7$  Hz], 6.99-7.1 [m, 6H].  $^{13}\text{C}\{^1\text{H}\}$  NMR ( $\text{C}_6\text{D}_6$ ):  $\delta$  24.11, 28.71, 123.84, 126.23 (br), 144.17 (br), 155.92 (br).

***N,N'*-Bis(2-tert-butylphenyl)formamidine (4a)**. Prepared according to the above general procedure (160 °C) and was obtained in 85% yield as a white solid.  $^1\text{H}$  NMR ( $\text{CD}_2\text{Cl}_2$ ):  $\delta$  1.50 [s, 18H], 7-7.5 [m, 8H], 7.86 [s, 1H].  $^{13}\text{C}\{^1\text{H}\}$  NMR ( $\text{CD}_2\text{Cl}_2$ ):  $\delta$  30.81, 35.55, 121.99, 124.27, 127.01, 127.52, 148.22. HRMS (FAB<sup>+</sup>) calculated for  $\text{C}_{21}\text{H}_{29}\text{N}_2$  [ $\text{M}^+$ ] 309.2331, observed 309.2325.

### General Procedure for the Preparation of Unsymmetric Formamidines

Acetic acid (86  $\mu\text{L}$ , 1.5 mmol) was added to a round bottom flask charged with the first aniline (30 mmol, 1 equiv) and triethyl orthoformate (5 mL, 30 mmol, 1 equiv). The flask was fitted with a distillation head and was heated with stirring to 140 °C until ethanol (3.5 ml, 60 mmol, 2 equiv) was collected by distillation. The second substituted

aniline (30 mmol, 1 equiv) was then added to the reaction mixture. Heating at 140 °C continued until ethanol (1.75 mL, 30 mmol, 1 equiv) was collected by distillation. Upon cooling to room temperature, the solution solidified. The crude product was triturated with cold hexanes and collected by vacuum filtration. Solids were then dissolved in minimal hot acetone and recrystallized at -15 °C to remove traces of symmetric formamidine byproducts. The crystals were collected by vacuum filtration and dried *in vacuo*, providing pure product (82%-86%). The following formamidines were prepared by this procedure:

***N*-(2,6-difluorophenyl)-*N'*-(2,4,6-trimethylphenyl)formamidine (5a).** Prepared according to the above general procedure in 86% yield as colorless needles.  $^1\text{H}$  NMR (DMSO- $d_6$ ):  $\delta$  2.21 [s, 6H], 2.23 [s, 3H], 6.89-7.1 [m, 5H], 7.83 [s, 1H], 8.70 [s, 1H].  $^{13}\text{C}\{^1\text{H}\}$  NMR (DMSO- $d_6$ ):  $\delta$  18.20, 20.51, 111.34, 111.54, 111.65, 121.41, 128.35, 128.81, 133.10, 134.74, 135.30, 152.34.  $^{19}\text{F}\{^1\text{H}\}$  NMR (DMSO- $d_6$ ):  $\delta$  -126.87 [s]. HRMS (FAB $^+$ ) calculated for  $\text{C}_{16}\text{H}_{17}\text{N}_2\text{F}_2$  [ $\text{M}^+$ ] 275.1357, observed 275.1360.

***N*-(2,6-diisopropylphenyl)-*N'*-(2-methylphenyl)formamidine (6a).** Prepared according to the above general procedure in 82% yield as faintly pink plates. In  $\text{CDCl}_3$  (25 °C) this formamidine exists in two isomeric forms in a 2:1 ratio (unassigned).  $^1\text{H}$  NMR chemical shifts that differ between isomers will be denoted by (maj) and (min).  $^1\text{H}$  NMR ( $\text{CDCl}_3$ ):  $\delta$  1.22 [d, 12H,  $J_{\text{HH}} = 6.9$  Hz], 1.975(min) [s, 1H], 2.31(maj) [s, 2H], 3.13(min) [sept, 0.68H,  $J_{\text{HH}} = 6.9$  Hz], 3.24(maj) [sept, 1.32H,  $J_{\text{HH}} = 6.9$  Hz], 6.95-7.26 [m, 7H], 7.79(maj) [s, 0.66H], 7.91(min) [d, 0.34H,  $J_{\text{HH}} = 11$  Hz].  $^{13}\text{C}\{^1\text{H}\}$  NMR ( $\text{CD}_2\text{Cl}_2$ ):  $\delta$  18.15, 18.24, 23.83, 24.01, 28.55, 116.90, 118.30, 123.31, 123.58, 123.74, 123.85, 123.97, 124.35, 126.80,

126.85, 126.89, 127.38, 127.76, 131.04, 131.52, 139.18, 143.98. HRMS (FAB<sup>+</sup>) calculated for C<sub>20</sub>H<sub>27</sub>N<sub>2</sub> [M<sup>+</sup>] 295.2174, observed 295.2175.

### Preparation of Imidazolinium Chlorides

Three procedures were used to prepare the imidazolinium chlorides.

#### From the Corresponding Formamidine

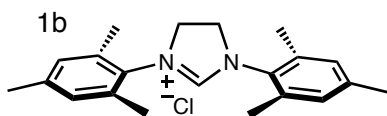
**Method A:** Diisopropylethylamine (0.96 mL, 5.5 mmol, 1.1 equiv) was added to a stirred solution of formamidine (5 mmol, 1 eq) and dichloroethane (3.8 mL, 50 mmol, 10 equiv) in a Schlenk tube. The tube was evacuated until the solvent began to bubble, then sealed under static vacuum and heated to 120 °C for 24-168 hours. The reaction mixture was then cooled to room temperature, and excess dichloroethane was removed *in vacuo*. The residue was triturated with acetone or hot toluene, and the product was collected by vacuum filtration, washed with excess solvent and dried *in vacuo*, providing pure product as a colorless powder (85%-95%). Upon sitting overnight, the diisopropylethylamine hydrochloride precipitated from the filtrate.

**Method B:** Dichloroethane (7.6 mL, 100 mmol, 10 equiv) was added to a Schlenk flask charged with formamidine (10 mmol, 1 equiv). The tube was evacuated until the solvent began to bubble, then sealed under static vacuum and heated to 120 °C for 24-168 hours. The reaction mixture was then cooled to room temperature, and excess dichloroethane was removed *in vacuo*. The residue was triturated with acetone or hot toluene, and the product was collected by vacuum filtration, washed with excess solvent and dried *in vacuo*, providing pure product as a colorless powder (85%-95%). Upon sitting overnight, the formamidine hydrochloride precipitated from the filtrate.

### From the Corresponding Aniline

Dichloroethane (1.9 mL, 25 mmol, 5 equiv) was added to a Schlenk flask charged with the aniline (10 mmol, 2 equiv) and triethyl orthoformate (0.83 mL, 5 mmol, 1 equiv). The tube was evacuated until solvent began to bubble, then sealed under static vacuum and heated to 120 °C for 24-36 hours. The reaction mixture was then cooled to room temperature. Unreacted substrates were then removed *in vacuo*. The residue was triturated with acetone or hot toluene, and the product was collected by vacuum filtration, washed with excess solvent and dried *in vacuo*, providing pure product as a colorless powder (85%-95%). Upon sitting overnight, the formamidine hydrochloride precipitated from the filtrate.

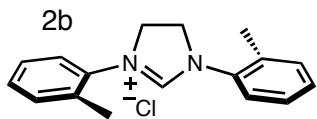
**1,3-Bis(2,4,6-trimethylphenyl)-imidazolinium chloride (1b).** Prepared according to



methods **A** (92%), **B** (49%), and **C** (45%) in 24 hours.

The product was collected as a white solid after trituration with boiling toluene. The NMR data are in accordance with those reported.<sup>16</sup> <sup>1</sup>H NMR (CDCl<sub>3</sub>): δ 2.29 [s, 6H], 2.31 [s, 12H], 4.49 [s, 4H], 6.87 [s, 4H], 9.46 [s, 1H]. <sup>13</sup>C{<sup>1</sup>H} NMR (CDCl<sub>3</sub>): δ 18.09, 21.15, 52.02, 130.03, 130.39, 135.07, 140.41, 160.14.

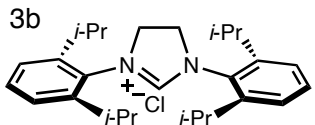
**1,3-Bis(2-methylphenyl)-imidazolinium chloride (2b).** Prepared according to methods



**A** (43%), **B** (48%), and **C** (26%) in 24 hours. The product

was collected as a white solid after trituration with acetone. The NMR data are in accordance with those reported.<sup>17</sup> <sup>1</sup>H NMR (CDCl<sub>3</sub>): δ 2.43 [s, 6H], 4.64 [s, 4H], 7.21-7.79 [m, 8H], 8.86 [s, 1H]. <sup>13</sup>C{<sup>1</sup>H} NMR (CDCl<sub>3</sub>): δ 18.34, 53.07, 126.82, 127.80, 130.0, 131.78, 133.66, 134.57, 157.68.

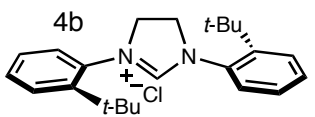
**1,3-Bis(2,6-diisopropylphenyl)-imidazolinium chloride (3b).** Prepared according to



methods **A** (91%), **B** (46%), and **C** (42%) in 36 hours. The product was collected as a white solid after trituration with minimal acetone. The NMR data are in accordance with

those reported.  $^1\text{H}$  NMR ( $\text{CDCl}_3$ ):  $\delta$  1.22 [d, 12H,  $J_{\text{HH}} = 6.9$  Hz], 1.35 [d, 12H,  $J_{\text{HH}} = 6.9$  Hz], 2.97 [sept, 4H,  $J_{\text{HH}} = 6.9$  Hz], 4.77 [s, 4H], 7.2-7.5 [m, 6H], 8.56 [s, 1H].  $^{13}\text{C}\{^1\text{H}\}$  NMR ( $\text{CDCl}_3$ ):  $\delta$  23.90, 25.61, 29.36, 55.52, 125.14, 129.39, 131.73, 146.24, 158.46.

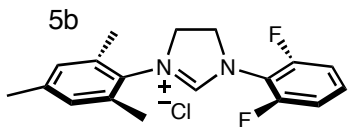
**1,3-Bis(2-tert-butylphenyl)-imidazolinium chloride (4b).** Prepared according to



methods **A** (91%) and **B** (46%) in 168 hours (7 days). The product was collected as a white solid after trituration in

acetone.  $^1\text{H}$  NMR ( $\text{CDCl}_3$ ):  $\delta$  1.46 [s, 18H], 4.86 [s, 4H], 7.35-7.50 [m, 6H], 7.97 [s, 1H], 8.70 [br, 2H].  $^{13}\text{C}\{^1\text{H}\}$  NMR ( $\text{CDCl}_3$ ):  $\delta$  32.36, 35.96, 56.68, 128.21, 128.98, 130.93, 132.43, 134.14, 146.28, 159.19. HRMS (FAB $^+$ ) calculated for  $\text{C}_{23}\text{H}_{31}\text{N}_2$  [ $\text{M}^+$ ] 335.2487, observed 335.2479.

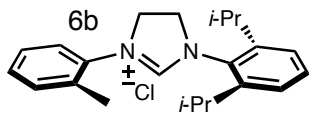
**1-(2,6-difluorophenyl)-3-(2,4,6-trimethylphenyl)-imidazolinium chloride (5b).**



Prepared according to methods **A** (75%) and **B** (41%) in 36 hours. The product was collected as a white solid after trituration with acetone. The NMR data are in accordance

with those reported.  $^{18}\text{H}$  NMR ( $\text{DMSO}-d_6$ ):  $\delta$  2.29 [s, 3H], 2.31 [s, 6H], 4.42-4.5 [m, 2H], 4.6-4.7 [m, 2H], 7.1 [s, 2H], 7.41-7.47 [m, 2H], 7.57-7.67 [m, 2H], 9.45 [s, 1H].  $^{13}\text{C}\{^1\text{H}\}$  NMR ( $\text{DMSO}-d_6$ ):  $\delta$  17.15, 20.57, 51.53, 112.88, 113.17, 129.5, 130.7, 135.13, 139.84, 161.06.  $^{19}\text{F}\{^1\text{H}\}$  NMR ( $\text{DMSO}-d_6$ ):  $\delta$  -119.84 [s].

**1-(2,6-diisopropylphenyl)-3-(2-methylphenyl)-imidazolinium chloride (6b).** Prepared



according to methods **A** (80%) and **B** (43%) in 24 hours. The product was collected as a white solid after trituration with acetone.  $^1\text{H}$  NMR ( $\text{CDCl}_3$ ):  $\delta$  1.22 [d, 6H,  $J_{\text{HH}} = 6.6$  Hz], 1.28 [d, 6H,  $J_{\text{HH}} = 6.6$  Hz], 2.41 [s, 3H], 3.05 [sept, 2H,  $J_{\text{HH}} = 6.6$  Hz], 4.44-4.52 [m, 2H], 4.76-4.83 [m, 2H], 7.18-7.28 [m, 5H], 7.36-7.41 [m, 1H], 7.6-7.63 [m, 1H], 9.15 [s, 1H].  $^{13}\text{C}\{^1\text{H}\}$  NMR ( $\text{CDCl}_3$ ):  $\delta$  18.16, 24.07, 25.18, 28.83, 53.25, 54.43, 124.83, 126.05, 127.72, 129.83, 131.13, 131.87, 133.15, 134.18, 146.31, 158.58. HRMS ( $\text{FAB}^+$ ) calculated for  $\text{C}_{25}\text{H}_{29}\text{N}_2$  [ $\text{M}^+$ ] 321.2331, observed 321.2342.

## References and Notes

---

- (1) Arduengo, A. J., III; Harlow, R. L.; Kline, M. A. *J. Am. Chem. Soc.* **1991**, *113*, 361–363.
- (2) (a) Bourissou, D.; Guerret, O.; Gabbai, F. P.; Bertrand, G. *Chem. Rev.* **2000**, *100*, 39–91. (b) Herrmann, W. A. *Angew. Chem., Int. Ed.* **2002**, *41*, 1290–1309. (c) Peris, E.; Crabtree, R. H. *Coord. Chem. Rev.* **2004**, *248*, 2239–2246. (d) Crudden, C. M.; Allen, D. P. *Coord. Chem. Rev.* **2004**, *248*, 2247–2273. (e) Diez-Gonzalez, S.; Nolan, S. P. *Coord. Chem. Rev.* **2007**, *251*, 874–883.
- (3) (a) Scholl, M.; Trnka, T. M.; Morgan, J. P.; Grubbs, R. H. *Tetrahedron Lett.* **1999**, *40*, 2247–2250. (b) Scholl, M.; Ding, S.; Lee, C. W.; Grubbs, R. H. *Org. Lett.* **1999**, *1*, 953–956. (c) Huang, J. K.; Stevens, E. D.; Nolan, S. P.; Peterson, J. L. *J. Am. Chem. Soc.* **1999**, *121*, 2674–2678.
- (4) For a review of recent work, see: Marion, N.; Diez-Gonzalez, S.; Nolan, S. P. *Angew. Chem., Int. Ed.* **2007**, *46*, 2988–3000.
- (5) (a) Öfele, K. *J. Organomet. Chem.* **1968**, *12*, P42–P43. (b) Herrmann, W. A.; Köcher, C.; Goossen, L. J.; Artus, G. R. *J. Chem.-Eur. J.* **1996**, *2*, 1627–1636. (c) Méry, D.; Aranzaes, J. R.; Astruc, D. *J. Am. Chem. Soc.* **2006**, *128*, 5602–5603.
- (6) Arduengo, A. J., III *Preparation of 1,3-Disubstituted Imidazolium Salts*, **1991**, U.S. Patent No. 5077414.
- (7) Arduengo, A. J., III; Krafczyk, R.; Schmutzler, R. *Tetrahedron* **1999**, *55*, 14523–14534.
- (8) For recent examples, see: (a) Ritter, T.; Day, M. W.; Grubbs, R. H. *J. Am. Chem. Soc.* **2006**, *128*, 11788–11789. (b) Stylianides, N.; Danopoulos, A. A.; Pugh, D.;

- 
- Hancock, F.; Zanotti-Gerosa, A. *Organometallics*, **2007**, *26*, 5627–5635.
- (c) Courchay, F. C.; Sworen, J.C.; Ghiviriga, I.; Abboud, A.; Wagener, K. B. *Organometallics* **2006**, *25*, 6074–6086. (d) Beletskaya, I. P.; Bessmertnykh, A. G.; Averin, A. D.; Denat, F.; Guillard, R. *Eur. J. Org. Chem.* **2005**, 261–280.
- (9) (a) Vougioukalakis, G. C.; Grubbs, R. H. *Organometallics* **2007**, *26*, 2469–2472. (b) Winkelmann, O.; Linder, D.; Lacuor, J.; Näther, C.; Lüning, U. *Eur. J. Org. Chem.* **2007**, *22*, 3687–3697.
- (10) (a) Jazzar, R.; Liang, H.; Donnadiu, B.; Bertrand, G. *J. Organomet. Chem.* **2006**, *691*, 3201–3205. (b) Jazzar, R.; Bourg, J. B.; Dewhurst, R. D.; Donnadiu, B.; Bertrand, G. *J. Org. Chem.* **2007**, *72*, 3492–3499.
- (11) Compounds are numbered according to their entry number in Table 4.1; (a) denotes the formamidine and (b) denotes the imidazolinium chloride.
- (12) Dains, F. B.; Malleis, O. O.; Meyer, J. T. *J. Am. Chem. Soc.* **1913**, *35*, 970–976.
- (13) (a) Yield in parentheses based on a 50% theoretical yield with half of the substrate considered as a sacrificial base.
- (14) (a) Isolated yield of the desired imidazolinium chloride. (b) Yield in parentheses based on a 50% theoretical yield with half of the substrate considered as a sacrificial base. (c) A suitable non-nucleophilic base could not be found to replace the formamidine as base. (d) While neither reaction had reached 100% conversion, the reactions were stopped after 7 days.
- (15) (a) Isolated yield of the desired imidazolinium chloride. (b) Yield in parentheses based on a 50% theoretical yield with half of the substrate considered as a sacrificial base.
- (16) A. J. Arduengo III et al. *Tetrahedron* **1999**, *55*, 14523–14534.

- 
- (17) Stewart, I. C.; Ung, T.; Pletnev, A. A.; Berlin, J. M.; Grubbs, R. H.; Schrodi, Y.  
*Org. Lett.* **2007**, *9*, 1589–1592.
- (18) Vougioukalakis, G. C.; Grubbs, R. H.; *Organometallics* **2007**, *26*, 2469–2472.

## Chapter 5

### Chiral Triazolylidenes and CAACs as Ligands for Use in Enantioselective Olefin Metathesis Catalysts

**Abstract**

Both chiral triazolylidenes and cyclic alkyl amino carbenes (CAACs) were chosen as ligands for the preparation of chiral ruthenium olefin metathesis catalysts. These  $C_1$  symmetric ligands were chosen to create non-conformationally flexible environments in proximity to the ruthenium center, potentially bringing chirality extremely close to the site of catalysis. These new motifs for ligand architecture show great promise. The moderate enantioselectivities obtained herein for AROCM and ARCM indicate a potential utility for both synthetic methodology and mechanistic insight. Due to the abundance of chiral starting materials and facile ligand synthesis, the most rational approach to understanding the structure/enantioselectivity relationship in these systems is the preparation of related ligands.

***Enantioselective Olefin Metathesis***

To date, olefin metathesis has played only a supporting role in the synthesis of optically pure materials. In general, optically pure olefin products are derived from optically pure substrates or are resolved from racemic product mixtures.<sup>1</sup> Although these methods have proven effective in many cases, it would be advantageous to transform achiral or racemic substrates into complex optically pure olefin metathesis products via olefin metathesis.

A highly enantioselective olefin metathesis catalyst could produce chiral molecules in a single step that are typically unavailable by other methods or that can only be reached by multi-step reaction pathways. Because no  $sp^3$ -hybridized carbons are formed during a metathesis reaction, asymmetric induction in the reaction does not seem possible at first glance. Instead, asymmetric metathesis reactions form chiral compounds through either kinetic resolutions of racemates or desymmetrizations of

achiral or meso compounds. Metathesis applications already commonly in use are thus easily rendered asymmetric (Figure 5.1).

The kinetic resolutions ideally involve selective ring closing of one enantiomer of a chiral diene while leaving the other enantiomer untouched. Asymmetric ring-closing metathesis (ARCM) and asymmetric cross-metathesis (ACM) are intramolecular and intermolecular reactions that result in the formation of a chiral center through desymmetrizations of trienes or dienes, respectively. Asymmetric ring-opening/cross-metathesis (AROCM) reactions create multiple chiral centers by desymmetrizing meso compounds.

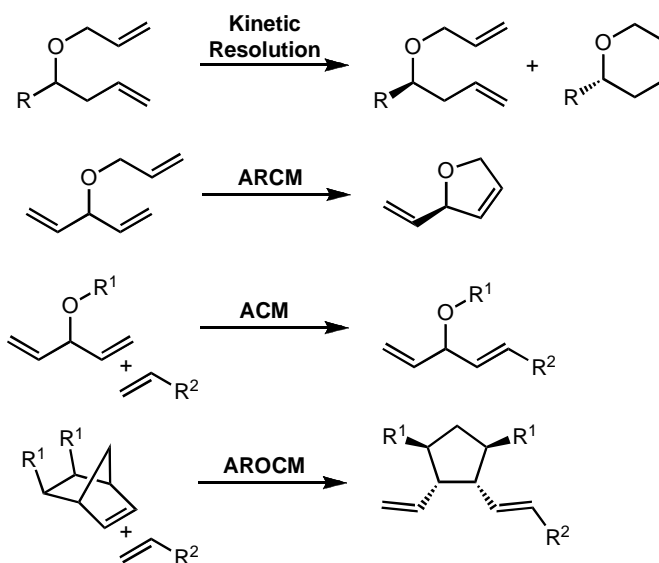


**Figure 5.1.** Examples of asymmetric olefin metathesis.

### Asymmetric Molybdenum Catalysts

Fujmura and Grubbs made a major advancement in the field of enantioselective olefin metathesis with the development of the first chiral molybdenum catalyst (**5.1**) that demonstrated mild selectivity in kinetic resolution reactions (Figure 5.2).<sup>2</sup> Since then, Hoveyda and Schrock have prepared numerous catalysts based on the same bidentate chiral ligand motif, such as **5.2**, that show high enantioselectivity in ring-closing and ring-

opening metathesis reactions.<sup>3</sup> More recently, they have found great success with molybdenum complexes that are both stereogenic at the metal and bear only monodentate ligands. For example, complex **5.3** was used successfully in the total synthesis of the natural product (+)-quebrachamine.<sup>4</sup>

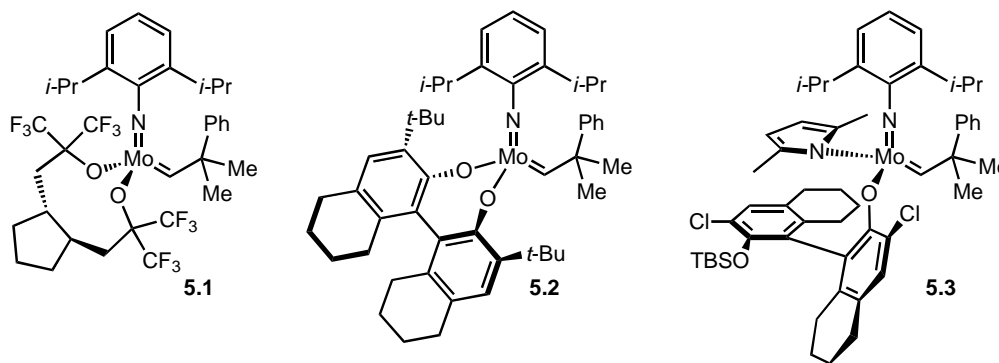


**Figure 5.2.** Representative asymmetric molybdenum catalysts.

Unfortunately, the above molybdenum catalysts possess the same functional group tolerance and stability problems of earlier molybdenum catalysts. Most molybdenum systems also require specific substrate-to-catalyst matching, necessitating the preparation of numerous catalysts and extensive reaction optimization.

### Asymmetric Ruthenium Catalysts

Due to the expected increase in functional group tolerance and stability, the development of ruthenium-based enantioselective olefin metathesis catalysts has been of considerable interest. Although the utilization of either chiral phosphine or chiral *N*-heterocyclic carbene (NHC) ligands could be envisioned to provide the necessary chirality in the standard systems, studies have focused on NHCs due to the increased activity and stability of the resulting catalysts. Furthermore, *N*-heterocyclic carbenes are quite suitable for chiral modification.<sup>5</sup>

Three classes of chiral ruthenium catalysts have been explored (Figure 5.3). The first class, developed by Grubbs and co-workers, contains  $C_2$ -symmetric monodentate

NHCs (**5.4**).<sup>6</sup> The second, developed by Hoveyda and co-workers, contains  $C_1$ -symmetric bidentate NHCs (**5.5**).<sup>7</sup> Recent work by Collins has shown that  $C_1$ -symmetric monodentate NHCs are also viable as ligands in the ruthenium-based systems (**5.6**).<sup>8</sup>

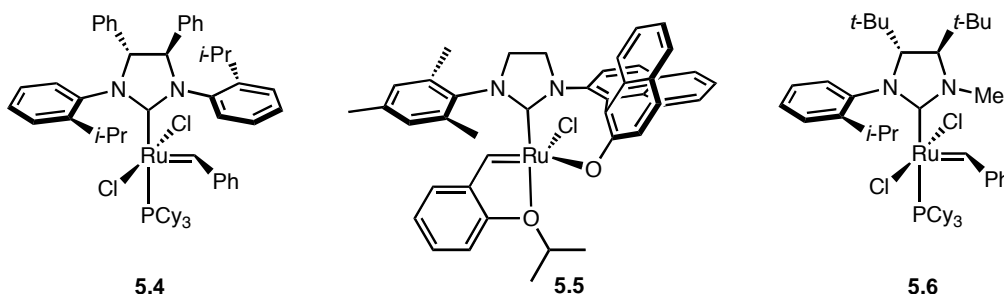


**Figure 5.3.** Examples of ruthenium-based asymmetric olefin metathesis catalysts.

Despite these successes, there still remains a need for further catalyst development. Chiral ruthenium catalysts developed to date still lack substrate generality: enantioselectivity drops dramatically with only minor changes in the substrate structure. Furthermore, a complex that can efficiently catalyze the asymmetric cross metathesis of olefins has yet to be developed. Further catalyst development should continue to employ NHCs due to their functional group tolerance, ease of use, and the myriad of possibilities in chiral modification.

Intrigued by Collins' successful use of  $C_1$ -symmetric monodentate NHCs in catalyst design, exploration of novel  $C_1$ -symmetric carbenes was envisioned. Unfortunately, while chiral transfer through gearing has proven mildly effective, the large degree of rotational freedom about the  $N$ -bound arenes may result in inadequate transfer and lower enantioselectivity. With that in mind, chiral triazolylidenes (**5.7**) and cyclic alkyl amino carbenes (CAACs) (**5.8**) were chosen as ligands (Figure 5.4) to create non-conformationally flexible environments in proximity to the ruthenium center, engendering constrained chiral space at the site of catalysis.

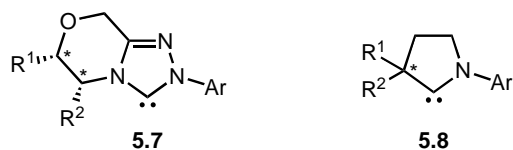


**Figure 5.4.**  $C_1$ -symmetric monodentate ligands chosen for study.

## Results and Discussion

### Chiral Triazolylidenes<sup>†</sup>

Triazolyl NHCs, conveniently prepared from readily available chiral amino-alcohols using a modified literature procedure,<sup>10b</sup> have been previously employed, among others, in the Benzoin condensation<sup>9</sup> and Stetter reaction.<sup>10</sup> The abundance of chiral amino-alcohols allows for direct ligand modification and optimization. Triazolium salts, the carbene precursors, are air- and water-stable crystalline solids. The chiral amino-alcohol (1*R*, 2*S*)-(+)-*cis*-1-amino-2-indanol was initially chosen as the building block for ligand design due to the rigid steric environments that its structure would create in the ruthenium systems.

### Complex 5.13

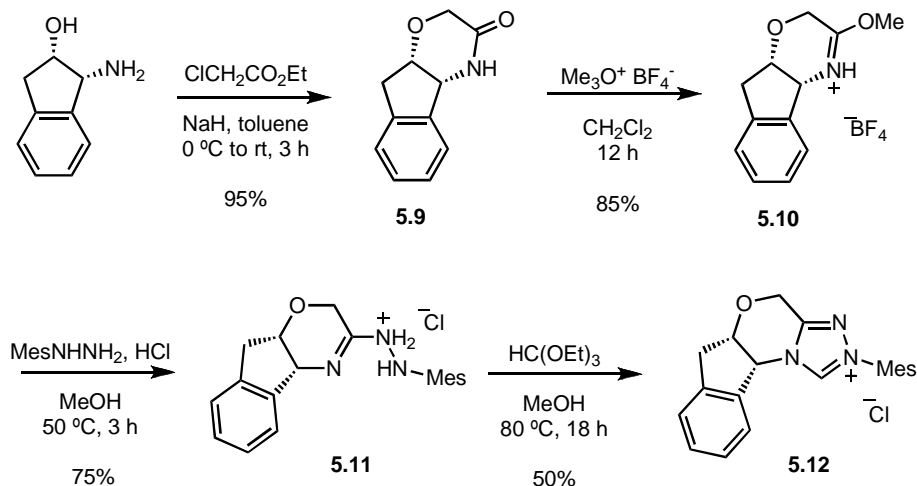
First, the triazolium salt (**5.12**) was prepared from commercially available (1*R*, 2*S*)-(+)-*cis*-1-amino-2-indanol (Scheme 5.1). Reaction of the amino-alcohol and ethyl chloroacetate, using the method of Clarke,<sup>11</sup> led to substituted morpholin-3-one **5.9**. Methylation with Meerwein's reagent afforded imino ether **5.10**, and subsequent reaction with mesitylhydrazine hydrochloride gave amidrazone hydrochloride **5.11**. Heating with

---

<sup>†</sup> This work was completed in 2005 and is reproduced in part from my candidacy progress report.

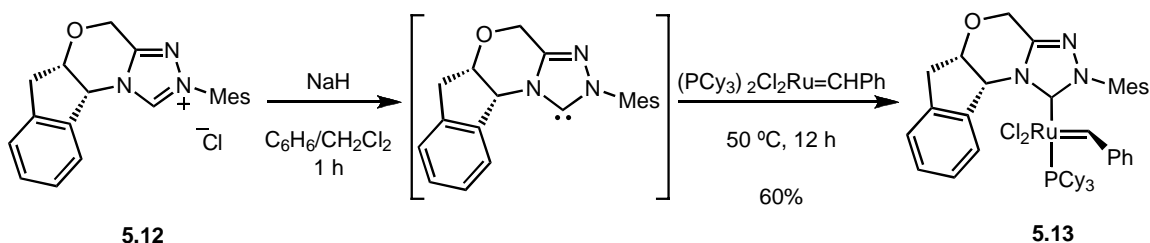
triethyl orthoformate effected the formylation and cyclization of **5.11**, cleanly yielding triazolium salt **5.12** (29% overall yield from the amino-alcohol).

**Scheme 5.1.** Synthesis of aminoindanol-derived triazolium salt **5.12**.



In situ formation of the carbene from **5.12** by deprotonation with NaH in a 50/50 solvent mixture of benzene and methylene chloride (Scheme 5.2), followed by the addition of  $(\text{PCy}_3)_2\text{Cl}_2\text{Ru}=\text{CHPh}$  and subsequent heating to 50 °C, resulted in a 60% yield of the desired complex (5,6-Indenyl-2-Mes-Tri) $(\text{PCy}_3)(\text{Cl})_2\text{Ru}=\text{CHPh}$  (**5.13**). This reaction could be performed on up to a 200 mg scale without loss in efficiency.

**Scheme 5.2.** Synthesis of chiral triazolylidene complex **5.13**.

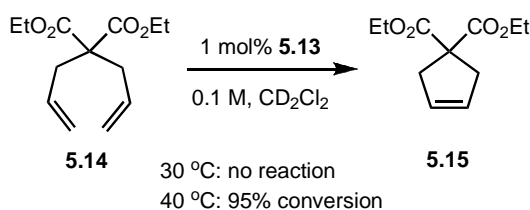


The complex displays a singlet at 19.9 ppm in the  $^1\text{H}$  NMR ( $\text{C}_6\text{D}_6$ ) and a singlet at 36.3 ppm in the  $^{31}\text{P}$  NMR. Compound **5.13** was found to be stable in benzene for over 24 hours at ambient temperature, as well as stable to heating for 24 hours at 40 °C. In addition, the complex is stable to air in the solid state and to flash chromatography on silica gel. To date, crystallization efforts have proven unsuccessful.

### Activity in Olefin Metathesis

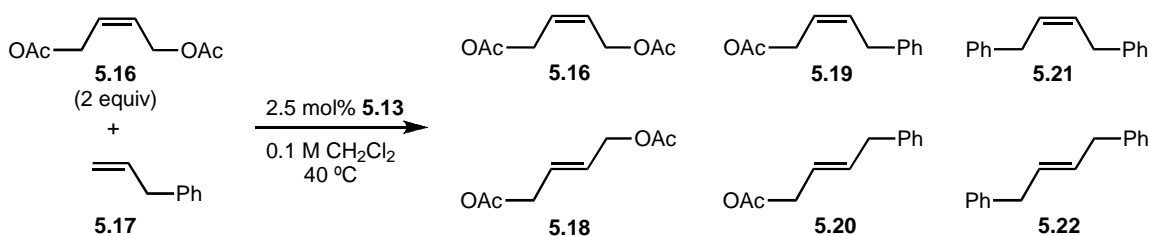
General metathesis activity of **5.13** was first evaluated in the RCM of diethyl diallyl malonate (**5.14**) (Scheme 5.3). Standard procedure calls for the reaction to be at 30 °C, but initial attempts at this temperature resulted in no reaction.<sup>12</sup> Increasing the reaction temperature to 40 °C resulted in 95% conversion to **5.15** after a thirty-minute reaction time. The necessary increase in temperature is most likely due to slow initiation of the catalyst into the catalytic cycle or slow propagation due to the steric bulk of the ligand. Studies to understand this temperature effect have not yet been undertaken.

**Scheme 5.3.** Screening of complex **5.13** in RCM.



The reactivity and diastereoselectivity of catalyst **5.13** were then tested in the olefin cross metathesis of *cis*-1,4-diacetoxy-2-butene (**5.16**) with allyl benzene (**5.17**) (Scheme 5.4). This reaction allows for examination of both the catalyst's diastereoselectivity in the formation of the cross product (**5.19** versus **5.20**) and the catalyst's propensity for secondary metathesis by monitoring the isomerization of **5.16** to **5.18**. Reaction progress was monitored via gas chromatography using tridecane as an internal standard.

**Scheme 5.4.** Screening diastereoselectivity of complex **5.13**.



The cross metathesis reaction catalyzed by **5.13** was monitored for 24 hours and did not reach completion. The results, in terms of both reactivity and selectivity, were comparable to the chiral bidentate catalyst (**5.5**). Figure 5.5 illustrates the isomerization of the *cis*-1,4-diacetoxy-2-butene starting material (**5.16**) as a function of the disappearance of the cross partner, allyl benzene (**5.17**).

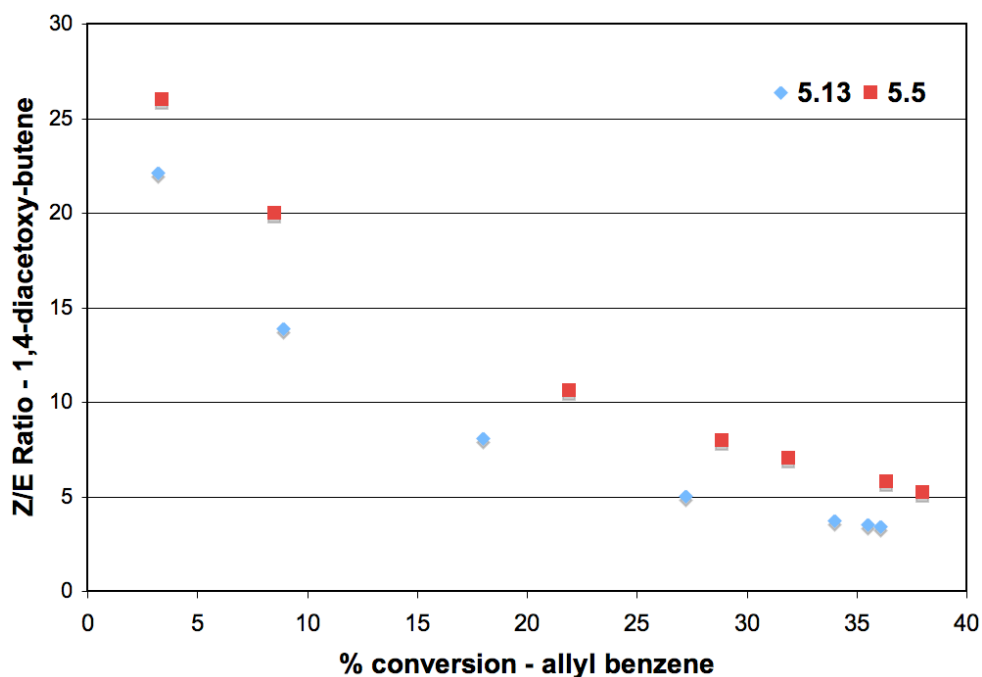


**Figure 5.5.** Isomerization of **5.16** by complex **5.13**.

With a *Z*-selective catalyst, isomerization of the predominantly *cis* starting material should be minimal, as any non-productive metathesis should regenerate the *cis*-olefin. However, as seen in Figure 5.5, the starting material was isomerized to the *trans*-olefin. Another strong indication of a *Z*-selective catalyst would be a low *E/Z* ratio of the cross-metathesis product. However, the major product observed at equilibrium was the *trans* product (**5.20**). Figure 5.6 compares this result with **5.5**, as well as the much more active **5.23** ( $\text{H}_2\text{IMes})(\text{PCy}_3)\text{Cl}_2\text{Ru}=\text{CHPh}$ . This comparison illustrates both the poor activity and diastereoselectivity of **5.13** in cross metathesis.

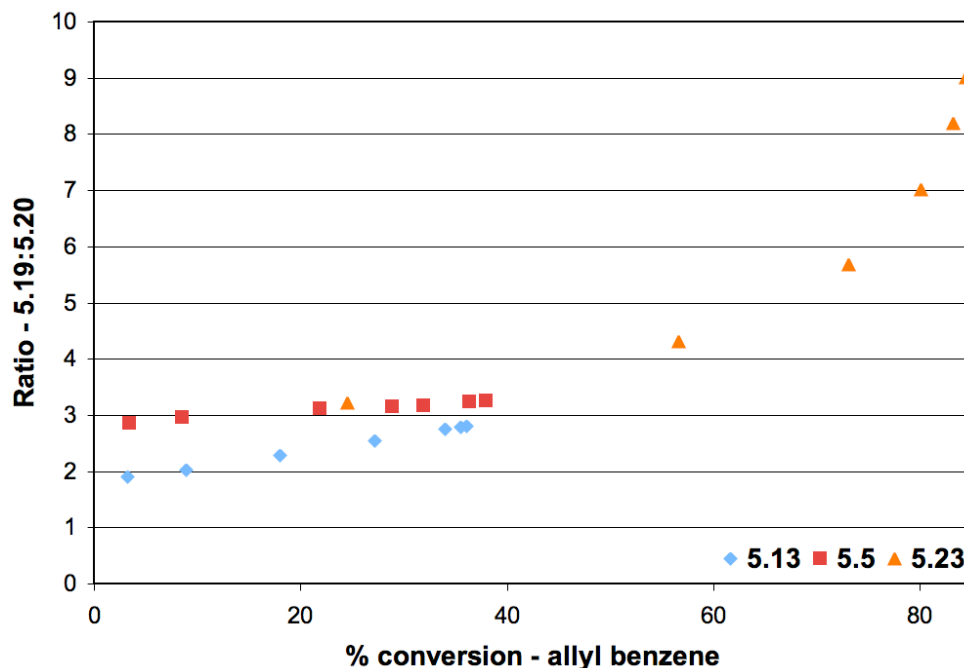
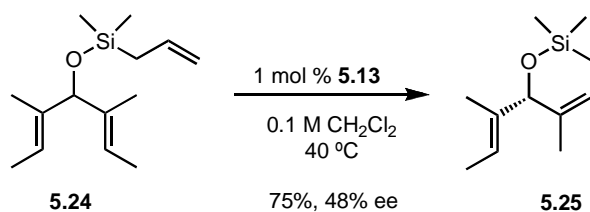


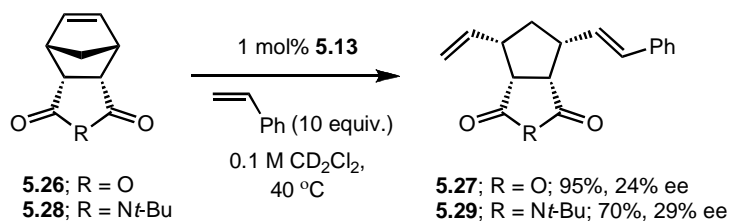
**Figure 5.6.** E/Z ratio of cross-metathesis products.

The enantioselectivity of **5.13** was then studied using several standard, asymmetric olefin metathesis reactions.<sup>6</sup> The ARCM of substrate **5.24** resulted in a promising 75% conversion to **5.25** with 48% ee (Scheme 5.5). For comparison, complex **5.4** provides the product in 98% yield and 83% ee. Despite the moderate enantioselectivity, this reaction set precedence for triazolyl *N*-heterocyclic carbene-ligated ruthenium complexes transferring chirality in metathesis.

**Scheme 5.5.** ARCM of **5.24** with complex **5.13**.



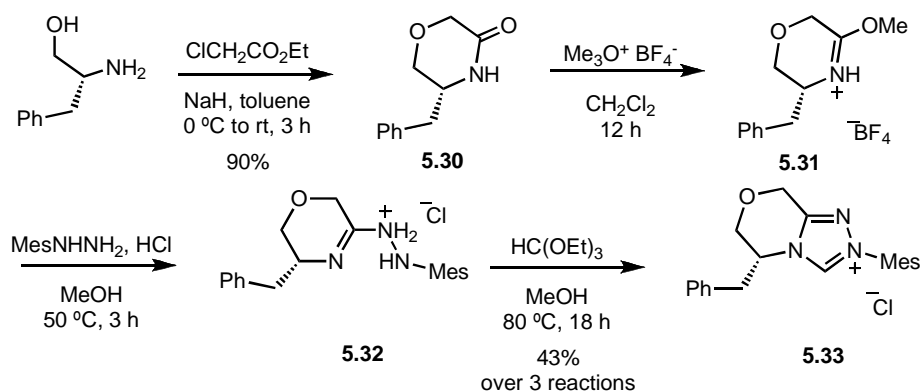
Results in asymmetric ring-opening cross metathesis were less promising. The AROCM of **5.26** and **5.28** resulted in the complete conversion to **5.27** and **5.29** with only 24% and 29% ee, respectively (Scheme 5.6).

**Scheme 5.6.** AROCM with complex **5.13**.

Although the enantioselectivity shown by **5.13** in AROCM and ARCM was lower than the previously reported chiral catalysts, the new motif for ligand design does show promise.<sup>6</sup> Employing an alternative amino alcohol starting material should provide a new steric environment around the metal, and comparison of this new complex to **5.13** could provide insight into the mode of enantioselectivity provided by the triazolium ligand motif.

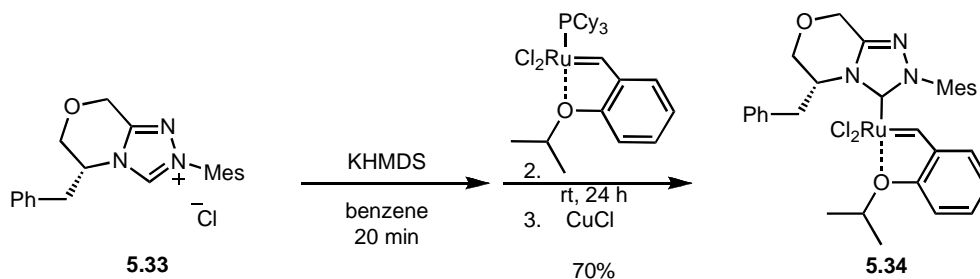
**Complex 5.34**

With that in mind, a triazolylidene ligand based on (*R*)-2-amino-3-phenyl-1-propanol was synthesized. Unlike in **5.12**, the phenyl functionality of the ligand has the potential for rotation, creating a less sterically rigid environment. Triazolium salt **5.33**, derived from commercially available (*S*)-2-Amino-3-phenyl-1-propanol, was synthesized by modifying the synthetic route to **5.12** and obtained in 39% overall yield from the amino-alcohol (Scheme 5.7).

**Scheme 5.7.** Synthesis of (*S*)-2-Amino-3-phenyl-1-propanol-derived triazolium salt **5.33**.

Standard carbene formation from **5.33** by deprotonation with KHMDS followed by addition of  $(\text{PCy}_3)\text{RuCl}_2=\text{CH}(\text{o-O}i\text{PrC}_6\text{H}_4)$  gave 70% conversion to two products after 24 hours at room temperature. After the addition of CuCl to scavenge free tricyclohexylphosphine, **5.34** was formed as the exclusive product (Scheme 5.8). This complex, purified by column chromatography, was found to be stable in benzene for over 24 hours at ambient temperature, but decomposition was evident after only four hours at 40 °C. To date, crystallization efforts have proven unsuccessful.

**Scheme 5.8.** Synthesis of chiral triazolylidene complex **5.34**.



The general metathesis activity of **5.34** was first tested in the RCM of diethyl diallyl malonate (**5.14**) but no reaction was evident at 30 °C. An increase in the reaction temperature to 40 °C resulted in only 20% conversion to **5.15** after two hours. This result was coupled with complete decomposition of the catalyst during the reaction period, as monitored by total loss of peaks in the alkylidene region of the  $^1\text{H}$  NMR. The attempted AROCM of **5.26** and of **5.28** with styrene also resulted in no reaction at room temperature or 30 °C. A reaction temperature of 40 °C resulted in complete catalyst decomposition without evidence of olefin metathesis. No decomposition products from these reactions could be isolated or identified.

Taken together, these results provided few clues about the structure/enantioselectivity relationship in the triazolylidene systems, which would allow for a rational approach in future research. With that in mind, further investigation into this motif was not conducted.

## Chiral CAACs<sup>§</sup>

Recently, another class of ruthenium based olefin metathesis catalysts, featuring  $C_1$  symmetric cyclic (alkyl) (amino) carbenes (CAACs), has emerged (Figure 5.7).<sup>13</sup> In some cases these species, such as **5.35** and **5.36**, compete or surpass the activity and/or selectivity observed with traditional NHC based catalysts.

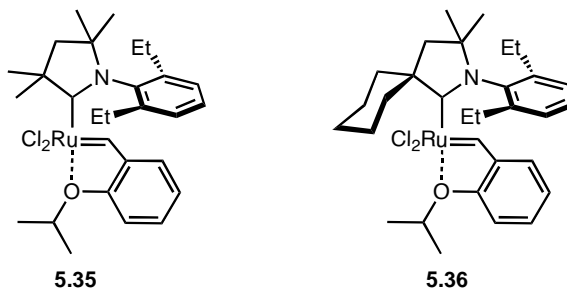


**Figure 5.7.** Examples of CAAC-based olefin metathesis catalysts.

CAACs differ from traditional NHCs in that they contain a quaternary carbon atom adjacent to the carbene center. The presence of this  $sp^3$  carbon atom increases the electron-donating ability of the ligand, and at the same time produces an unusual steric environment around the metal center. Moreover, due to the quaternary carbon atom in the  $\beta$ -position of the metal center, CAAC ligands have the potential to bring chirality closer to the site of catalysis.

It was anticipated that ruthenium alkylidenes containing a chiral CAAC ligand would afford highly efficient and enantioselective olefin metathesis catalysts. With that in mind, menthone was initially chosen as the building block for ligand design due to the rigid steric environment that its structure would create in the ruthenium systems.

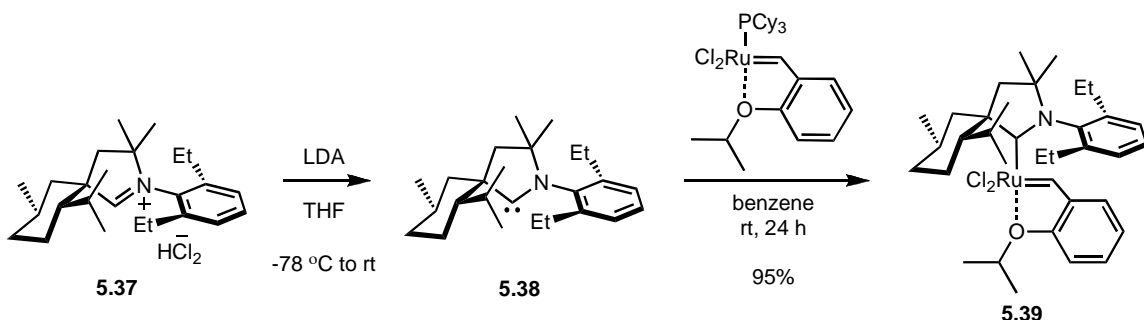
---

<sup>§</sup> This work has been completed in collaboration with Dr. Vincent Lavallo and Jean Li. Vince completed ligand synthesis and Jean has completed many of the metathesis reactions reported. I would like to thank them for their contribution to the project.

### Complex 5.39

Cyclic (alkyl) (amino) carbenes based on (-)-menthone have been previously reported by Bertrand and co-workers.<sup>14</sup> Under analogous experimental conditions, iminium chloride **5.37**, featuring a 2,6-diethylphenyl group was obtained in good yield. With this precursor in hand, the corresponding free carbene (**5.38**) was generated by treatment with lithium diisopropylamide (LDA) (Scheme 5.9). **5.38** was then reacted with commercially available  $(\text{PCy}_3)\text{RuCl}_2=\text{CH}(o\text{-O}i\text{PrC}_6\text{H}_4)$  at room temperature, affording the phosphine-free chelating ether complexes **5.39** over the course of 24 hours. This complex was isolated as a crystalline green solid after flash column chromatography.

**Scheme 5.9.** Synthesis of chiral CAAC complex **5.39**.



### Structural Analysis

To probe the electronic and steric effects of the ligated CAAC, crystals of **5.39** were grown and its molecular structure was confirmed by single-crystal X-ray crystallographic analysis (Figure 5.8). Like other ruthenium-based olefin metathesis catalysts, the complex exhibits a distorted square pyramidal geometry with the benzylidene moiety occupying the apical position.

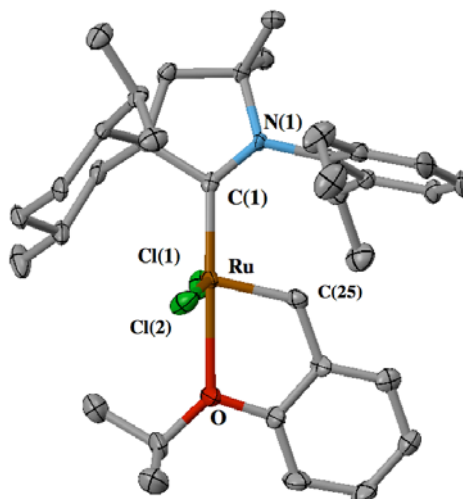


**Figure 5.8.** X-ray crystal structure of complex **5.39** is shown. Displacement ellipsoids are drawn at 50% probability. For clarity, hydrogen atoms have been omitted.

When compared with its dimethyl CAAC analog (**5.35**) and  $(\text{H}_2\text{IMes})(\text{PCy}_3)\text{Cl}_2\text{Ru}=(\text{=CH-}o\text{-O/PrC}_6\text{H}_4)$  (**5.40**),<sup>13,15</sup> the menthone substitution of **5.39** results in significant differences in both the Ru-C(1) bond length and the Ru-O bond length (Table 5.1).

**Table 5.1.** Selected X-ray data for **5.35**, **5.39**, and **5.40**.

	<b>5.35</b>	<b>5.39</b>	<b>5.40</b>
<b>Bond Lengths (Å)</b>			
Ru-C <sub>carbene</sub>	1.9482	1.961	1.981
Ru-C <sub>benzylidene</sub>	1.8367	1.837	1.828
Ru-O	2.2978	2.380	2.261
<b>Bond Angles (deg)</b>			
C <sub>carbene</sub> -Ru-O	178.07	173.69	176.2
C <sub>benzylidene</sub> -Ru-O	78.54	77.37	79.3
Cl(1)-Ru-Cl(2)	154.542	157.2	156.5

The bond distance between the ligand carbene carbon and the Ru center is longer in **5.39** (1.961 Å) than in **5.35** (1.948 Å), suggesting that the bulk of the menthone substituent pushes the ligand away from the metal center. However, this bond distance is shorter in **5.39** than in **5.40** (1.980 Å). This observation is consistent with the

increased  $\sigma$ -donating properties of the CAAC ligands over than NHC counterparts. The increased Ru-O bond distance in **5.39** (2.381 Å), relative to **5.40** (2.261 Å), supports this conclusion.

### Activity in Olefin Metathesis

General metathesis activity of **5.39** was first evaluated by performing the RCM of diethyl diallylmalonate (**5.14**) (Figure 5.9). The reaction, utilizing 1 mol% catalyst in  $C_6D_6$  at 30 °C, was monitored by  $^1H$  NMR spectroscopy. Note that the plot of cycloalkene **5.15** concentration versus time reveals that complex **5.39** does effect the cyclization of **5.14**, but with a slower reaction rate than the standard NHC complex **5.40**.

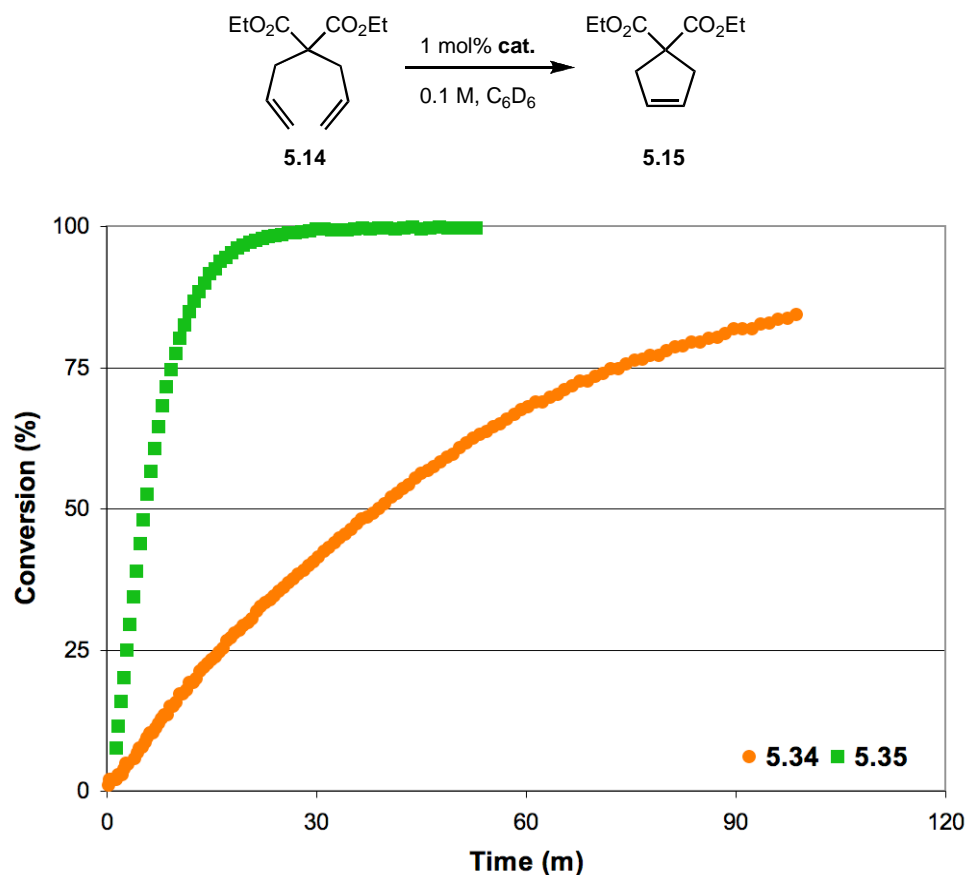
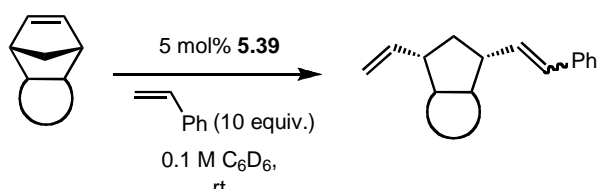


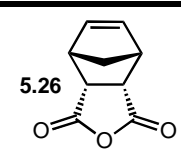
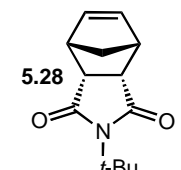
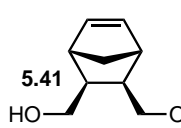
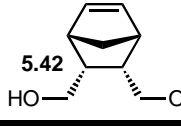
**Figure 5.9.** Screening of complex **5.39** in RCM.

As with the triazolylidene-based complexes, the enantioselectivity of CAAC-based complex (**5.39**) was then studied using known asymmetric olefin metathesis

reactions.<sup>6</sup> Preliminary results in asymmetric ring-opening cross metathesis were promising, but provided few details about how to move forward (Table 5.2). As was the case with the triazolylidene catalyst **5.13**, replacement of the anhydride oxygen with a *tert*-butylamine (**5.28**) increased the enantioselectivity of the reaction. When unprotected diols **5.41** and **5.42** were examined, the yields were dramatically reduced to 35% and ~38%, respectively. As discussed in the literature, substrate coordination to the catalyst may inhibit the reaction.<sup>6</sup> Surprisingly, the stereochemistry of the norbornene diols had little effect on the ee of the trans products as the *exo*-diol **5.41** gave 12% and the *endo*-diol **5.42** gave 19%.

**Table 5.2.** AROCM with complex **5.39**.

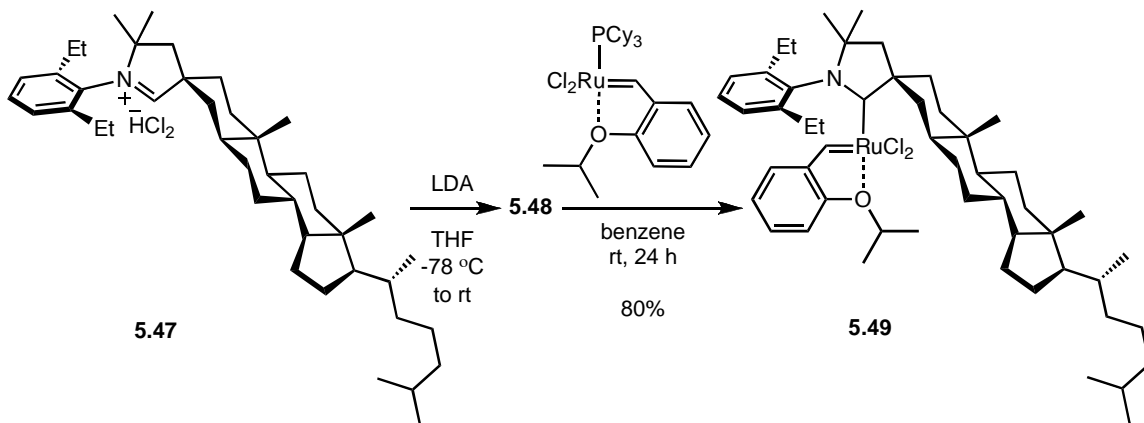


Substrate	ee E (Z)	Yield E (Z)
	18 % (n.d.)	64% (n.d.)
	91 % (-0)	70% (25%)
	12% (6%)	18% (17%)
	19% (29%)	37% (trace)



course of 24 hours. This complex was isolated as a crystalline green solid after flash column chromatography.

**Scheme 5.10.** Synthesis of chiral CAAC complex **5.49**.



**Structural Analysis**

Crystals of **5.49** were grown and its molecular structure was confirmed by single-crystal X-ray crystallographic analysis (Figure 5.11). Like other ruthenium-based olefin metathesis catalysts, the complex exhibits a distorted square pyramidal geometry with the benzylidene moiety occupying the apical position.

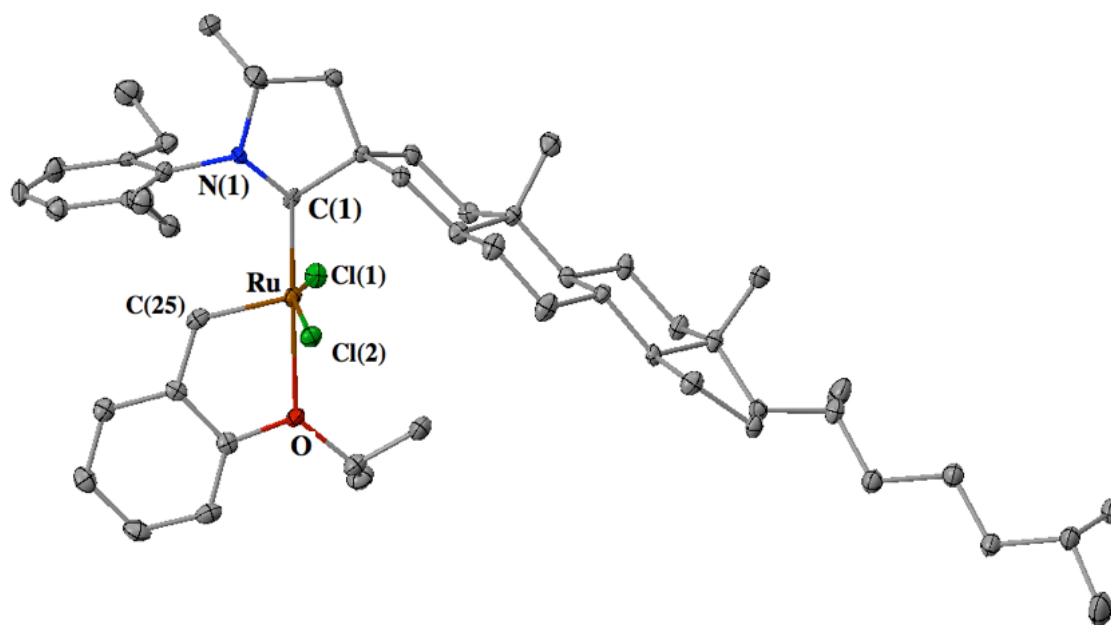


**Figure 5.11.** X-ray crystal structure of complex **5.49** is shown.

### ***Activity in Olefin Metathesis***

The general metathesis activity of **5.49** was first tested in the RCM of diethyl diallyl malonate (**5.14**) but no reaction was evident at 30-55 °C. An increase in the reaction temperature to 60 °C, however, resulted in 70% conversion to **5.15** after two hours. This result was coupled with complete decomposition of the catalyst during the reaction period, as monitored by total loss of peaks in the alkylidene region of the <sup>1</sup>H NMR. Subsequent experimentation with other substrates, including ethylene, has demonstrated that **5.49** is completely unreactive below 60 °C, suggesting that a major conformational change in the complex is necessary for reactivity.

### ***Conclusions***

Both chiral triazolylidenes and cyclic alkyl amino carbenes (CAACs) were chosen to create non-conformationally flexible environments in proximity to the ruthenium center in olefin metathesis catalysts. Although the enantioselectivity shown by these complexes in AROCM and ARCM was considerably lower than previously reported chiral catalysts, they represent an important proof of principle and work is ongoing to improve the yields and enantioselectivities for asymmetric olefin metathesis through modification of the ligand frameworks.

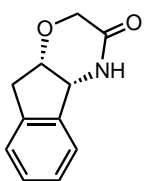
### ***Experimental***

NMR spectra were recorded using a Varian Mercury 300 or Varian Inova 500 MHz spectrometer. NMR chemical shifts are reported in parts per million (ppm) downfield from tetramethylsilane (TMS) with reference to internal solvent for <sup>1</sup>H and <sup>13</sup>C. Spectra are reported as follows: chemical shift (δ ppm), multiplicity, coupling constant (Hz), and integration. Gas chromatography data were obtained using an Agilent 6850

FID gas chromatograph equipped with a DB-Wax Polyethylene Glycol capillary column (J&W Scientific). High-resolution mass spectroscopy (FAB) was completed at the California Institute of Technology Mass Spectrometry Facility. X-ray crystallographic structures were obtained by the Beckman Institute X-ray Crystallography Laboratory of the California Institute of Technology. Crystallographic data have been deposited at the CCDC, 12 Union Road, Cambridge CB2 1EZ, U.K., and copies can be obtained on request, free of charge, by quoting the publication citation and the deposition numbers 696348 (**5.34**) and 735366 (**5.49**).

All reactions involving metal complexes were conducted in oven-dried glassware under a nitrogen atmosphere with anhydrous and degassed solvents, using standard Schlenk and glovebox techniques. Anhydrous solvents were obtained via elution through a solvent column drying system.<sup>16</sup> Silica gel used for the purification of organometallic complexes was obtained from TSI Scientific, Cambridge, MA (60 Å, pH 6.5–7.0).  $(\text{PCy}_3)\text{RuCl}_2(=\text{CH}-o\text{-O}i\text{PrC}_6\text{H}_4)$ , and  $(\text{PCy}_3)_2\text{RuCl}_2=\text{CHPH}$  were obtained from Materia, Inc. Unless otherwise indicated, all compounds were purchased from Aldrich or Fisher and used as obtained. The initial screening of the catalysts in RCM via  $^1\text{H}$  NMR spectroscopy was conducted according to literature procedures.<sup>17</sup> Screening in asymmetric olefin metathesis was also conducted according to literature procedures.<sup>6</sup>

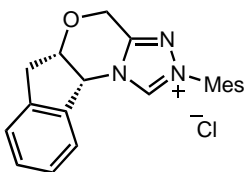
**(4aR,9aS)-4,4a,9,9a-tetrahydroindeno[2,1-b][1,4]oxazin-3(2H)-one (5.9)**



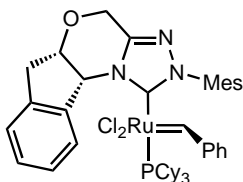
A flame-dried 100 mL two-neck round bottom flask with magnetic stir bar was charged with (1*R*, 2*S*)-(+)-*cis*-1-amino-2-indanol and toluene (0.5 M). The flask was cooled to 0 °C. Under argon, 1.5 equiv NaH (dispersed in oil, 60% by weight) was added to the flask. Ethyl chloroacetate, in slight excess, was added drop-wise over a 15 minute period. During this time, bubbling was evident in the flask. After this addition, the reaction was allowed to warm to room temperature (21-

26°C). The reaction was stirred for 3 hour at room temperature, then diluted with methylene chloride, washed with dilute aqueous HCl, dried (NaHCO<sub>3</sub>), and evaporated under reduced pressure. Crystallization from benzene gave the morpholin-3-one (1.2 g, 95%) as a white powder. Characterization data for **5.9** are identical to those reported in the literature.<sup>18</sup>

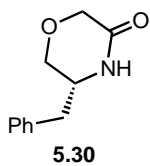
**(5a*S*,10b*R*)-2-mesityl-4,5a,6,10b-tetrahydroindeno[2,1-*b*][1,2,4]triazolo[4,3-*d*][1,4]oxazin-2-ium chloride (5.12)**



A flame-dried 100 mL round bottom flask was charged with **5.9** and methylene chloride (0.5 M). Trimethyloxonium tetrafluoroborate, in slight excess was added and the reaction mixture was allowed to stir for 12 hours at 23 °C. 1 equiv mesitylhydrazine was added and the reaction mixture stirred for 3 hours. The solvent was removed under reduced pressure and the mixture was transferred to a Schlenk tube. The mixture was then heated with an excess of triethyl orthoformate–methanol (2:1) in the sealed tube at 80 °C for 12 hours. Upon cooling, volatiles were removed under reduced pressure. Crystallization from hexanes:toluene 10:1 gave the triazolium salt (0.31 g, 32%) as an orange crystal. <sup>1</sup>H NMR (300 MHz, CDCl<sub>3</sub>) δ 11.44 (s, 1H), 7.66-7.71 (m, 2H), 7.21-7.43 (m, 4H), 6.14 (d, 1H, *J* = 4.1 Hz), 5.17 (dd, 1H, *J* = 16, 37.7 Hz), 4.94 (ddd, 1H, *J* = 3.8, 3.8, 1.4 Hz), 3.93 (dd, 1H, *J* = 16, 37.7 Hz), 3.16 (d, 1H, *J* = 17.2 Hz), 2.97 (d, 1H, *J* = 17.2 Hz), 2.37 (s, 3H), 2.12 (s, 6H).

**(5,6-Indenyl-2-Mes-Tri)(PCy<sub>3</sub>)(Cl)<sub>2</sub>Ru=CHPh (5.13)**

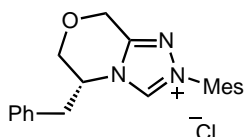
In a glove box, a Schlenk flask was charged with triazolium chloride **5.12** (147 mg, 0.4 mmol) and NaH in oil (60% by wt.) (16 mg, 0.4 mmol). Benzene (3 mL) was added, and the ligand **5.12** was allowed to deprotonate by stirring at room temperature for 20 minutes. Ruthenium complex (PCy<sub>3</sub>)<sub>2</sub>RuCl<sub>2</sub>=CHPH (220 mg, 0.27 mmol) was then added as a solution in methylene chloride (3 mL). The sample was sealed and removed from the glove box. The reaction mixture was stirred for 12 hours at 50 °C. The reaction mixture was cooled to room temperature, filtered, and concentrated *in vacuo*. Column chromatography (gradient from 10:90 to 50:50 ethyl ether/hexanes) of the concentrate gave purified complex **34** as a brown solid in 60% yield. <sup>1</sup>H NMR (C<sub>6</sub>D<sub>6</sub>) δ 19.9 (s, 1H), 6.96-7.4 (m, 11H), 6.22 (d, 1H, *J* = 4.1 Hz), 4.37 (d, 2H, *J* = 2.1 Hz) 1.5-3.1 (m, 44H) . <sup>31</sup>P NMR (C<sub>6</sub>D<sub>6</sub>): δ 36.3 ppm. HRMS (FAB) analysis *m/z*: calculated [M<sup>+</sup>] 873.2895, found 873.2912.

**(R)-3-(Phenylmethyl)morpholin-2-one (5.30)**

A flame-dried 100 mL two-neck round bottom flask with magnetic stir bar was charged with (*R*)-2-Amino-3-phenyl-1-propanol (1.0 g, 6.6 mmol) and toluene (0.5 M). The flask was cooled to 0 °C. Under Argon, 1.5 equiv NaH (dispersed in oil -60% by weight) was added to the flask. Ethyl chloroacetate, in slight excess, was added drop-wise over a 15 minute period. During this time, bubbling was evident in the flask. After this addition, the reaction was allowed to warm to room temperature (21-26 °C). The reaction was stirred for 3 hours at room temperature, then diluted with methylene chloride, washed with dilute aqueous HCl, dried (NaHCO<sub>3</sub>), and evaporated under reduced pressure. Crystallization from benzene

gave the morpholin-3-one (1.14 g, 90%) as a white powder. Characterization data for **5.30** are identical to those reported in the literature.<sup>19</sup>

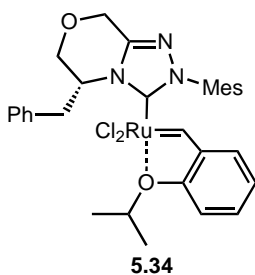
**(R)-5-benzyl-2-mesityl-6,8-dihydro-5H-[1,2,4]triazolo[3,4-c][1,4]oxazin-2-ium chloride (5.33)**



**5.33**

A flame-dried 100 mL round bottom flask was charged with **5.30** and methylene chloride (0.5 M). Trimethyloxonium tetrafluoroborate, in slight excess was added and the reaction mixture was allowed to stir for 12 hours at 23 °C. 1 equiv mesitylhydrazine was added and the reaction mixture stirred for 3 hours. The solvent was removed under reduced pressure and the mixture was transferred to a Schlenk tube. The mixture was then heated with an excess of triethyl orthoformate–methanol (2:1) in the sealed tube at 80 °C for 12 hours. Upon cooling, volatiles removed under reduced pressure. Purification by column chromatography (CH<sub>2</sub>Cl<sub>2</sub>/MeOH) gave the triazolium salt (0.5 g, 43%) as tan powder. <sup>1</sup>H NMR (CDCl<sub>3</sub>) δ 11.64 (s, 1H), 6.44-7.47 (m, 7H), 5.09 (dd, 1H, *J* = 16.5, 31.1 Hz), 4.64 (dd, 1H, *J* = 16.6, 18.4 Hz), 4.0-4.12 (m, 2H), 3.44 (dd, 1H, *J* = 6.9, 7.2 Hz), 3.18-3.34 (m, 1H), 2.8-2.96 (m, 1H), 2.38 (s, 6H), 2.1 (s, 3H).

**(5-Bn-2-Mes-Tri)(Cl)<sub>2</sub>Ru=CH-*o*-OPr<sup>i</sup>C<sub>6</sub>H<sub>4</sub> (5.34)**

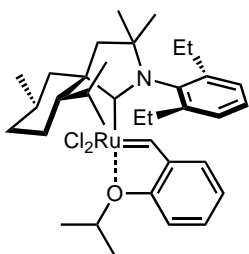


**5.34**

In a glove box, a Schlenk flask was charged with triazolium chloride **5.33** (120 mg, 0.325 mmol) and KHMDS (75 mg, 0.375 mmol). Benzene (5 mL) was added, and the ligand **5.33** was allowed to deprotonate by stirring at room temperature for 20 minutes. Ruthenium complex RuCl<sub>2</sub>(PCy<sub>3</sub>)(=CH-*o*-OPr<sup>i</sup>C<sub>6</sub>H<sub>4</sub>) (250 mg, 0.25 mmol) was then added as a solution in benzene (3 mL). The sample was sealed and removed from the glove box. The reaction mixture was stirred for 24 hours at

room temperature, then CuCl was added to the flask under positive argon. The heterogeneous mixture was stirred vigorously for 1 hour. The reaction mixture was then filtered, and concentrated *in vacuo*. Column chromatography (gradient from 0:100 to 5:95 methanol/methylene chloride) of the concentrate gave purified complex **5.34** as a brown solid in 70% yield.  $^1\text{H NMR}$  ( $\text{C}_6\text{D}_6$ )  $\delta$  16.8 (s, 1H), 6.7-7.4 (m, 11H), 5.97 (dd, 1H,  $J = 4.0, 7.9$  Hz), 5.5 (d, 1H,  $J = 14.7$  Hz), 5.24 (dd, 1H,  $J = 3.54, 9.5$  Hz), 3.2-3.6 (m, 4H), 1.5-2.4 (m, 16H). HRMS (FAB) analysis  $m/z$ : calculated  $[\text{M}^+]$  653.115, found 653.1161.

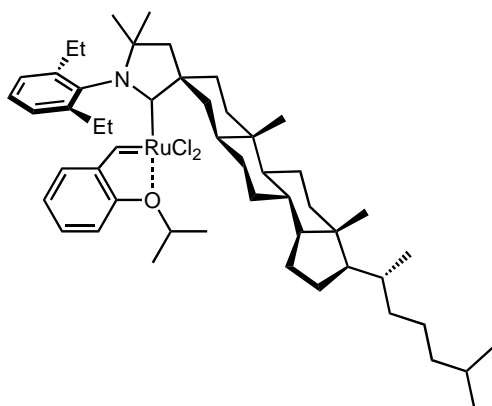
### $\text{RuCl}_2(\text{menthone-CAAC})(=\text{CH}-o\text{-O}i\text{PrC}_6\text{H}_4)$ (**5.39**)



To a solution of free CAAC (**5.37**) (2 equiv) in benzene was added ruthenium complex  $\text{RuCl}_2(\text{PCy}_3)(=\text{CH}-o\text{-O}i\text{PrC}_6\text{H}_4)$  and the mixture was stirred for 24 hours at room temperature. After concentrating the mixture *in vacuo*, the mixture was purified by column chromatography on TSI silica (eluent: toluene). The green band was collected and volatiles were removed under vacuum, providing **5.39** as a green solid in 95% yield. Crystals suitable for X-ray crystallography were grown from a saturated solution of hexanes (0 °C).  $^1\text{H NMR}$  (500 MHz,  $\text{C}_6\text{D}_6$ , 25 °C):  $\delta$  0.61 [s, 3H], 0.657-0.697 [m, 6H], 0.718 [s, 3H], 0.879 [d, 3H,  $J = 6.59$  Hz], 0.946-0.99 [m, 1H], 1.1 [d, 2H,  $J = 6.18$  Hz], 1.268-1.304 [m, 9H], 1.445-1.511 [m, 1H], 1.68 [d, 1H,  $J = 12.76$  Hz], 1.815 [br s, 3H], 2.068-2.18 [m, 2H], 2.396 [br s, 2H], 2.254-2.605 [m, 2H], 2.862 [br s, 1H], 3.318 [d,  $J = 7$  Hz], 4.25-4.323 [m, 1H], 6.147 [d, 1H,  $J = 8.23$ ], 6.38 [t, 1H,  $J = 7.42$ ], 6.7-6.72 [m, 1H], 6.92-6.937 [m, 2H], 7.019 [t, 1H,  $J = 7.42$  Hz], 16.463 [s, 1H].  $^{13}\text{C NMR}$  (125 MHz,  $\text{C}_6\text{D}_6$ ):  $\delta$  14.794, 14.890, 20.419, 22.050, 22.076, 25.268, 25.701, 29.503, 50.935, 71.369, 74.244, 75.987, 113.618, 121.780, 124.071, 124.489, 125.507, 126.866, 126.957, 128.689, 130.880, 140.467, 143.655, 143.700, 144.456, 145.246, 152.699,

268.009, 303.565. HRMS (FAB<sup>+</sup>) calculated for C<sub>35</sub>H<sub>51</sub>Cl<sub>2</sub>NORu [M<sup>+</sup>] 673.2392, observed 673.2413.

**RuCl<sub>2</sub>(cholestenone-CAAC)(=CH-*o*-O*Pr*C<sub>6</sub>H<sub>4</sub>) (5.49)**



To a solution of free cholestenone-CAAC (2 equiv) in benzene was added ruthenium complex RuCl<sub>2</sub>(PCy<sub>3</sub>)(=CH-*o*-O*Pr*C<sub>6</sub>H<sub>4</sub>) and the mixture was stirred for 24 hours at room temperature. After concentrating the mixture *in vacuo*, the mixture was purified by column chromatography on TSI silica (eluent: toluene).

The green band was collected and volatiles were removed under vacuum, providing **5.49** as a green solid in 70% yield. Crystals suitable for X-ray crystallography were grown from a slow diffusion of pentane into a saturated solution of toluene (0 °C). <sup>1</sup>H NMR (500 MHz, C<sub>6</sub>D<sub>6</sub>) δ 16.76 (s, 1H), 7.31 (t, J = 7.7, 1H), 7.22 (dd, J = 7.7, 2.2, 2H), 7.19 – 7.14 (m, 6H), 7.02 (dd, J = 7.5, 1.7, 2H), 6.69 – 6.63 (m, 1H), 6.41 (d, J = 8.5, 1H), 4.65 (hept, J = 6.1, 1H), 3.26 – 3.09 (m, 1H), 3.04 – 2.72 (m, 3H), 2.42 (ddq, J = 15.0, 10.5, 7.4, 2H), 2.14 (dd, J = 9.1, 3.4, 1H), 2.11 (s, 1H), 2.02 – 1.90 (m, 2H), 1.90 – 1.80 (m, 1H), 1.79 – 1.70 (m, 1H), 1.64 – 1.11 (m, 16H), 1.10 (d, J = 3.3, 1H), 1.08 (d, J = 2.8, 1H), 0.98 (dd, J = 4.6, 2.8, 2H), 0.96 (d, J = 2.1, 1H), 0.95 – 0.92 (m, 3H), 0.82 (s, 3H), 0.43 (s, 1H). <sup>13</sup>C NMR (126 MHz, C<sub>6</sub>D<sub>6</sub>) δ 301.41, 267.05, 153.10, 145.58, 144.06, 143.81, 140.93, 131.97, 130.79, 130.04, 129.49, 123.07, 121.85, 114.66, 76.35, 74.44, 74.30, 60.59, 57.65, 56.87, 55.38, 46.19, 43.66, 40.57, 37.24, 36.33, 35.76, 29.39, 26.64, 26.42, 25.47, 23.90, 23.53, 23.32, 15.83, 15.61. HRMS (FAB<sup>+</sup>) calculated for C<sub>52</sub>H<sub>79</sub>Cl<sub>2</sub>NORu [M<sup>+</sup>] 905.4583, observed 905.4540.

<b>Complex</b>	<b>5.34</b>	<b>5.49</b>
<b>CCDC #</b>	696348	735366
<b>Empirical formula</b>	C <sub>35</sub> H <sub>51</sub> NOCl <sub>2</sub> Ru	C <sub>52</sub> H <sub>79</sub> NOCl <sub>2</sub> Ru
<b>Formula weight</b>	673.74	906.13
<b>Crystallization solvent</b>	Hexanes	Toluene/pentane
<b>Crystal color</b>	Olive green	Green
<b>T (K)</b>	100(2)	100(2)
<b>θ range (°)</b>	2.21 to 31.91	2.21 to 27.49
<b>a (Å)</b>	8.8753(7)	12.7795(11)
<b>b (Å)</b>	18.4415(13)	13.2943(12)
<b>c (Å)</b>	10.1004(8)	28.071(3)
<b>α (Å)</b>		
<b>β (Å)</b>	92.987(4)	
<b>γ (Å)</b>		
<b>V (Å<sup>3</sup>)</b>	1650.9(2)	4769.2(8)
<b>Crystal system</b>	Monoclinic	Orthorhombic
<b>Space group</b>	P2 <sub>1</sub>	P2 <sub>1</sub> 2 <sub>1</sub> 2 <sub>1</sub>
<b>d<sub>calc</sub> (g/cm<sup>3</sup>)</b>	1.355	1.262
<b>μ (mm<sup>-1</sup>)</b>	0.664	0.478
<b>GOF on F<sup>2</sup></b>	1.704	1.323
<b>R<sub>1</sub>, wR<sub>2</sub> [I &gt; 2σ(I)]</b>	0.0444, 0.0584	0.0320, 0.0408

**References and Notes**

---

- (1) For example, see: (a) Hourri, A. F.; Xu, Z.; Cogan, D. A.; Hoveyda, A. H. *J. Am. Chem. Soc.* **1995**, *117*, 2943-2944. (b) Limanto, J.; Snapper, M. L. *J. Am. Chem. Soc.* **2000**, *122*, 8071-8072. (c) Nicolaou, K. C.; Wissinger, N.; Pastor, J.; Ninkovic, S.; Sarabia, F.; He, Y.; Vourloumis, D.; Yang, Z.; Li, T.; Giannakakou, P.; Hamel, E. *Nature* **1997**, *387*, 268-272. (d) Fürstner, A.; Thiel, O. R. *J. Org. Chem.* **2000**, *65*, 1738-1742.
- (2) (a) Fujmura, O.; Grubbs, R. H. *J. Am. Chem. Soc.* **1996**, *118*, 2499-2500. (b) Fujmura, O.; Grubbs, R. H. *J. Org. Chem.* **1998**, *63*, 824-832.
- (3) (a) For a review of molybdenum-catalyzed enantioselective metathesis, see: Hoveyda, A. H.; Schrock, R. R. *Chem. Eur. J.* **2001**, *7*, 945-950. (b) Alexander, J. B.; La, D. S.; Cefalo, D. R.; Hoveyda, A. H.; Schrock, R. R. *J. Am. Chem. Soc.* **1998**, *120*, 4041-4042. (c) La, D. S.; Alexander, J. B.; Cefalo, D. R.; Graf, D. D.; Hoveyda, A. H.; Schrock, R. R. *J. Am. Chem. Soc.* **1998**, *120*, 9720-9721. (d) Zhu, S. S.; Cefalo, D. R.; La, D. S.; Jamieson, J. Y.; Davis, W. M.; Hoveyda, A. H.; Schrock, R. R. *J. Am. Chem. Soc.* **1999**, *121*, 8251-8252. (e) La, D. S.; Sattely, E. S.; Ford, J. G.; Schrock, R. R.; Hoveyda, A. H. *J. Am. Chem. Soc.* **2001**, *123*, 7767-7768.
- (4) (a) Malcomson, S. J.; Meek, S. J.; Sattely, E. S.; Schrock, R. R.; Hoveyda, A. H. *Nature* **2008**, *456*, 933-937. (b) Sattely, E. S.; Meek, S. J.; Malcomson, S. J.; Schrock, R. R.; Hoveyda, A. H. *J. Am. Chem. Soc.* **2009**, *131*, 943-953. (c) Ibrahim, I.; Yu, M.; Schrock, R. R.; Hoveyda, A. H. *J. Am. Chem. Soc.* **2009**, *131*, 3844-3845.

- 
- (5) (a) Enders, D.; Gielen, H.; Breuer, K. *Tetrahedron: Asymmetry* **1997**, *8*, 3571–3574. (b) Herrmann, W. A.; Goossen, L. J.; Spiegler, M. *Organometallics* **1998**, *17*, 2162–2168. (c) Lee, S.; Hartwig, J. F. *J. Org. Chem.* **2001**, *66*, 3402–3415.
- (6) (a) Seiders, T. J.; Ward, D. W.; Grubbs, R. H. *Org. Lett.* **2001**, *3*, 3225–3228. (b) Funk, T. W.; Berlin, J. M.; Grubbs, R. H. *J. Am. Chem. Soc.* **2006**, *128*, 1840–1846. (c) Berlin, J. M.; Goldberg, S. D.; Grubbs, R. H. *Angew. Chem., Int. Ed.* **2006**, *45*, 7591–7595. (d) Ward, D. W.; Berlin, J. M.; Grubbs, R. H. Unpublished results; California Institute of Technology, 2003–2006.
- (7) (a) Van Veldhuizen, J. J.; Gillingham, D. G.; Garber, S. B.; Kataoka, O.; Hoveyda, A. H. *J. Am. Chem. Soc.* **2003**, *125*, 12502–12508. (b) Van Veldhuizen, J. J.; Garber, S. B.; Kingsbury, J. S.; Hoveyda, A. H. *J. Am. Chem. Soc.* **2002**, *124*, 4954–4955.
- (8) (a) Fournier, P. A.; Collins, S. K. *Organometallics* **2007**, *26*, 2945–2949. (b) Grandbois, A.; Collins, S. K. *Chem. Eur. J.* **2008**, *14*, 9323–9329. (c) Fournier, P. A.; Savoie, J.; Stenne, B.; Bedard, M.; Grandbois, A.; Collins, S. K. *Chem. Eur. J.* **2008**, *14*, 8690–8695.
- (9) (a) Knight, R. L.; Leeper, F. J. *J. Chem. Soc., Perkin Trans.* **1998**, *12*, 1891–1893. (b) Enders, D.; Kalfass, U. *Angew. Chem., Int. Ed.* **2002**, *41*, 1743–1745. (c) Pesch, J.; Harms, K.; Bach, T. *Eur. J. Org. Chem.* **2004**, *9*, 2025–2035.
- (10) (a) Kerr, M. S.; Read de Alaniz, J.; Rovis, T. *J. Am. Chem. Soc.* **2002**, *124*, 10298–10299. (b) Kerr, M. S.; Read de Alaniz, J.; Rovis, T. *J. Org. Chem.* **2005**, *70*, 5275–5278.
- (11) Clarke, F. H. *J. Org. Chem.* **1962**, *27*, 3251–3253.
- (12) Ritter, T.; Hejl, A.; Wenzel, A. G.; Funk, T. W.; Grubbs, R. H. *Organometallics* **2006**, *25*, 5740–5745.

- 
- (13) (a) Anderson, D. R.; Lavallo, V.; O'Leary, D. J.; Bertrand, G.; Grubbs, R. H. *Angew. Chem. Int. Ed.* **2007**, *46*, 7262–7265. (b) Anderson, D. R.; Ung, T.; Mkrtumyan, G.; Bertrand, G.; Grubbs, R. H.; Schrodi, Y. *Organometallics* **2008**, *27*, 563–566.
- (14) (a) Lavallo, V., Canac, Y., Prasang, C., Donnadiu, B., Bertrand, G. *Angew. Chem. Int. Ed.* **2005**, *44*, 5705–5709. (b) Jazzar, R.; Bourg, J.-B.; Dewhurst, R. D.; Donnadiu, B.; Bertrand, G. *J. Org. Chem.* **2007**, *72*, 3492–3499.
- (15) Garber, S. B.; Kingsbury, J. S.; Gray, B. L.; Hoveyda, A. H. *J. Am. Chem. Soc.* **2000**, *122*, 8168–8179.
- (16) Pangborn, A. B.; Giardello, M. A.; Grubbs, R. H.; Rosen, R. K.; Timmers, F. J. *Organometallics* **1996**, *15*, 1518–1520.
- (17) Ritter, T.; Hejl, A.; Wenzel, A. G.; Funk, T. W.; Grubbs, R. H. *Organometallics* **2006**, *25*, 5740–5745, and literature cited therein.
- (18) Ghosh, A.; McKee, S. P.; Sanders, W. M. *Tet. Lett.* **1991**, *32*, 711–714.
- (19) Norman, B. H.; Kroin, J. S. *J. Org. Chem.* **1996**, *61*, 4990–4998.

## Appendix A

### Ruthenium Olefin Metathesis Catalysts Bearing Acenaphthylene-Annulated N-Heterocyclic Carbene Ligands

**Abstract**

A series of ruthenium olefin metathesis catalysts bearing acenaphthylene-annulated N-heterocyclic carbene (NHC) ligands with varying degrees of *N*-aryl substitution have been prepared. Initial evaluation of their performance in olefin metathesis demonstrated that these complexes show greater resistance to decomposition, resulting in increased catalyst lifetimes. While this work has great potential, the results are preliminary. To fully understand the effect that these ligands can have on ruthenium complexes, related ligands need to be developed and compared against standard NHC analogs.

**Introduction**

As discussed in depth in chapters two and three, an important challenge in ring-closing metathesis (RCM) is to substantially decrease “standard” catalyst loading, thereby reducing both reaction cost and challenges associated with product purification, an especially critical concern when reaction products are intended for pharmaceutical use.<sup>1</sup> To this effect, our goal has been to increase catalyst efficiency by developing even more stable and robust catalysts that still retain high catalytic activity. Preliminary work in this project was completed concurrently with the methyl-substitution studies discussed in chapter two. As in that study, we expected that the backbone substitution in acenaphthylene-annulated NHCs could play a central role in increased activity and catalyst lifetimes. We were also very interested in the effects of the forced syn-conformation of the *N*-aryl substituents on catalyst activity and stability.

## Results

### Catalyst Syntheses

The preparation of the mesityl and 2,6-diisopropylphenyl substituted acenaphtho-imidazolium chlorides have been previously reported by Çetinkaya and Grubbs, respectively.<sup>2</sup> Under analogous experimental conditions, acenaphtho-imidazolium chlorides **A.1** and **A.2** were obtained in good yields (Figure A.1).

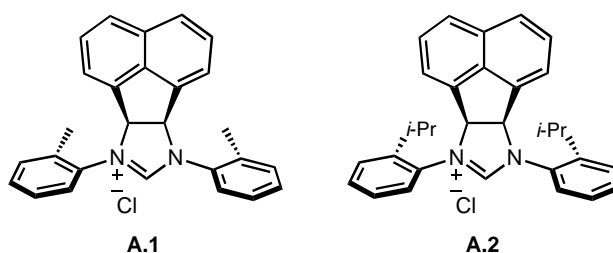
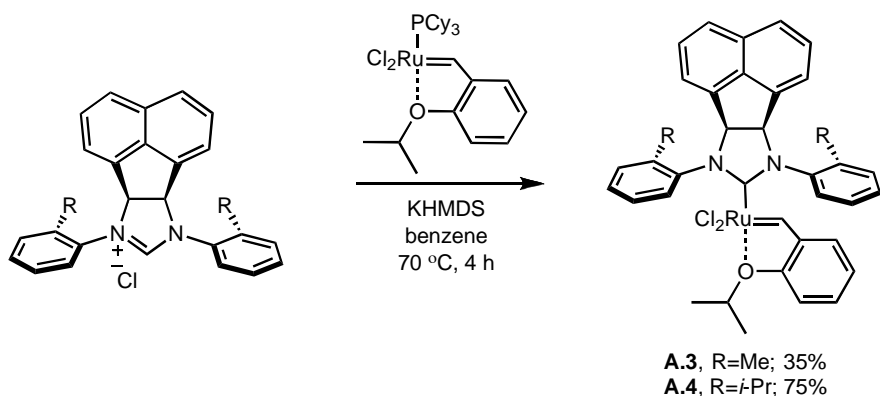


**Figure A.1.** Acenaphtho-imidazolium chlorides.

With these precursors in hand, the corresponding free carbenes were generated by treatment of the imidazolium salts with potassium hexamethyldisilazide (KHMDs) at room temperature (Scheme A.1). These carbenes (prepared in situ) were reacted with commercially available (PCy<sub>3</sub>)RuCl<sub>2</sub>=CH(*o*-O/PrC<sub>6</sub>H<sub>4</sub>) at 70 °C, affording the phosphine-free chelating ether complexes **A.3** and **A.4**. These complexes were isolated as crystalline green solids after flash column chromatography, and as solids are both air and moisture stable under standard conditions.

**Scheme A.1.** Synthesis of ruthenium complexes **A.3** and **A.4**.



**Structural Analyses**

To probe the electronic and steric effects of this new backbone substitution, crystals of **A.3** and **A.4** were grown and their molecular structures were confirmed by single-crystal X-ray crystallographic analysis (Figures A.2 and A.3). As expected, the complexes exhibit a distorted square pyramidal geometry with the benzylidene moiety occupying the apical position. As desired, the N-aryl substituents are on the same face in both examples.

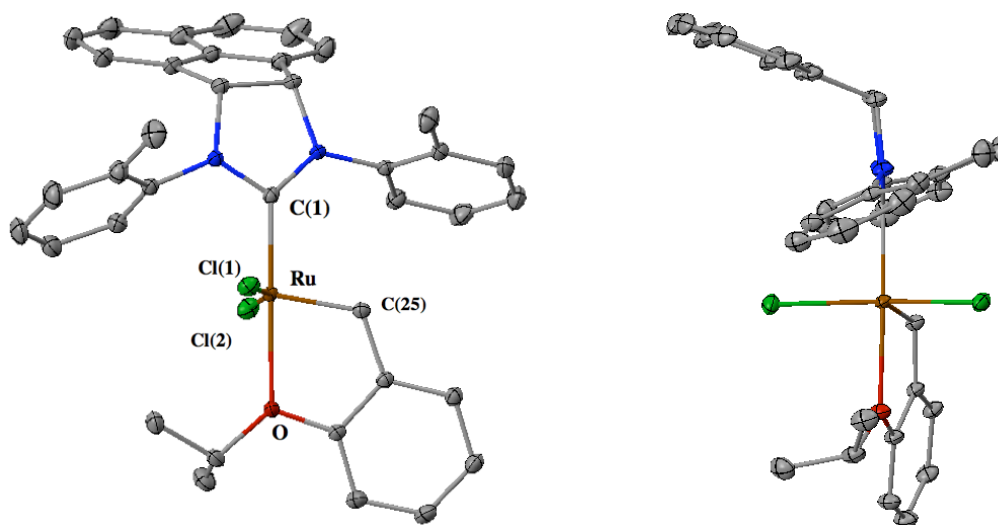


**Figure A.2.** X-ray crystal structure of complex **A.3**, including side view.

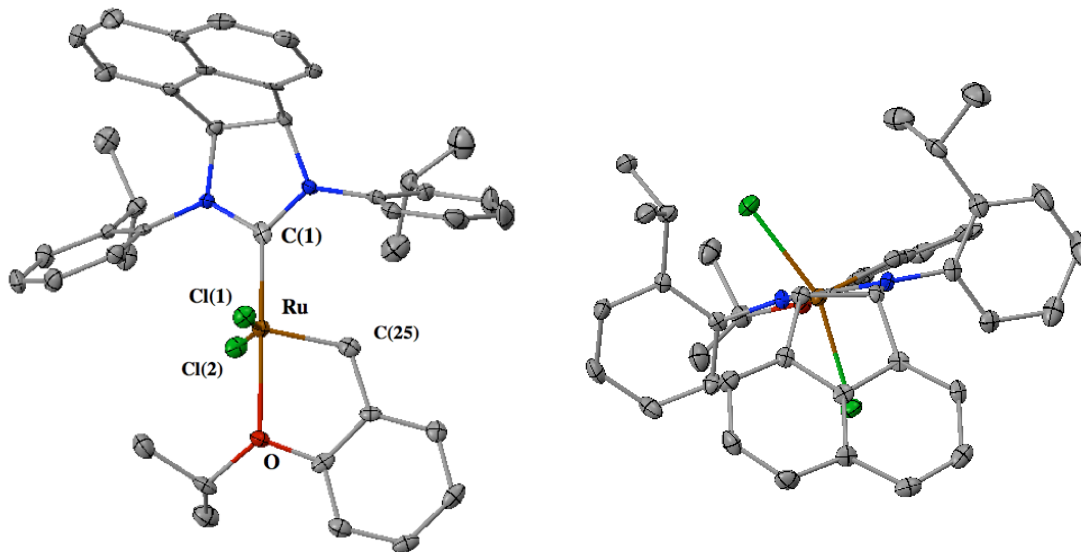


**Figure A.3.** X-ray crystal structure of complex **A.4**, including top view.

### Activity in Olefin Metathesis

Catalysts **A.3** and **A.4** were compared to highly active complex **A.5** ( $(H_2ITol)(PCy_3)Cl_2Ru=CHPh$  ( $H_2ITol = 1,3\text{-di-}o\text{-tolylimidazolidine-2-ylidene}$ )). First, they were examined in the ring-closing metathesis of diethyl diallylmalonate (**A.6**) (Figure A.4). The reaction, utilizing 1 mol% catalyst in  $CD_2Cl_2$  at 30 °C, was monitored by  $^1H$  NMR spectroscopy. While **A.3** and **A.4** both complete the reaction, they initiate much slower than complex **A.5**. The same trend was observed for the cyclization of diethyl allylmethylmalonate **A.8** to form trisubstituted cyclic olefin **A.9** (Figure A.5), and in the challenging RCM of diethyl dimethylmalonate (**A.10**) (Figure A.6).

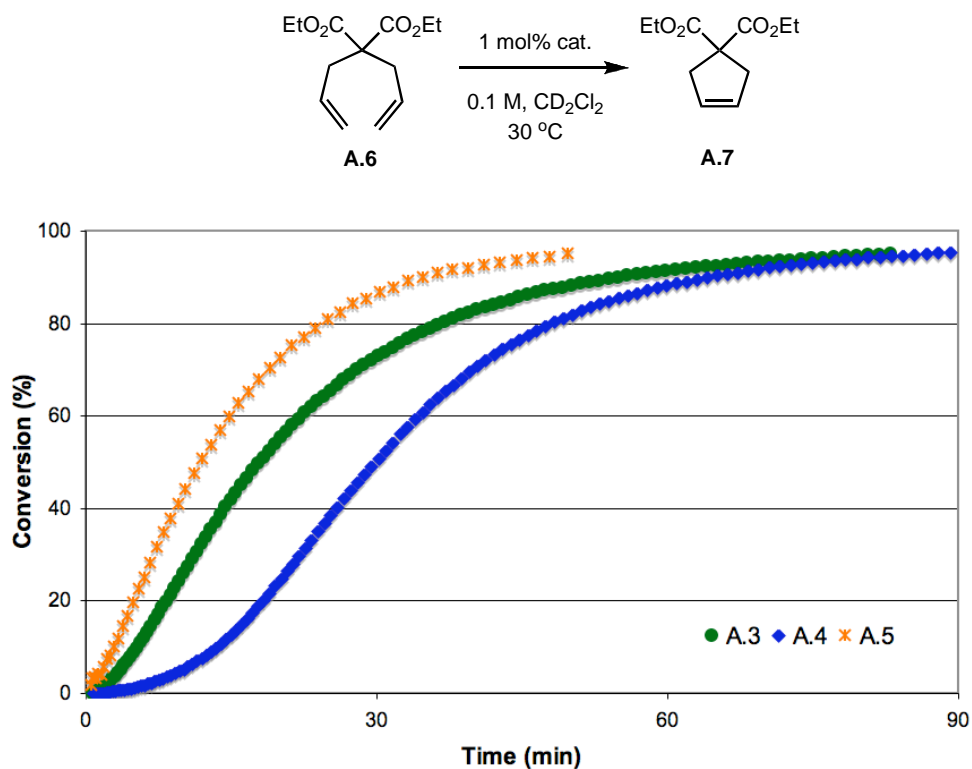


**Figure A.4.** RCM of diene **A.6** to disubstituted cycloalkene **A.7**.

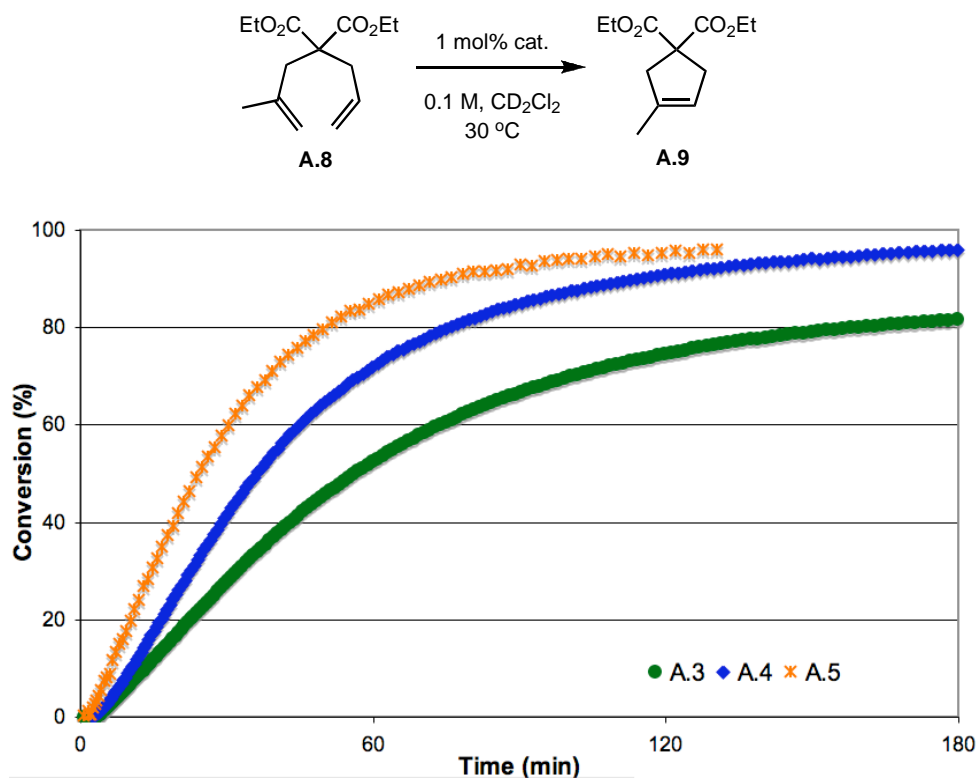


**Figure A.5.** RCM of diene **A.8** to trisubstituted cycloalkene **A.9**.

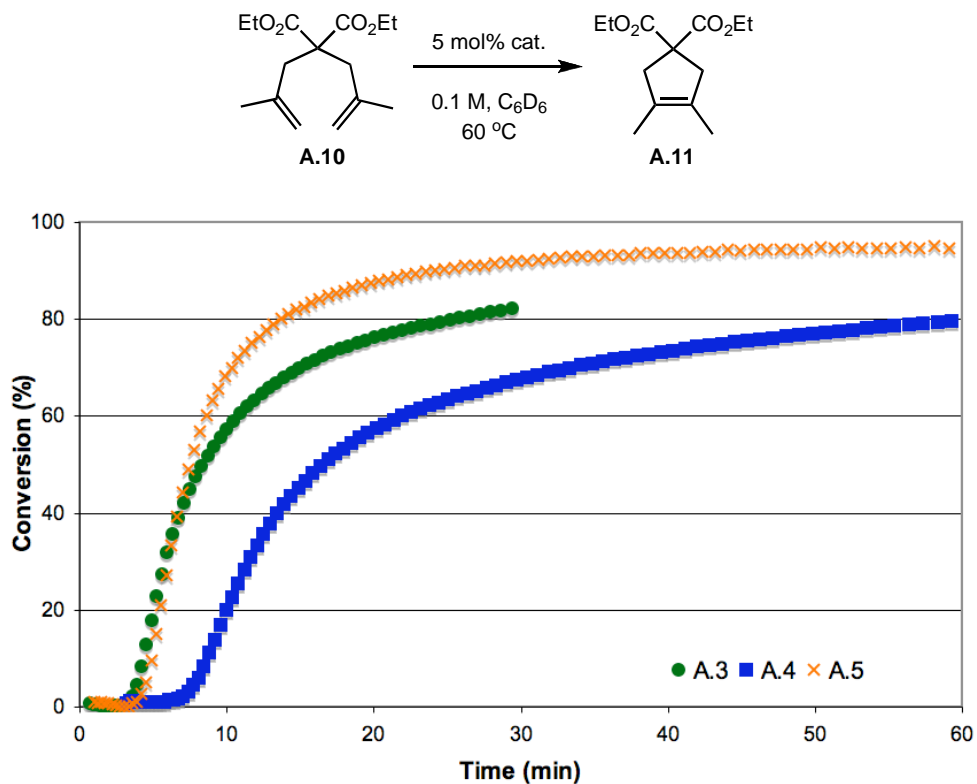


**Figure A.6.** RCM of diene **A.10** to tetrasubstituted cycloalkene **A.11**.

As in chapter two, these initial results provide little insight into the effects of ligand modification on total catalyst efficiency. While it was clear that the acenaphthol-annulated ligands decreased the initiation rate of the catalysts, we remained interested in catalyst lifetimes relative to standard catalysts. With that in mind, the highly sensitive assay designed in chapter two was implemented to compare complexes **A.4** and **A.5** (Figure A.7). At these very low catalyst loadings (250 ppm), acenaphthylene substitution resulted in higher conversions to cyclic olefin **A.7**. The data suggest that the higher conversions are a direct result of longer catalyst lifetimes. However, as observed during the initial studies, the backbone substitution decreases reaction rate.

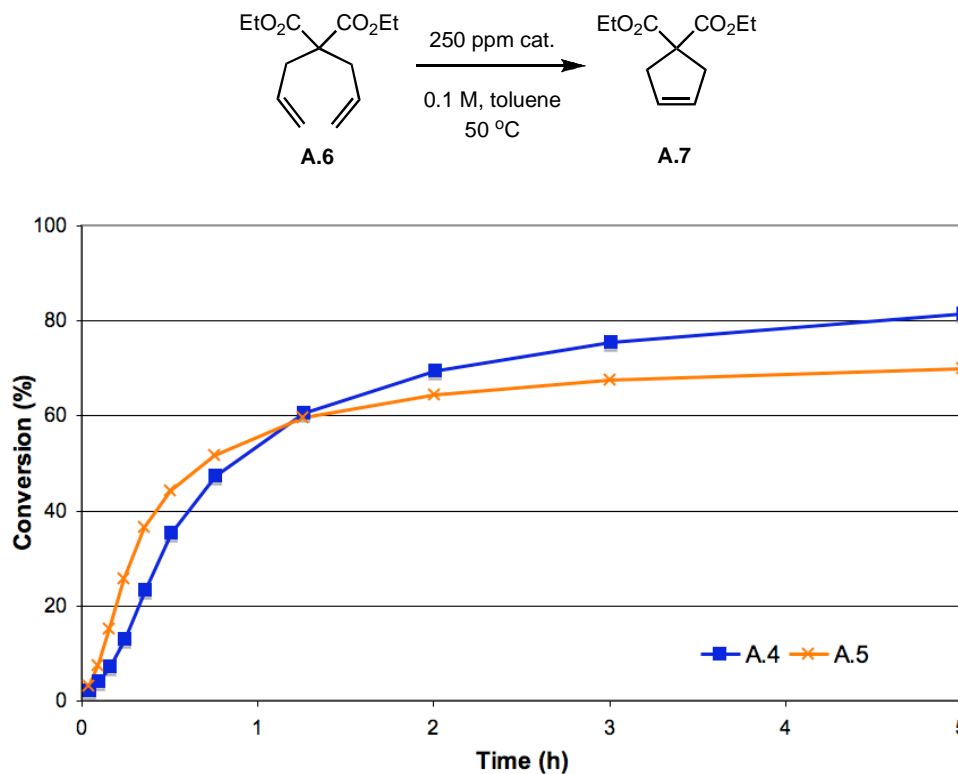


**Figure A.7.** Low ppm assay for RCM of **A.6** utilizing complexes **A.4** and **A.5**.

### ***Future Directions***

This preliminary work has demonstrated that the acenaphthylene annulation of NHCs has great potential. To fully understand the effect that these ligands can have on ruthenium complexes in metathesis, related ligands need to be developed and compared against standard NHC analogs. Future work should focus on the preparation and testing of the N-phenyl derivative of these complexes. Ideally, this new complex will exhibit high activity while showing greater resistance to decomposition, resulting in increased catalyst lifetimes and larger turnover numbers.

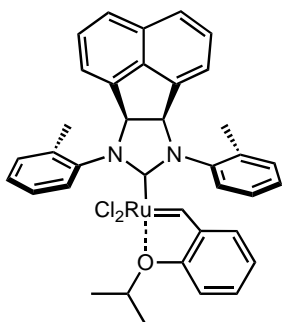
### ***Experimental***

NMR spectra were recorded using a Varian Mercury 300 or Varian Inova 500 MHz spectrometer. NMR chemical shifts are reported in parts per million (ppm) downfield from tetramethylsilane (TMS) with reference to internal solvent for  $^1\text{H}$  and  $^{13}\text{C}$ .

Spectra are reported as follows: chemical shift ( $\delta$  ppm), multiplicity, coupling constant (Hz), and integration. Gas chromatography data was obtained using an Agilent 6850 FID gas chromatograph equipped with a DB-Wax Polyethylene Glycol capillary column (J&W Scientific). High-resolution mass spectroscopy (FAB) was completed at the California Institute of Technology Mass Spectrometry Facility. X-ray crystallographic structures were obtained by the Beckman Institute X-ray Crystallography Laboratory of the California Institute of Technology. Crystallographic data have been deposited at the CCDC, 12 Union Road, Cambridge CB2 1EZ, U.K., and copies can be obtained on request, free of charge, by quoting the publication citation and the deposition numbers 687311 (**A.3**) and 684753 (**A.4**).

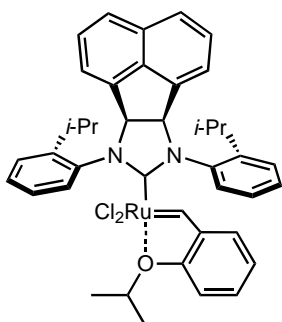
All reactions involving metal complexes were conducted in oven-dried glassware under a nitrogen atmosphere with anhydrous and degassed solvents, using standard Schlenk and glovebox techniques. Anhydrous solvents were obtained via elution through a solvent column drying system.<sup>3</sup> Silica gel used for the purification of organometallic complexes was obtained from TSI Scientific, Cambridge, MA (60 Å, pH 6.5–7.0).  $(\text{PCy}_3)_2\text{RuCl}_2(=\text{CH}-o\text{-O}i\text{PrC}_6\text{H}_4)$ , was obtained from Materia, Inc. Unless otherwise indicated, all compounds were purchased from Aldrich or Fisher and used as obtained. The initial screening of the catalysts, in RCM via  $^1\text{H}$  NMR spectroscopy was conducted according to literature procedures.<sup>4</sup> Low ppm level screening was conducted according to procedures outlined in chapter two and the related literature.<sup>5</sup>

**RuCl<sub>2</sub>[1,3-di-2-methylphenylacenaphtho[1,2-d]imidazolin-2-ylidene](=CH-*o*-O*i*PrC<sub>6</sub>H<sub>4</sub>) (A.3)**



In a glove box, a Schlenk flask was charged with **A.1** (2 equiv) and KHMDS (2.1 equiv). Benzene (10 mL) was added, and the ligand was allowed to deprotonate by stirring at room temperature for 20 minutes. Ruthenium complex RuCl<sub>2</sub>(PCy<sub>3</sub>)(=CH-*o*-O*i*PrC<sub>6</sub>H<sub>4</sub>) was then added. The sample was sealed and removed from the glove box. The reaction mixture was stirred for 4 hours at 70 °C. After concentrating the mixture *in vacuo*, the mixture was purified by column chromatography on TSI silica (eluent: toluene). The green band was collected and volatiles were removed under vacuum, providing **A.3** as a green solid in 35% yield. Crystals suitable for X-ray crystallography were grown from a saturated solution of methanol (0 °C). <sup>1</sup>H NMR (500 MHz, C<sub>6</sub>D<sub>6</sub>, 25 °C): δ 16.20 (s, 1H), 8.27(s, 1H), 7.1-7.2 (m, 3H), 6.6-6.8 (m, 6H), 6.25-6.4 (m, 4H), 6.0-6.1 (m, 1H), 5.5-5.6 (m, 2H), 4.1-4.2 (m, 1H), 2.27-2.47 (m, 6H), 0.97-1.09 (m, 6H). HRMS Calculated for C<sub>37</sub>H<sub>34</sub>Cl<sub>2</sub>N<sub>2</sub>ORu: 694.1092. Found: 694.1073.

**RuCl<sub>2</sub>[1,3-di-2-isopropylphenylacenaphtho[1,2-d]imidazolin-2-ylidene](=CH-*o*-O*i*PrC<sub>6</sub>H<sub>4</sub>) (A.4)**



In a glove box, a Schlenk flask was charged with **A.2** (2 equiv) and KHMDS (2.1 equiv). Benzene (10 mL) was added, and the ligand was allowed to deprotonate by stirring at room temperature for 20 minutes. Ruthenium complex RuCl<sub>2</sub>(PCy<sub>3</sub>)(=CH-*o*-O*i*PrC<sub>6</sub>H<sub>4</sub>) was then added. The sample was sealed and removed from the glove box. The reaction mixture was stirred for 4 hours at 70 °C. After concentrating the mixture *in vacuo*, the

mixture was purified by column chromatography on TSI silica (eluent: toluene). The green band was collected and volatiles were removed under vacuum, providing **A.4** as a green solid in 70% yield. Crystals suitable for X-ray crystallography were grown from a saturated solution of methanol (0 °C). <sup>1</sup>H NMR (500 MHz, C<sub>6</sub>D<sub>6</sub>): δ 16.63 (s, 1H), 8.60(d, 2H, J=8.0Hz), 7.17-7.47 (m, 8H), 6.92-7.04 (m, 4H), 6.48-6.7 (m, 4H), 6.28 (d, 1H, J=8.7Hz), 5.90-6.13 (m, 2H), 4.37 (m, 1H), 3.70-3.84 (m, 2H), 1.63-1.66 (m, 3H), 1.27-1.42 (m, 12H), 1.19-1.25 (m, 3H). HRMS Calculated for C<sub>41</sub>H<sub>42</sub>Cl<sub>2</sub>N<sub>2</sub>ORu: 750.1718. Found: 750.1690.

<b>Complex</b>	<b>A.3</b>	<b>A.4</b>
<b>CCDC #</b>	687311	684753
<b>Empirical formula</b>	C <sub>37</sub> H <sub>34</sub> N <sub>2</sub> OCl <sub>2</sub> Ru	C <sub>41</sub> H <sub>42</sub> N <sub>2</sub> OCl <sub>2</sub> Ru
<b>Formula weight</b>	694.63	750.74
<b>Crystallization solvent</b>	Methanol	Methanol
<b>Crystal color</b>	Dichroic – brown/green	Green
<b>T (K)</b>	100(2)	100(2)
<b>θ range (°)</b>	2.41 to 46.41	2.23 to 28.76
<b>a (Å)</b>	18.3236(7)	24.1277(7)
<b>b (Å)</b>	12.3481(5)	13.2139(4)
<b>c (Å)</b>	28.3579(10)	25.2901(7)
<b>α (Å)</b>		
<b>β (Å)</b>	94.035(2)	117.6880(10)
<b>γ (Å)</b>		
<b>V (Å<sup>3</sup>)</b>	6400.4(4)	7139.7(4)
<b>Crystal system</b>	Monoclinic	Monoclinic
<b>Space group</b>	C2/c	P2 <sub>1</sub> /n
<b>d<sub>calc</sub> (g/cm<sup>3</sup>)</b>	1.442	1.397
<b>μ (mm<sup>-1</sup>)</b>	0.689	0.624
<b>GOF on F<sup>2</sup></b>	1.602	1.324
<b>R<sub>1</sub>, wR<sub>2</sub> [I &gt; 2σ(I)]</b>	0.0395, 0.0743	0.0400, 0.0491

## References and Notes

---

- (1) Governmental recommendations for residual ruthenium are now routinely less than 10 ppm. For recent guidelines, see: (a) Zaidi, K. *Pharmacoepial Forum* **2008**, *34*, 1345–1348. (b) Criteria given in the EMEA Guideline on the Specification Limits for Residues of Metal Catalysts, available at: [www.emea.europa.eu/pdfs/human/swp/444600.pdf](http://www.emea.europa.eu/pdfs/human/swp/444600.pdf)
- (2) (a) Türkmen, H.; Sahin, O.; Büyükgüngör, O.; Çetinkaya, B. *Eur. J. Inorg. Chem.* **2006**, 4915–4921. (b) Grubbs, R. H.; Scholl, M. PCT Int. Appl. WO 0071554, **2000**.
- (3) Pangborn, A. B.; Giardello, M. A.; Grubbs, R. H.; Rosen, R. K.; Timmers, F. J. *Organometallics* **1996**, *15*, 1518–1520.
- (4) Ritter, T.; Hejl, A.; Wenzel, A. G.; Funk, T. W.; Grubbs, R. H. *Organometallics* **2006**, *25*, 5740–5745, and literature cited therein.
- (5) Kuhn, K. M.; Bourg, J. B.; Chung, C. K.; Virgil, S. C.; Grubbs, R. H. *J. Am. Chem. Soc.* **2009**, *131*, 5313–5320.

## Appendix B

### Additional Results: Cyclic Carbamates via RCM

## Abstract

In chapter three, a high-throughput assay was utilized to screen a series of ruthenium catalysts for the ring-closing metathesis (RCM) of acyclic carbamates to form the corresponding di-, tri-, and tetrasubstituted five-, six-, and seven-membered cyclic carbamates. Due to the large amount of data collected, the discussion in chapter three focused on only a small portion of the results from this study, providing an overall assessment of catalyst activity with the carbamate substrates. Because the additional results are relevant and provide additional insight into the trends discussed in chapter three, they have been reported in this appendix.

## Results

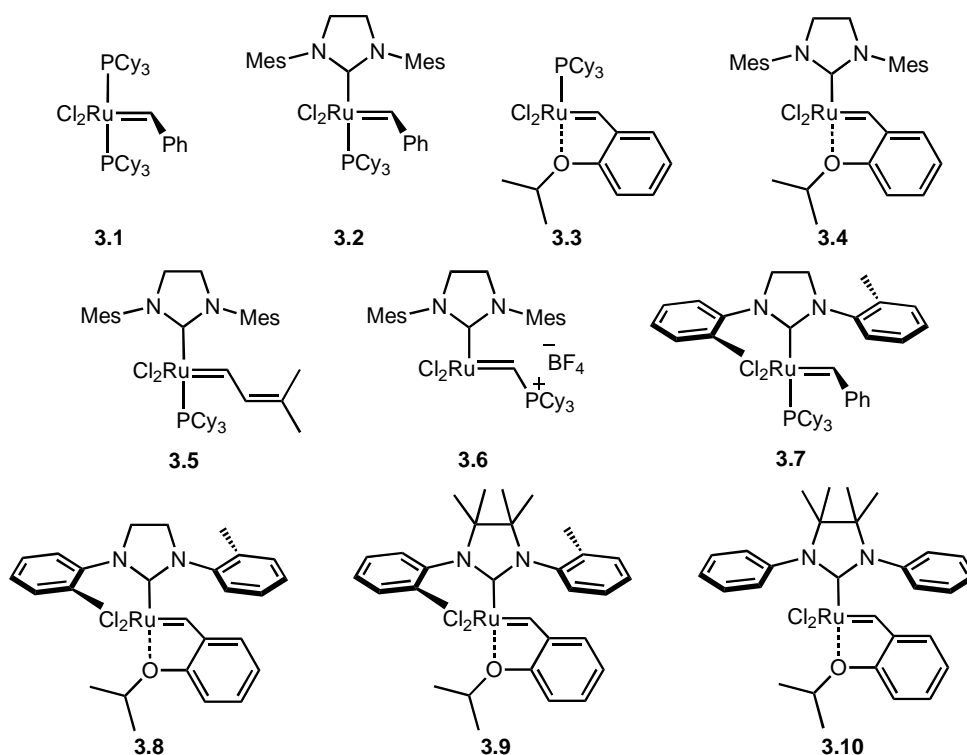


**Figure B.1.** Ruthenium-based olefin metathesis catalysts utilized in this study.

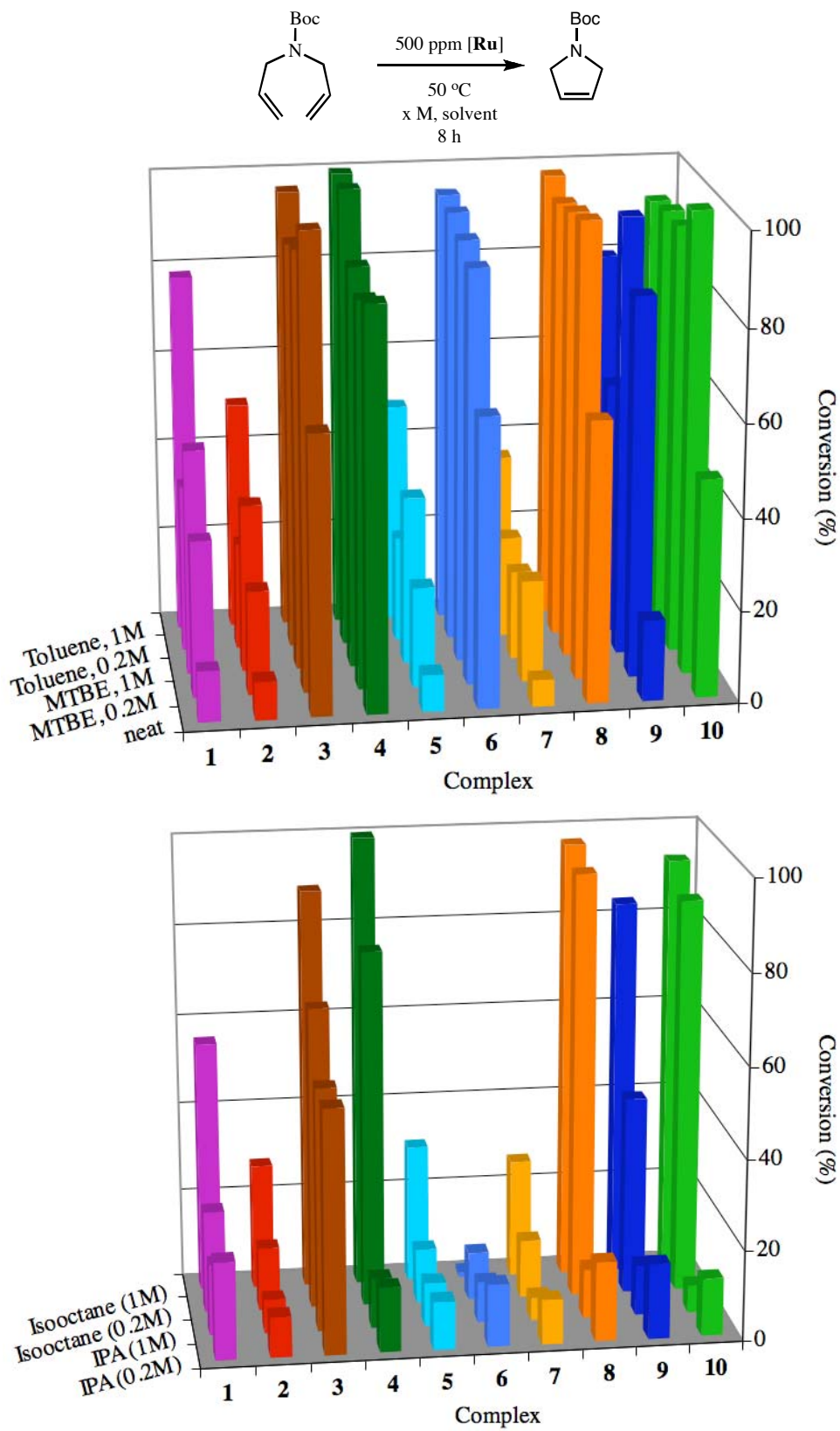


**Figure B.2.** RCM of 3.11 utilizing complexes 3.1–3.10 at 50 °C.

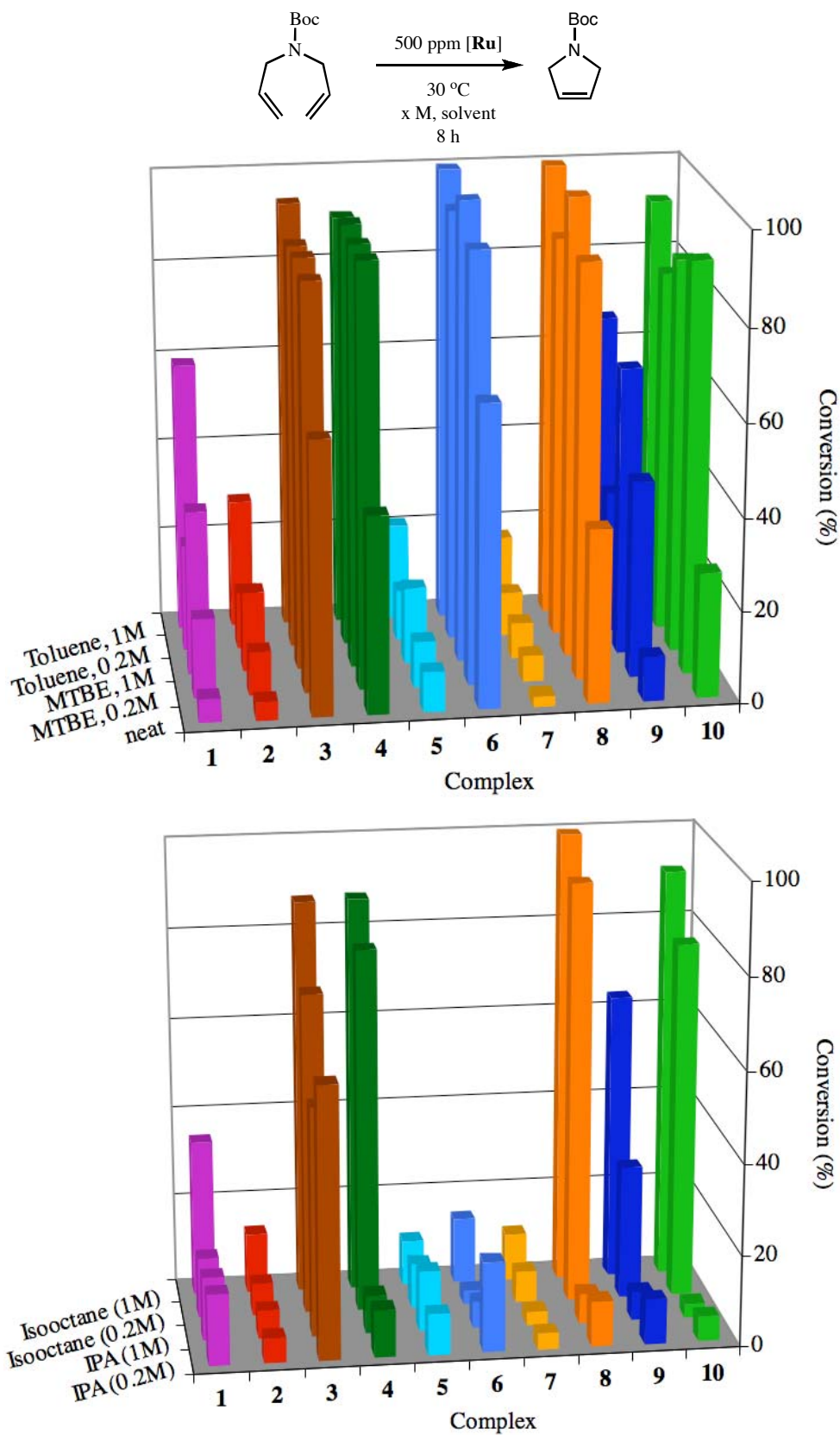


**Figure B.3.** RCM of **3.11** utilizing complexes **3.1–3.10** at 30 °C.

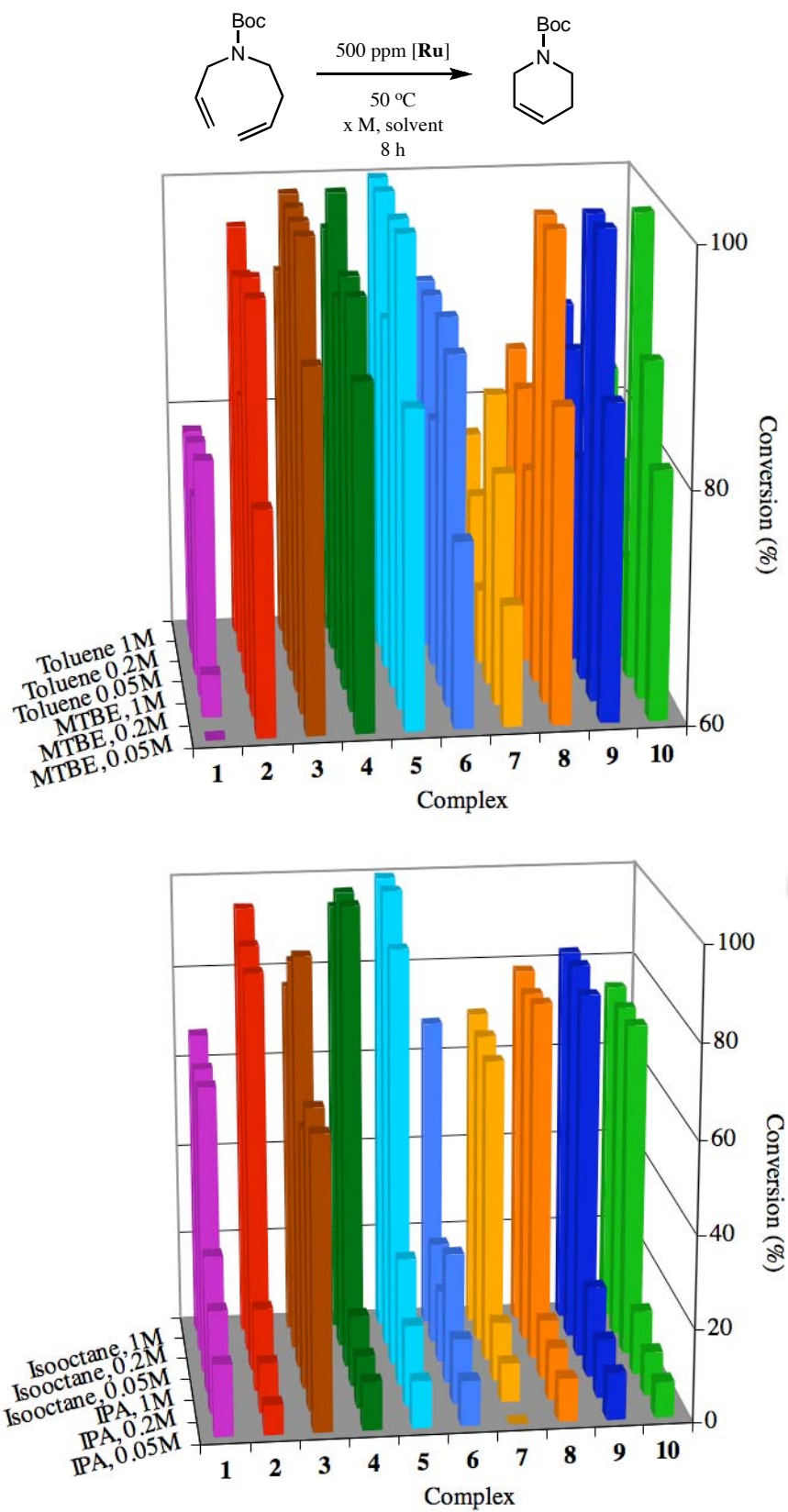


**Figure B.4.** RCM of **3.13** utilizing complexes **3.1–3.10** at 50 °C.

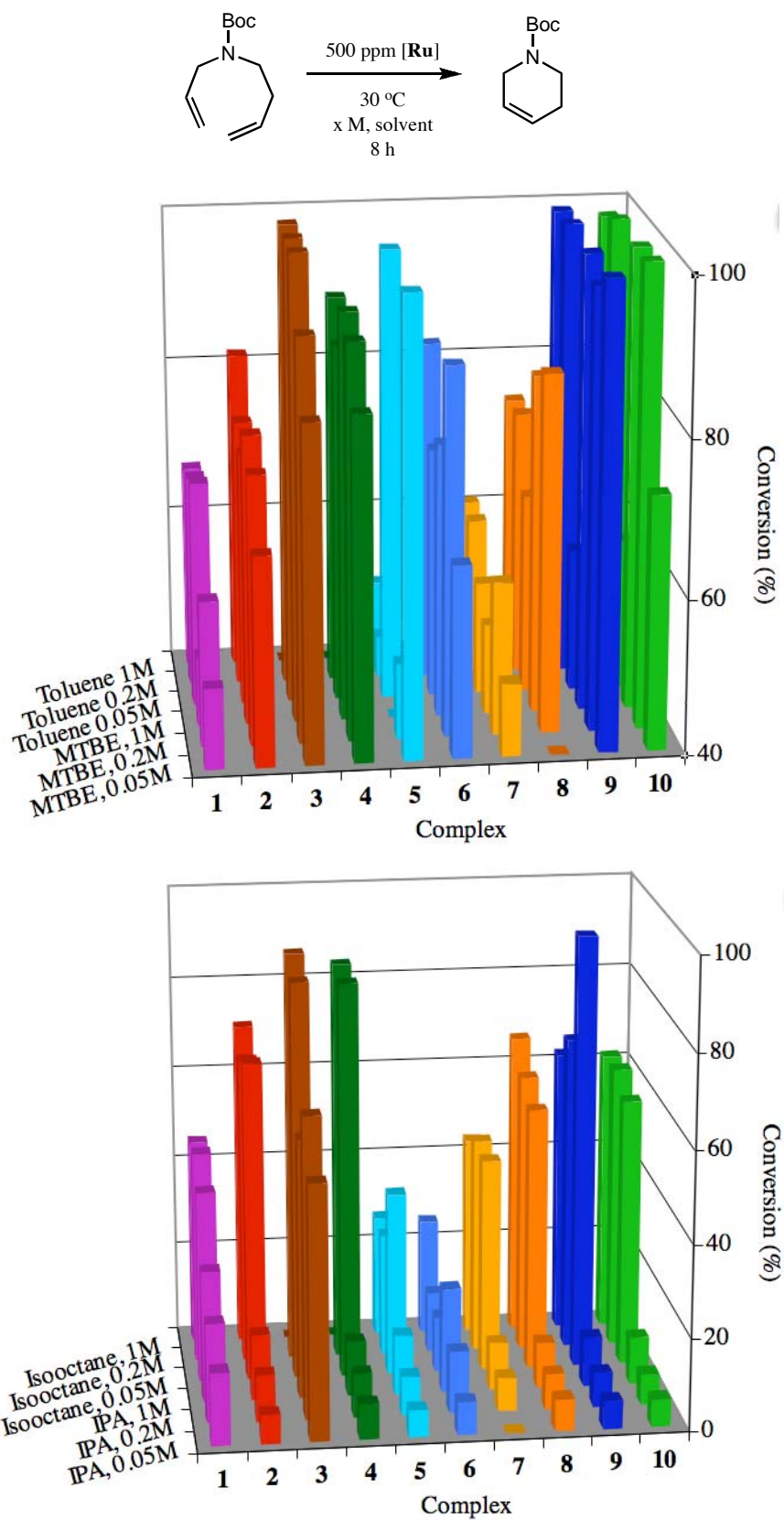


**Figure B.5.** RCM of 3.13 utilizing complexes 3.1–3.10 at 30 °C.

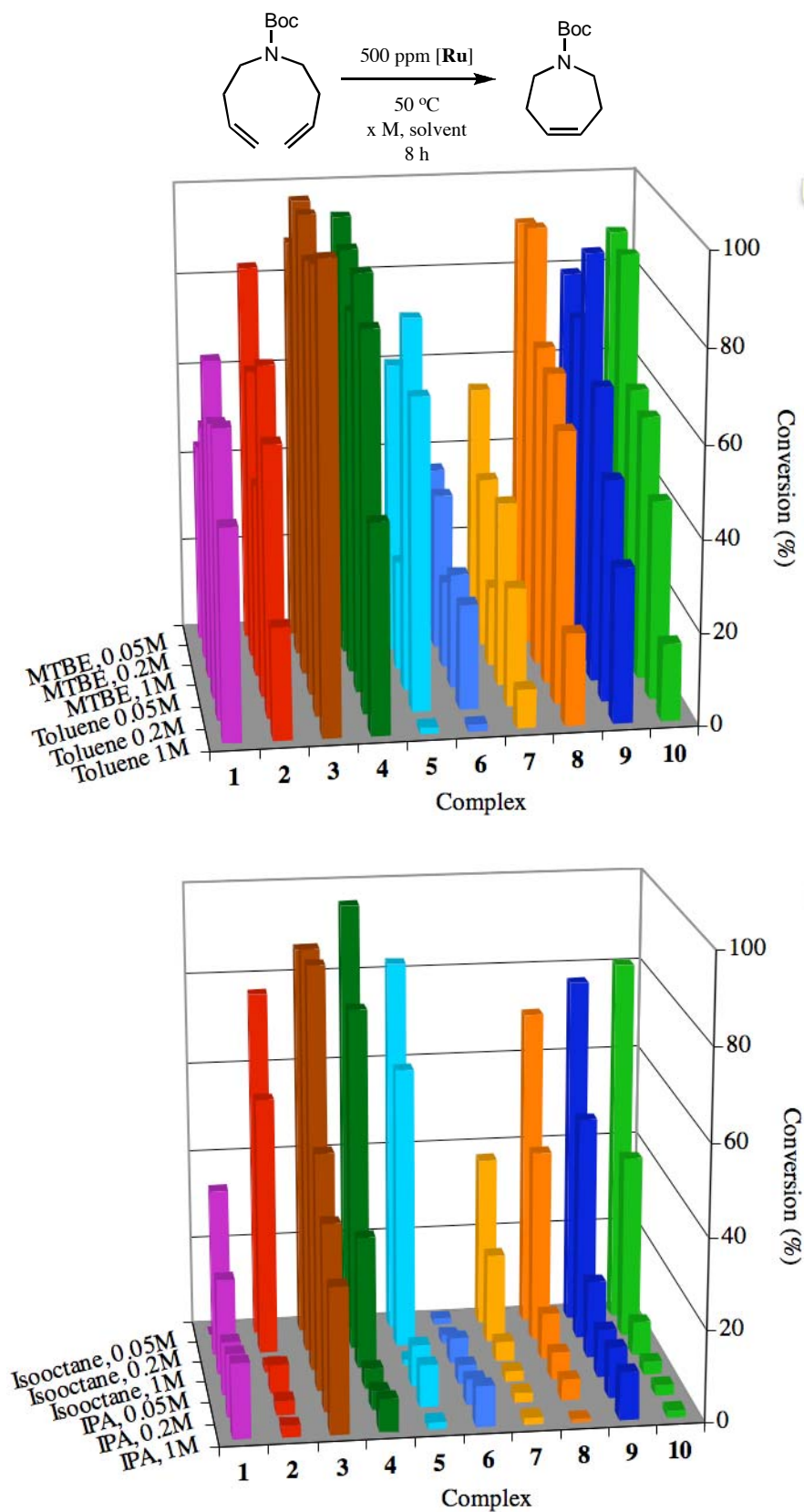


**Figure B.6.** RCM of **3.15** utilizing complexes **3.1–3.10** at 50 °C.

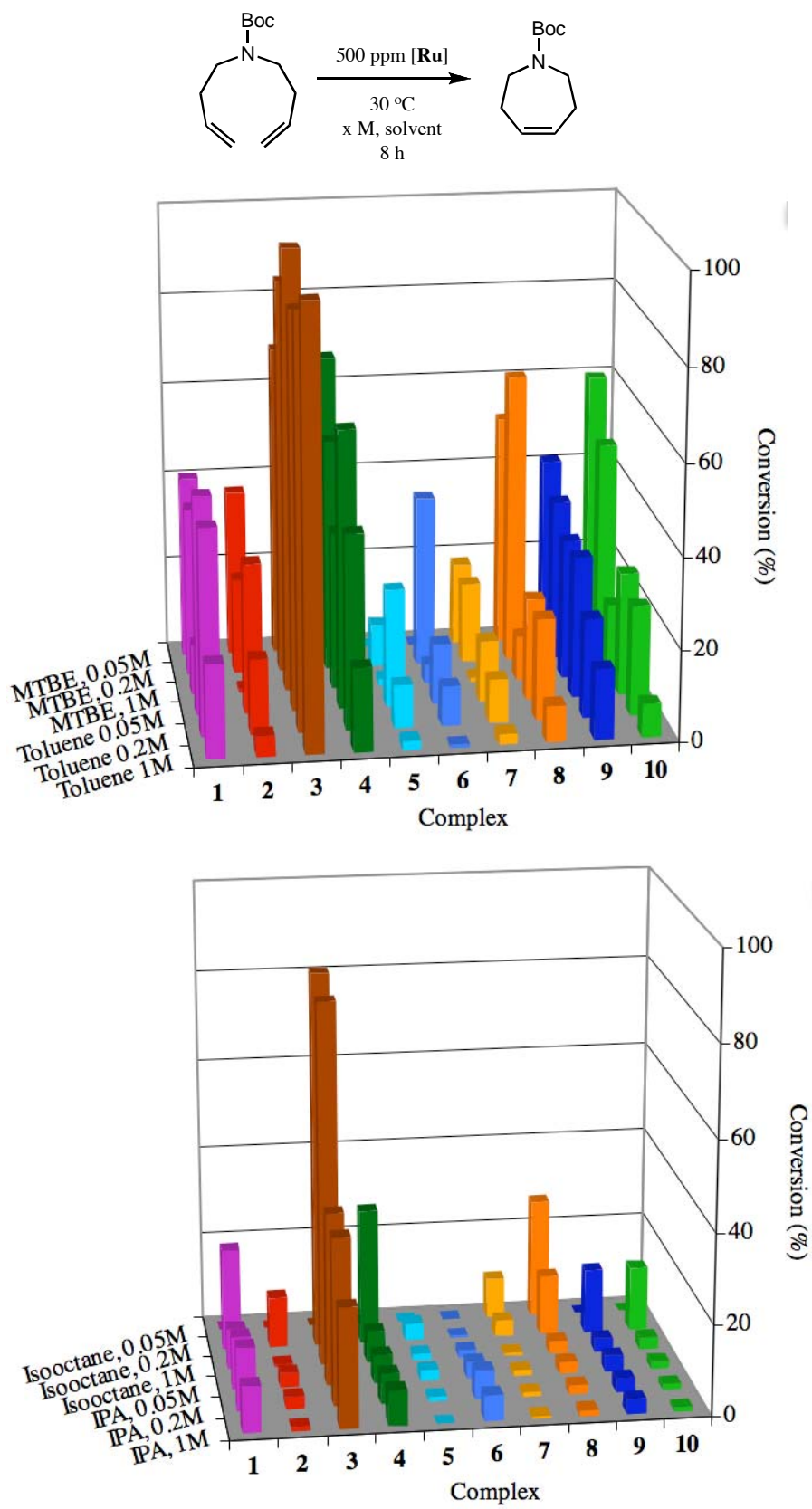


**Figure B.7.** RCM of **3.15** utilizing complexes **3.1–3.10** at 30 °C.

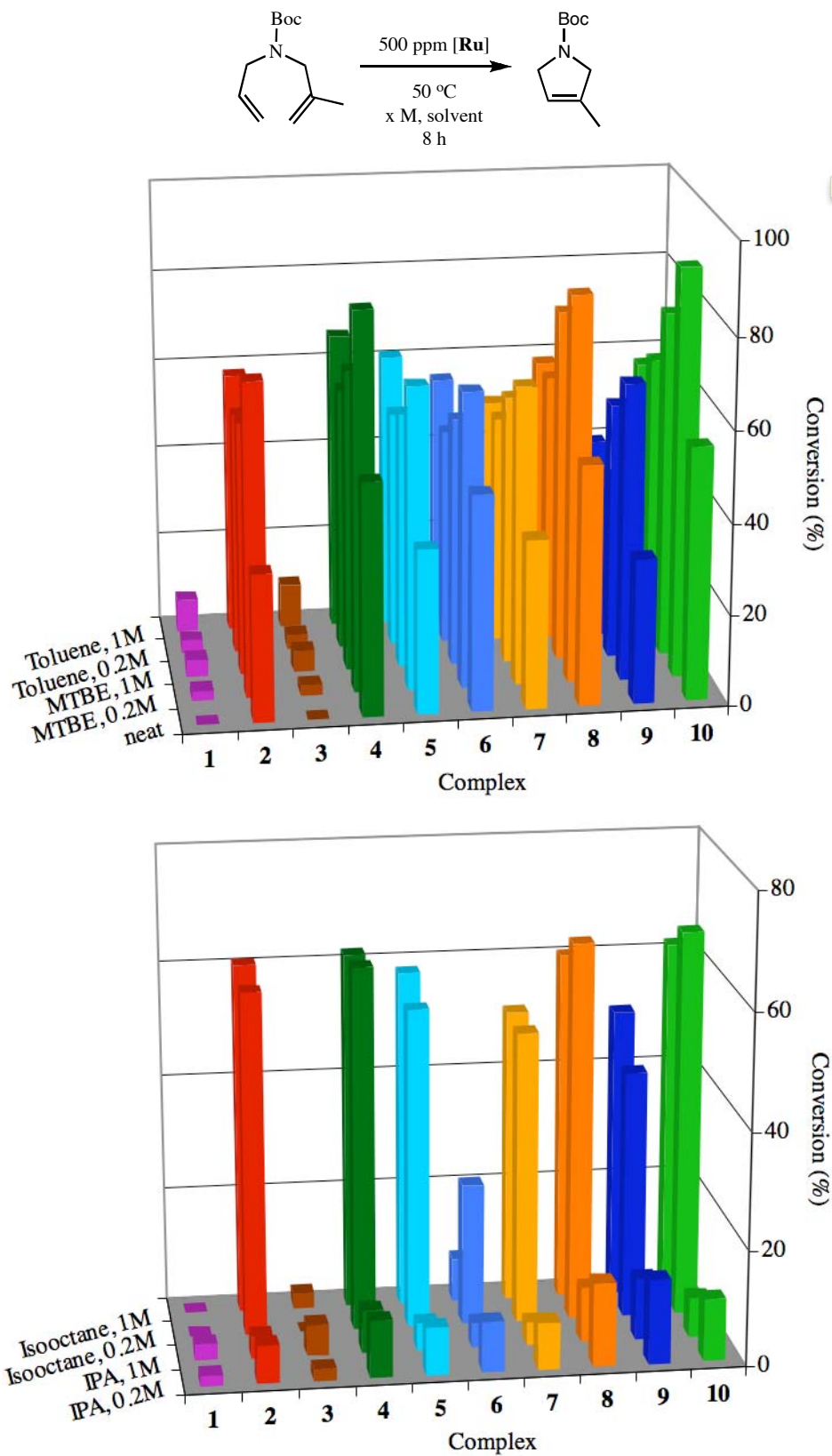


**Figure B.8.** RCM of 3.17 utilizing complexes 3.1–3.10 at 50 °C.

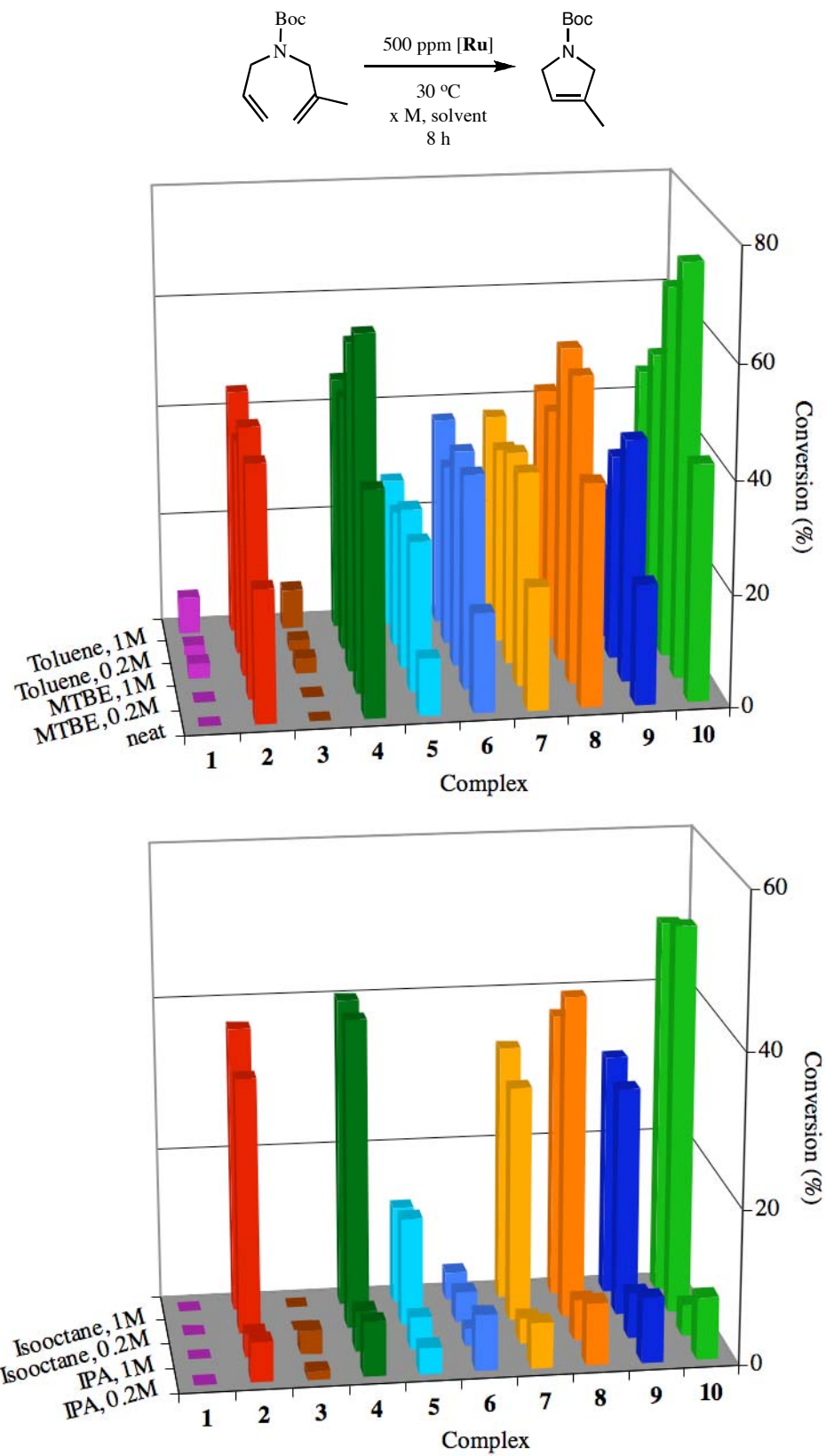


**Figure B.9.** RCM of 3.17 utilizing complexes 3.1–3.10 at 30 °C.

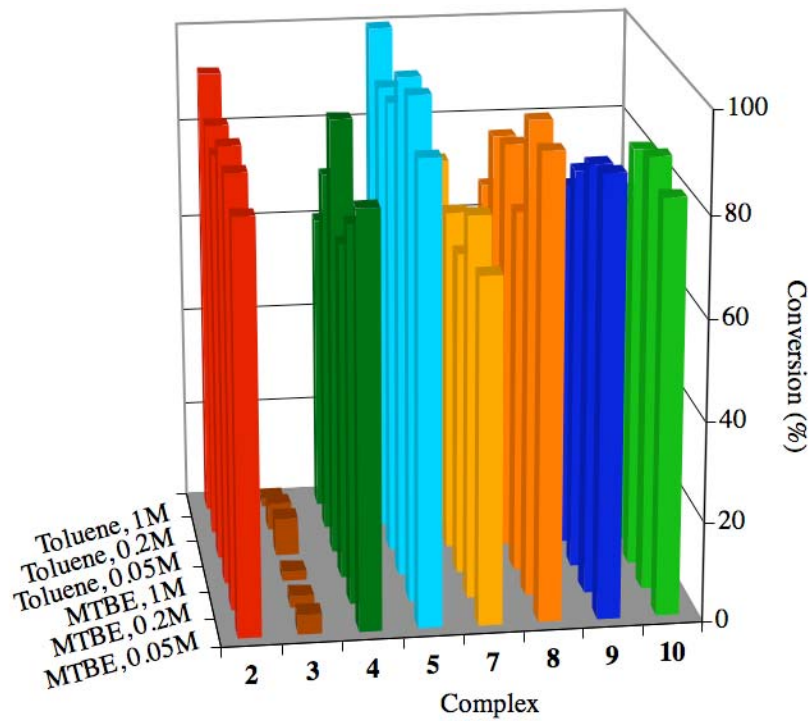
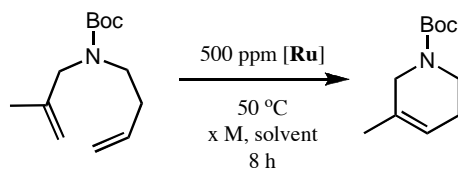


**Figure B.10.** RCM of **3.19** utilizing complexes **3.2–3.5** and **3.7–3.10** at 50 °C.

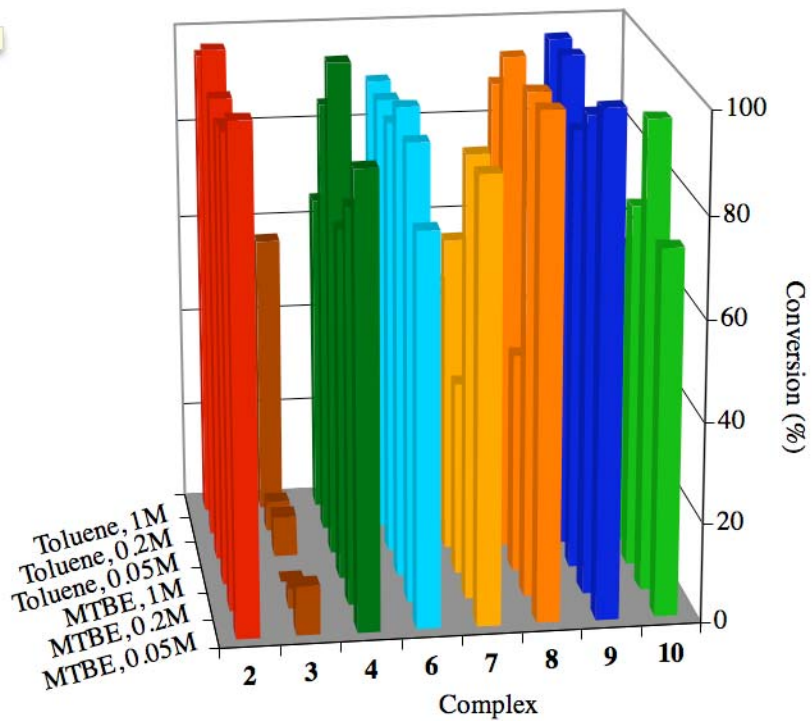
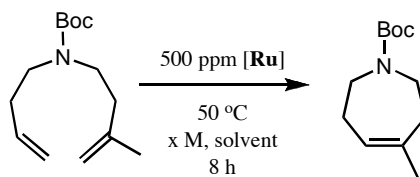


**Figure B.11.** RCM of **3.21** utilizing complexes **3.2–3.4** and **3.6–3.10** at 50 °C.

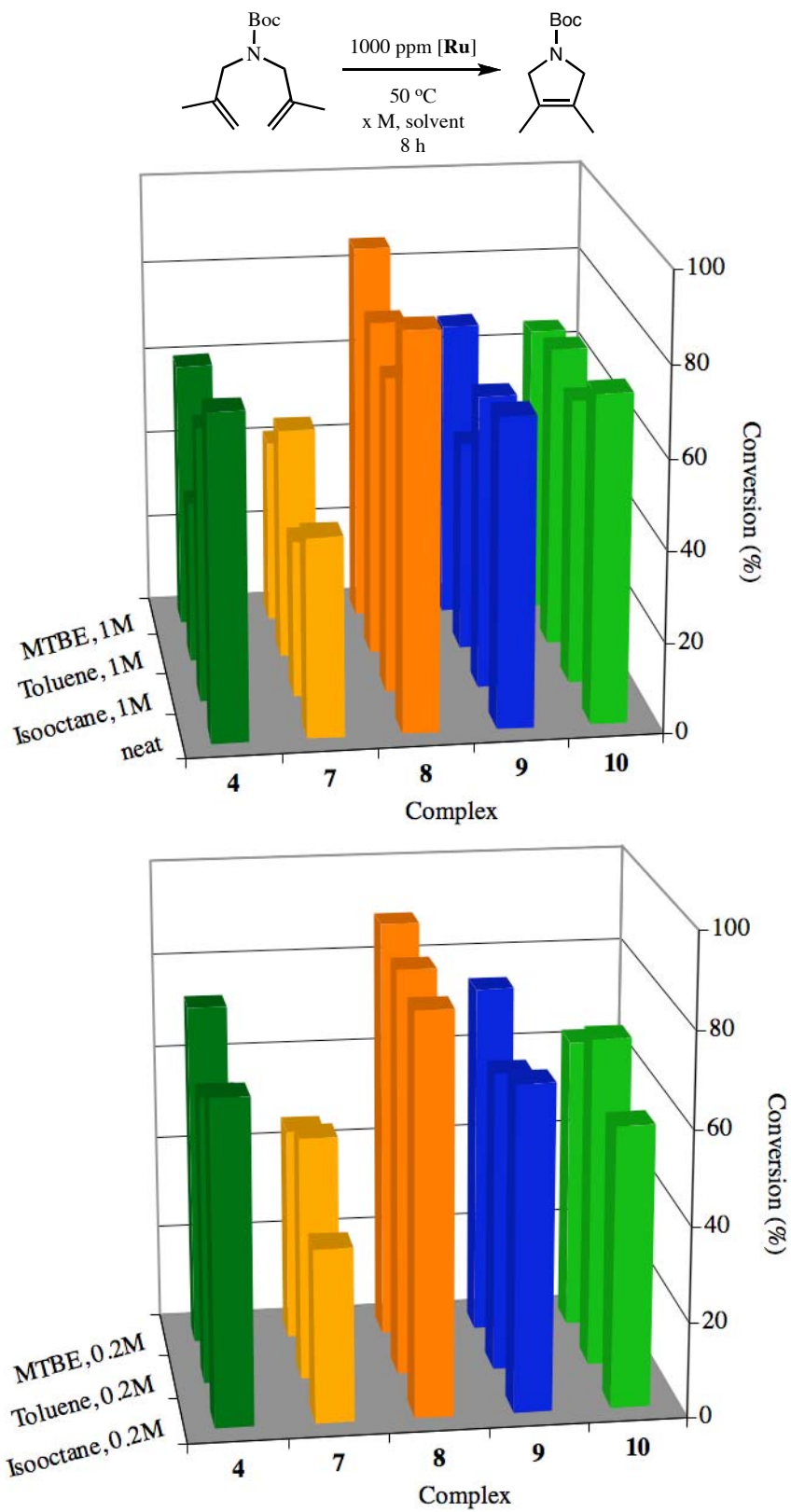


**Figure B.12.** RCM of **3.23** utilizing complexes **3.4** and **3.7–3.10** at 50 °C.

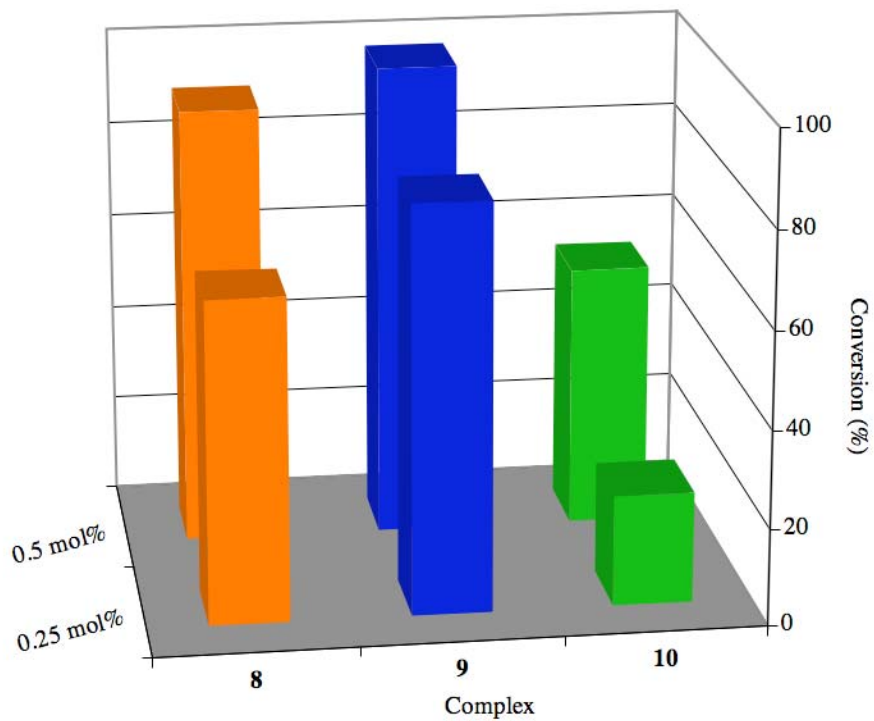
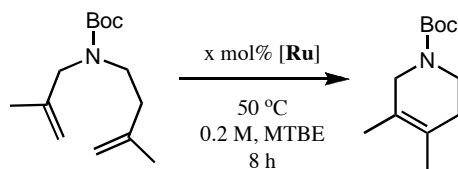


**Figure B.13.** RCM of 3.25 utilizing complexes 3.8–3.10 at 50 °C.

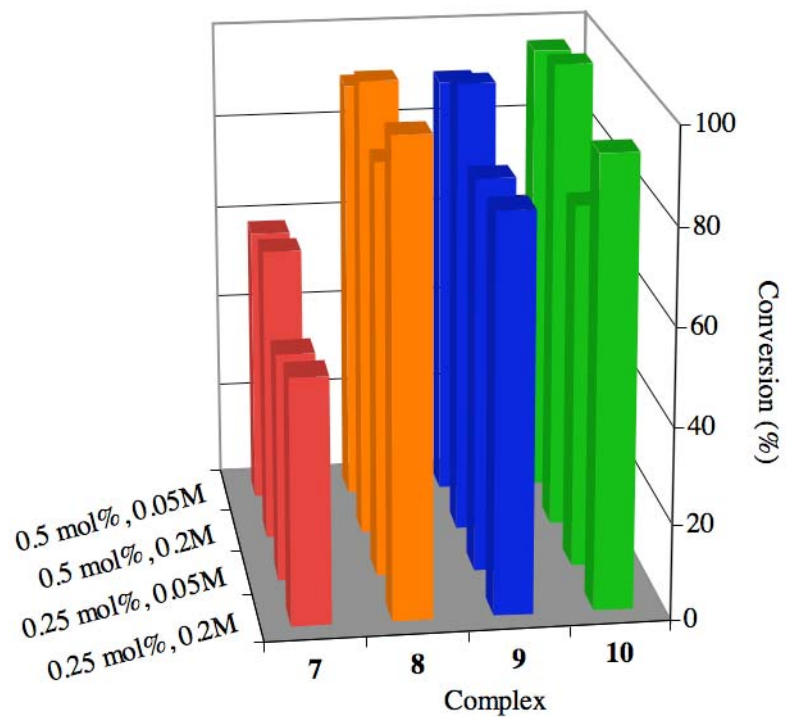
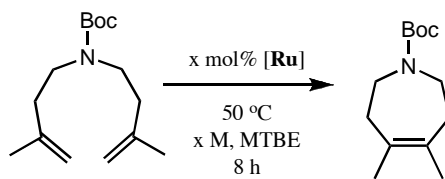


**Figure B.14.** RCM of **3.27** utilizing complexes **3.7–3.10** at  $50 \text{ }^\circ\text{C}$ .



L. Bencze